

**Engineering Sciences**

76

**Branch Library**

**MATHEMATICAL MODELING  
OF SEDIMENTATION TRANSIENTS  
IN SAND-BED CHANNELS**

by

**Khalid Mahmood**

and

**V. Miguel Ponce**



**Colorado State University  
Engineering Research Center  
Fort Collins, Colorado  
80523**

April 1976

018483 0079374

**CER75-76KM-VMP28**

## ABSTRACT

A mathematical model of sedimentation transients in straight alluvial channels is presented for subcritical flow. Both the bed load and suspended load components of the transport are separately accounted in the model. A coupled solution of the momentum and sediment continuity equations enables the numerical solution with longer time steps than are possible for uncoupled models. The model is particularly suitable for long-term simulations in sand-bed channels. In view of the markedly slow nature of the sedimentation transients, the water discharge is considered invariant at the time scale used to model the sedimentation transients. For the upstream boundary condition, either the depth of flow or bed elevation can be specified in time. A practical alternative is to specify the bed material transport in time, since it can be directly related to the depth of flow. For the downstream boundary condition, the model requires that the stage be specified in time.

A linearized implicit numerical scheme is used to solve the governing equations. The linearization assumes that during a discrete time step  $\Delta t$ , the proportional change in depth of flow,  $\Delta h/h$  is less than 0.10. The stability and convergence of the numerical scheme are given careful consideration, and criteria are developed to assess the convergence properties. Theoretically optimum values of the weighting factor  $\delta$  and a sedimentation Courant number  $cr$  are presented, where  $c$  is the celerity of small bed level perturbations and  $r = 2\Delta t/\Delta x$ .

Results of test runs derived from hypothetical examples are presented. The numerical model effectively simulates the formation of

a bed wave in the upstream reach of a straight alluvial channel due to a nonequilibrium sediment inflow hydrograph. There is no limitation to the shape of the sediment hydrograph that can be modeled, provided the linearization is valid ( $\Delta h/h \leq 0.10$ ) and  $cr$  is equal to or slightly greater than 2. Experience with this model shows that in order to insure stability of the numerical scheme, a value of  $\delta \approx 0.7$  is necessary.

Various types of aggradation and degradation problems can be simulated by this model. Examples of the following problems are presented: (1) the formation and migration of bed waves in alluvial channels, (2) the change in channel bed configuration caused by the change in tail water elevation, and (3) the transient effect of local sediment removal by means such as dredging and sediment ejection.

## ACKNOWLEDGEMENTS

The study reported herein is part of a continuing research effort in the Study of Alluvial River Mechanics with Full-Scale Verification on the Link Canals of Pakistan. This is supported by National Science Foundation Grant No. ENG72-00274A01.

Field data for the verification of this model are being observed under Alluvial Channels Observation Project (ACOP) in Pakistan. ACOP is a Special Foreign Currency Cooperative Research Project and is funded by National Science Foundation Grant No. OIP73-02277A01 to Water and Power Development Authority, Pakistan.

Help by Mr. Emmet Owens, Jr. in the final preparation of this report is acknowledged.

## TABLE OF CONTENTS

<u>Chapter</u>		<u>Page</u>
	ABSTRACT . . . . .	ii
	ACKNOWLEDGEMENTS . . . . .	iv
	LIST OF FIGURES . . . . .	vii
I	INTRODUCTION . . . . .	1
II	BASIC EQUATIONS . . . . .	5
	2.1 Introduction . . . . .	5
	2.2 Governing Equations . . . . .	6
	2.3 Supplementary Equations . . . . .	13
	2.4 Resistance Function . . . . .	14
	2.5 Velocity Distribution . . . . .	16
	2.6 Bed Load Function . . . . .	17
	2.7 Suspended Load Function . . . . .	18
	2.8 Summary . . . . .	20
III	NUMERICAL SOLUTION . . . . .	22
	3.1 Finite Difference Scheme . . . . .	22
	3.2 Discretization of the Equation for Bed Material Continuity . . . . .	24
	3.3 Discretization of the Equation of Motion . . . . .	26
	3.4 Boundary Conditions . . . . .	27
	3.5 Solution Algorithm . . . . .	30
IV	STABILITY AND CONVERGENCE . . . . .	32
	4.1 Introduction . . . . .	32
	4.2 Linearization of the Governing Equations. . . . .	33
	4.3 Diffusion and Dispersion Properties of the Differential System . . . . .	36
	4.4 Diffusion and Dispersion Functions for the Difference System . . . . .	40
	4.5 Convergence Ratios . . . . .	43
	4.6 Convergence Ratios for Prismatic Frictionless Systems . . . . .	44
	4.7 Convergence Ratios for Frictional Prismatic Systems . . . . .	48
	4.8 Convergence Ratios for Frictional Nonprismatic Systems . . . . .	51
	4.9 Summary . . . . .	56

<u>Chapter</u>		<u>Page</u>
V	NUMERICAL EXPERIMENTS . . . . .	58
	5.1 Introduction . . . . .	58
	5.2 Test Reach . . . . .	59
	5.3 Test Run 1 . . . . .	61
	5.4 Test Run 2 . . . . .	70
	5.5 Test Run 3 . . . . .	71
	5.6 Test Run 4 . . . . .	74
VI	CONCLUSIONS AND RECOMMENDATIONS . . . . .	77
	APPENDIX I . . . . .	81
	APPENDIX II . . . . .	83
	APPENDIX III . . . . .	113

## LIST OF FIGURES

<u>Figure</u>		<u>Page</u>
2.1	Alternate Bars in the Taunsa-Panjnab Link Canal . . . . .	7
2.2	Definition Sketch . . . . .	10
2.3	Characteristic Curves for Subcritical Flow in Sand- Bed Channels . . . . .	12
3.1	Definition Sketch for the Finite Difference Scheme . . . . .	23
4.1	Variation of Convergence Ratios with Discretization Parameters in a Frictionless System . . . . .	47
4.2	Variation of Convergence Ratios with Discretization Parameters in a Frictional System . . . . .	50
4.3	Variation of Convergence Ratios with Discretization Parameters (effect of increased frictional resistance) . . . . .	52
4.4	Variation of Convergence Ratios with Discretization Parameters (effect of increased bed material load) . . . . .	52
4.5	Variation of Convergence Ratios with Discretization Parameters for a Nonprismatic Channel, $dB/dx = 0.01$ . . . . .	54
4.6	Variation of Convergence Ratios with Discretization Parameters for a Nonprismatic Channel, $dB/dx = -0.01$ . . . . .	55
5.1	Bed Elevation of the Channel, Test Run 1. $\delta = 0.70$ . . . . .	63
5.2	Bed Elevation of the Channel, Test Run 1. $\delta = 0.60$ . . . . .	64
5.3	Test Run 1: Comparison of Results of the Formation of the Bed Wave, for $t = 120$ days . . . . .	65
5.4	Bed Elevation of the Channel, Test Run 2. $\delta = 0.70$ . . . . .	72
5.5	Bed Elevation of the Channel, Test Run 3. $\delta = 0.70$ . . . . .	75
5.6	Bed Elevation of the Channel, Test Run 4. $\delta = 0.70$ . . . . .	76
A.1	Program Setran Flowchart . . . . .	114

## CHAPTER I

## INTRODUCTION

The morphologic and bed material transport relations in alluvial channels are generally based on equilibrium flow conditions. An equilibrium flow through a finite reach of a channel is defined as a flow that possesses sediment inflow-outflow balance over a sufficiently long but finite time interval. Flow in natural and man-made alluvial channels is generally unsteady both in water and in sediment discharge. Therefore, a channel that is in equilibrium over longer time intervals may experience significant deviation from the equilibrium over shorter intervals. Deviations from equilibrium conditions in an alluvial channel may also occur when the base level has been changed due to man-made or natural causes and the channel is in the process of adjusting to the new boundary conditions. The regime associated with these deviations, pertaining to oscillations around an equilibrium state or to the transition from one equilibrium state to another, is herein called a "Sedimentation Transient" or in short a "Transient."

The transients in alluvial channels are primarily caused by the unsteady inflow-outflow conditions and the lag in channel response. They may develop during the passage of a discharge wave, due to a change in the base level and particularly when a large concentration of sediment is introduced into a channel. The sedimentation transients can relate to one or more sedimentation quantities, such as the channel bed-level, suspended load, bed material size, etc. Sand-bed channels exhibit transients more frequently due to a greater mobility of their beds than the coarse material or cohesive boundary channels.

A number of phenomena in sand-bed channels occur as related to transients. For example: (1) the average sediment transport rate in a channel with bed level transients is larger than the transport without a transient and the larger the amplitude of the bed-level transient, the larger is this difference; (2) the minimum available depth of flow in a channel is related to the amplitude of the existing largest positive bed-level transient; (3) bed-level transients phenomenologically reflect the time lag between the precipitation and the resulting sediment yield along a drainage basin, and (4) more importantly, the bed-level transients in straight sand-bed canals can introduce bed instability due to the effect of locally accelerated flow [1].

This report is related to the mathematical modeling of bed-level transients in sand-bed canals. It is inspired by the sedimentation transients that are experienced in large sand-bed link canals in Pakistan. The transients in the link canals are formed under a combination of the following conditions. During flood flows in their parent rivers, the link canals receive large bed material concentrations that cause bed aggradation. As the concentrations recede to their equilibrium levels, the bed-level at the head of the canal lowers and a bed wave is formed. This wave travels down the canal and is generally damped in amplitude. However, at any time there may be a number of waves in the channel that may coalesce and form larger waves. The water level at the tail regulator of a canal (the base level) also varies seasonally. When the level is above its equilibrium value, the bed in the reach under the backwater is aggraded. As the base level is lowered below the equilibrium value a negative wave is formed that

---

\* Numbers in brackets [ ] refer to Appendix I--References.

travels downstream. The combination of these factors gives rise to significant transients of different shapes and sizes.

The governing equations for the transients in sand-bed channels comprise the momentum equation for the water-sediment mixture, and the continuity equations for the water and sediment phases. These equations constitute a set of nonlinear hyperbolic partial differential equations for which an analytical solution is generally unavailable. In unsteady water-sediment routing in channels, these equations or their simplified forms are therefore numerically solved by using appropriate finite difference schemes. The solution techniques so far developed are restricted to the bed-load mode of sediment transport and mostly use an uncoupled model in which the hydraulic and sedimentation phases are studied sequentially.

When applied to bed-level transients in sand-bed channels, these techniques are generally deficient, because: (1) in sand-bed channels, most of the bed material load is transported in suspension and realistic results cannot be expected when this mode of transport is neglected; (2) the uncoupled models have to use a smaller time step than the coupled model and therefore increase the total computational time; (3) the bed waves in frictional flow systems undergo dispersion and damping. The numerical schemes can introduce dispersion and damping of their own so that the representation of the transients is distorted. It is not possible to analytically determine the bed wave dispersion and damping characteristics for uncoupled models and so the accuracy of their results is uncertain unless rather small space and time steps are used and finally; (4) models that neglect the suspended load or the models that are uncoupled cannot realistically represent the formation

of bed waves due to the influx of large sediment concentration at the head of a channel.

A mathematical model is developed herein that is especially suited for the study of bed-level transients in sand-bed channels. This model is based on a coupled solution of the hydraulic and sedimentation phenomena. It also accounts for the suspension mode of sediment transport. The governing equations for sedimentation transients are presented in Chapter II and the numerical solution based on a linearized-implicit-coupled scheme is presented in Chapter III. Chapter IV deals with the stability and convergence characteristics of the numerical scheme presented in Chapter III. Specifically, the damping and dispersion characteristics of the scheme are considered, and criteria for the errors introduced by the numerical scheme are developed. Chapter V presents the results of some numerical experiments that simulate the phenomena observed in the link canals. Chapter VI contains the conclusions of this study and recommendations for future research in this field. The computer program developed for using this model is presented in Appendix II along with a user's manual.

## CHAPTER II

## BASIC EQUATIONS

## 2.1 Introduction

The flow in sand-bed channels involves a three-dimensional two-phase flow, many aspects of which are not as yet fully understood. However, in solving practical problems related to alluvial channels, simplifying assumptions have been successfully used in the past. For example, the mass and momentum diffusion characteristics of clear water turbulent flows have been used in developing the sediment transport functions [2,3]. These simplifications are useful inasmuch as solutions can be obtained that otherwise are not possible. In this study of sedimentation transients, three basic assumptions are made with regard to the character of alluvial channel flow. These are:

1. The cross-sectional shape of the channel is constant, so that the hydraulic and sedimentation phenomena can be described as functions of average flow parameters such as the hydraulic depth, water surface width and the average velocity of flow.
2. The flow is one-dimensional and the channel phenomena can be modeled as functions only of the linear dimension along the direction of flow.
3. The hydraulic transients travel much faster than the sedimentation transients, so that the water flow can be considered as steady compared to the time scale of the sedimentation phenomena and over a given computational time step the sedimentation phenomena can be represented by the time averaged flows parameters.

The cross-sectional shape of sand-bed canals is determined by the flow and sediment characteristics [4]. The sedimentation characteristics such as the mineralogy and quantity of wash load are fairly constant regionally, so that a unified pattern of channel behavior is recognized (regime theory is a good example of regional pattern). For such channels the cross-sectional shape follows a uniform pattern, and the flow and sedimentation phenomena can be described in terms of average channel parameters.

Flow in wide and straight sand-bed channels exhibits three-dimensional flow patterns to some extent. For example the straight sand-bed canals form alternate bars of varying height (see Figure 2.1). However, the degree of asymmetry in their cross-section is generally small, so that the one-dimensional assumption is considered valid. The relative speeds of water and sedimentation transients on sand-bed channels and their effect on the governing equations has been specifically studied in the past. As a result, Iwagaki [5], de Vries [6] and Cunge and Perdreau [7] showed that the water discharge can be considered steady in the study of sedimentation transients.

## 2.2 Governing Equations

With the preceding assumptions and the usual assumptions of shallow water flow [8], the governing equations of flow through a wide rectangular channel with a variable bed level and bed width are:

Equation of Motion:

$$\frac{1}{g} \frac{\partial}{\partial t} \left( \frac{Q}{Bh} \right) + \frac{\partial}{\partial x} \left( \frac{Q^2}{2gB^2h^2} + y \right) + S_f = 0 \quad (2-1)$$

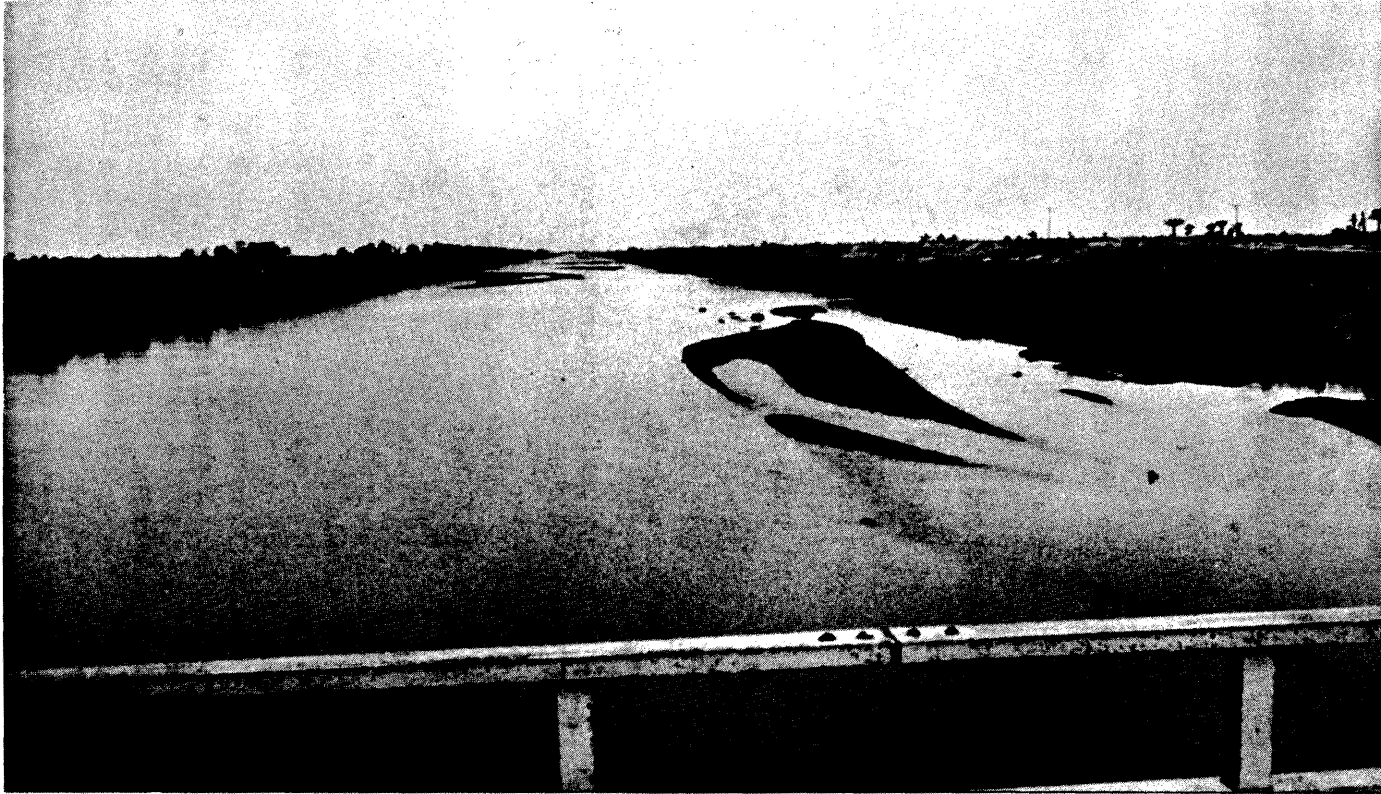


Fig. 2.1 Alternate Bars in the Taunsa-Panjnab Link Canal in Pakistan.

Equation of Continuity of Water-Sediment Mixture:

$$\frac{\partial}{\partial t} [\rho Q] = 0 \quad (2-2)$$

Equation of Continuity of the Bed Material:

$$\frac{\partial G_b}{\partial x} + \frac{\partial G_s}{\partial x} + \frac{\partial}{\partial t} (C_s B h) + (1-p) S_s \gamma_w \frac{\partial}{\partial t} (Bz) = 0 \quad (2-3)$$

where

$Q$  = the constant discharge in the channel,

$g$  = the gravitational acceleration,

$y$  = the water surface elevation,

$S_f$  = the energy gradient assumed to be equal to the energy gradient for a representative average discharge,

$\rho$  = the mass density of the sediment water mixture,

$G_b$  = the bed load,

$G_s$  = the suspended bed material load,

$C_s$  = the average spatial bed material concentration in the cross-section,

$p$  = the porosity of the channel bed,

$\gamma_w$  = the density of water

$S_s$  = specific gravity of solids

$z$  = the bed elevation,

$B$  = the deformable bed width, assumed equal to the width of the rectangular cross-section,

$h$  = the depth of flow ( $h=y-z$ ),

$x$  = the distance along the channel bed measured in the downstream direction and,

$t$  = the time.

The geometrical quantities defined above are also shown in Figure 2.2. All the terms in Equation (2-1) have units of slope and transport rates  $G_b$  and  $G_s$  in Equation (2-3) are expressed in units of weight per unit time. It is assumed that the mass density of the sediment water mixture in Equations (2-1) and (2-2) is the same as that of water and the width  $B$  is invariant in time. The governing equations then reduce to:

$$\frac{\partial}{\partial x} \left( \frac{Q^2}{2gB^2h^2} + y \right) + S_f = 0 \quad (2-4)$$

$$\frac{\partial}{\partial x} (g_b) + \frac{\partial}{\partial x} (g_s) + \frac{\partial}{\partial t} (C_s h) + p_* \frac{\partial z}{\partial t} + (g_b + g_s) \frac{1}{B} \frac{\partial B}{\partial x} = 0 \quad (2-5)$$

where the local acceleration term has been dropped in Equation (2-4) because its magnitude is much smaller than the other terms and its effect on the transient can be ignored [9]. In Equations (2-4) and (2-5),  $g_s$  and  $g_b$  are the suspended bed material load and the bed load, respectively, per unit width of the channel, defined as  $g_s = G_s/B$  and  $g_b = G_b/B$ , and  $p_* = (1-p)S_s\gamma_w$ .

In alluvial channel flow the quantities  $S_f$ ,  $g_s$ ,  $g_b$  and  $C_s$  used in Equations (2-4) and (2-5) are functions of the local velocity  $V$ , depth of flow  $h$  and bed material size  $D$ , besides the properties of water such as temperature, kinematic viscosity, etc. If the bed material size along a channel is initially known and is considered invariant in time (as in the case of the channel width) then these quantities can be expressed as functions of  $h(x,t)$  alone, so that

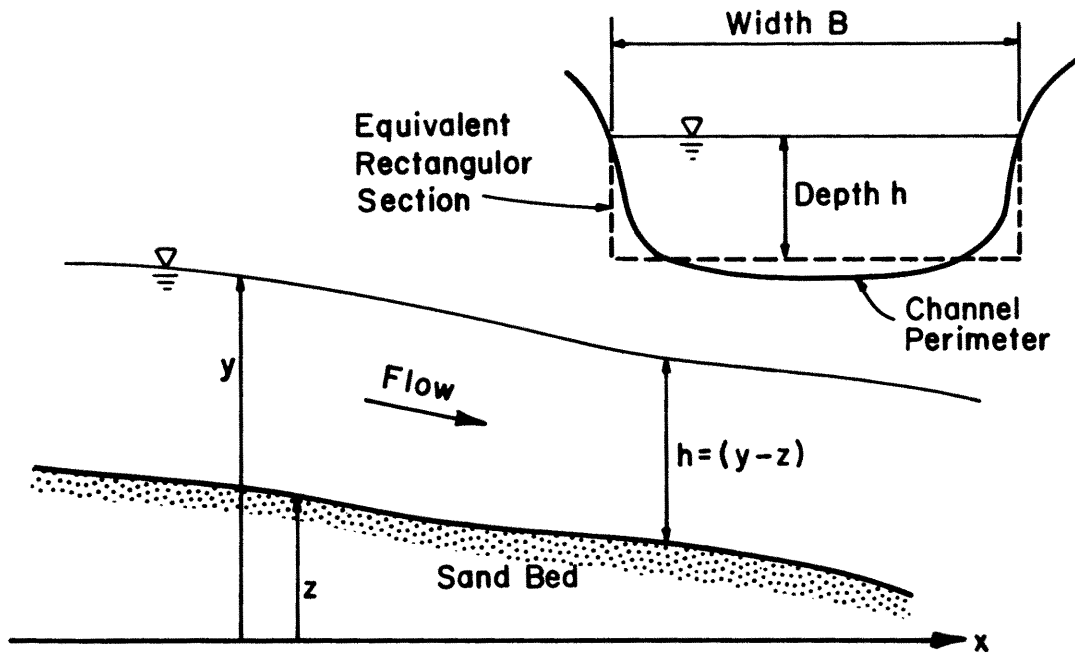


Fig. 2.2 Definition Sketch.

$$S_f = S_f(h) \quad (2-6)$$

$$g_t = (g_s + g_b) = g_t(h) \quad (2-7)$$

and

$$C_s = C_s(h) \quad (2-8)$$

Using these expressions, Equations (2-4) and (2-5) become:

$$(1-F^2) \frac{\partial y}{\partial x} + F^2 \frac{\partial z}{\partial x} = -S_f + \frac{Q}{gB^{3/2}} B' \quad (2-9)$$

$$C'_s \frac{\partial y}{\partial t} + g'_t \frac{\partial y}{\partial x} + (p_* - C'_s) \frac{\partial z}{\partial t} - g'_t \frac{\partial z}{\partial x} = -\frac{g_t}{B} B' \quad (2-10)$$

where the Froude number  $F = Q/\sqrt{gB^2h^3}$ , the mass density of the sand bed  $p_* = S_s \gamma_w (1-p)$  and prime superscript represents derivative with respect to  $h$ .

Equations (2-9) and (2-10) form a set of nonlinear first order partial differential equations for the dependent variables, water stage  $y$  and the bed elevation  $z$  with the two independent variables, distance along the direction of flow  $x$  and time  $t$ . These are hyperbolic equations with the characteristic equation

$$g' dt^2 + [p_*(1-F^2) - C'_s] dt dx = 0 \quad (2-11)$$

Equation (2-11) has two roots,

$$c_2 = \left(\frac{dx}{dt}\right)_2 = -\infty \quad (2-12)$$

and

$$c_3 = \left(\frac{dx}{dt}\right)_3 = \frac{-g'_t}{[p_*(1-F^2) - C'_s]} \quad (2-13)$$

The characteristic curves,  $c_2$  and  $c_3$  for subcritical flow are shown in Figure 2.3. These characteristic directions indicate that: (1) the effect of a small disturbance in  $y$  within the domain or at the downstream boundary will instantaneously extend to the upstream boundary

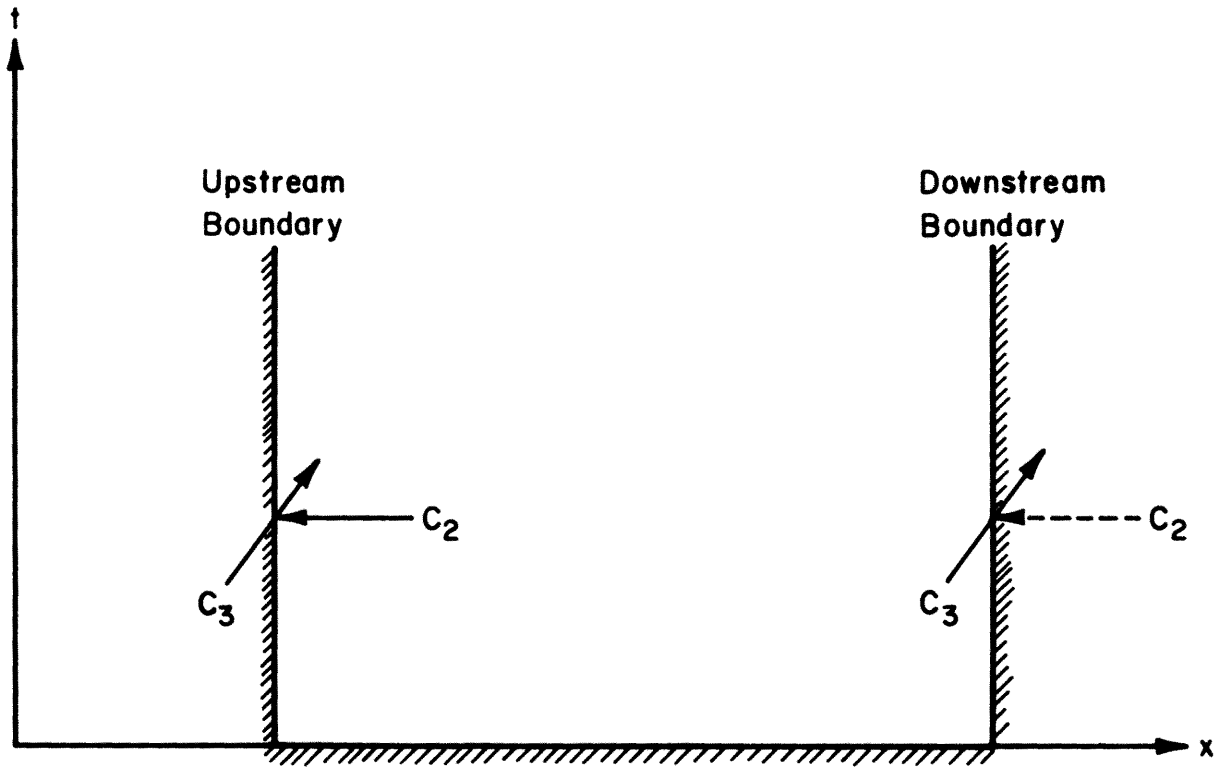


Fig. 2.3 Characteristic Curves for Subcritical Flow in Sand-Bed Channels.

and (2) a small disturbance in bed level  $z$ , will travel with celerity  $c_3$ . Equations (2-12) and (2-13) also indicate that for the mixed value problem (Equations (2-9) and (2-10)) to be well posed the following conditions need to be specified for the subcritical flow  $F < 1$ :

1. Initial Condition

$$y(x,0) \quad \text{and} \quad z(x,0), \quad 0 \leq x \leq L$$

2. Boundary Conditions

One boundary condition on the upstream boundary as

$$z(0,t), \quad 0 \leq t \leq T$$

and one boundary condition on the downstream boundary as

$$y(L,t), \quad 0 \leq t \leq T$$

where  $L$  is the length of the channel reach and  $T$  is the time span over which the governing equations are to be solved.

### 2.3 Supplementary Equations

Equations (2-4) and (2-5) contain  $S_f$ , the energy gradient of the flow, and quantities  $g_s$ ,  $g_b$  and  $C_s$ , associated with the transport of sediment by flow. In alluvial channel flow these quantities are functionally related to the bed material size and water discharge by resistance and transport functions.

The experience with resistance to flow in alluvial channels indicates that the resistance varies with the flow rate and that at least different resistance functions are applicable to different bed form regimes [3]. There is also a variety of resistance functions available for modeling that differ in their approach and range of applicability. For the purpose of modeling, it is not necessary to follow a particular resistance function. Rather, a functional form

that covers the range of conditions anticipated in the study and that has been validated by experience, can be conveniently used to relate  $S_f$  with other flow quantities. On the other hand, the sediment transport function used to model the sand-bed channel transients has to satisfy a few specific conditions. One, the transport function must have a sound phenomenological structure. This is necessary because in following sedimentation transients, a wide range of transport conditions from small to high transport rates is covered and to model the transients, it is necessary to realistically represent the change in transport associated with the change in hydraulic quantities. Two, the transport function should be able to separately compute the suspended and bed-load phases. This is important in sand-bed channels, because in these the suspension phase accounts for a major portion of the transport.

Based on the preceding consideration and the writers' experience, the following set of resistance and transport functions has been adopted. Essentially, the resistance function follows the empirically derived behavior of sand-bed channels [4], while the transport function is modeled for a unigranular material after Einstein's Bed-Load function and Mahmood's transport function [2,3].

#### 2.4 Resistance Function

In wide, straight sand-bed channels, the resistance to flow varies with the change of bed form dimensions. However, over a given range, such as the dune to antidune bed form regime, the resistance varies monotonically so that for a constant  $Q$ , the Manning's  $n$  decreases with an increase in Froude number of the flow. This behavior has been

observed in laboratory recirculating flumes and in the large sand-bed irrigation canals operating under equilibrium conditions [4]. It is stated as follows:

$$n = \frac{k_1 D^a}{F^b} \quad (2-14)$$

where  $n$  = Manning's roughness coefficient for the flow,  $D$  = a representative bed material size in feet,  $F$  = Froude number of the flow, and  $k_1$ ,  $a$  and  $b$  are real numbers. Equation (2-14) is dimensionally nonhomogeneous and for a given model  $k_1$ ,  $a$  and  $b$  are determined by calibration or from the available equilibrium data.

Part of the resistance to flow in Equation (2-6) is due to the grain roughness [2,3] and part due to the form roughness caused by the bed form and the presence of the sediment transport. It is necessary to calculate these components explicitly for later use in the transport functions. For the grain roughness, the Manning-Strickler equation is used as follows:

$$n' = 0.0342 D^{1/6} \quad (2-15)$$

where  $n'$  = grain-associated component of Manning's roughness coefficient. Using the functional form of Manning's roughness equation the component of the channel depth associated with the grain roughness is:

$$h' = h \left( \frac{n'}{n} \right)^{3/2} \quad (2-16)$$

The following hydraulic parameters of the flow can then be defined in terms of the constants of Equations (2-14) and (2-15).

$$h' = \ell_1 h^{m_1} B^{t_1} \quad (2-17)$$

$$S_f = \ell_2 h^{m_2} B^{t_2} \quad (2-18)$$

$$U_* = \sqrt{ghS_f} \quad (2-19)$$

$$U_*' = \sqrt{gh'S_f} \quad (2-20)$$

where

$$l_1 = \left[ \frac{0.0342 D^{(1/6-a)} Q^b}{k_1 g^{b/2}} \right]^{3/2} \quad (2-21)$$

$$m_1 = 1 - \frac{9}{4} b \quad (2-22)$$

$$t_1 = -\frac{3b}{2} \quad (2-23)$$

$$l_2 = \left[ \frac{k_1 D^a Q^{(1-b)} g^{b/2}}{1.486} \right]^2 \quad (2-24)$$

$$m_2 = 3b - \frac{10}{3} \quad (2-25)$$

and

$$t_2 = 2(b-1) \quad (2-26)$$

## 2.5 Velocity Distribution

The velocity distribution in the vertical is assumed to follow a power-law as

$$\frac{u}{U_*'} = a_2 \left( \frac{y}{D} \right)^{b_2} \quad (2-27)$$

where the shear velocity  $U_*'$  is the grain-associated shear velocity, exponent  $b_2 = 1/6$  and coefficient  $a_2$  can be determined by equating the grain-associated resistance factor from Equation (2-15) and from the integration of Equation (2-27):

$$a_2 = \frac{7 QD^{1/6}}{6BU_*'h^{7/6}} \quad (2-28)$$

or

$$a_2 = l_3 h^{m_3} B^{t_3} \quad (2-29)$$

where

$$k_3 = 7/6 \frac{QD^{1/6}}{\sqrt{gk_1k_2}} \quad (2-30)$$

$$m_3 = -\left(\frac{m_1}{2} + \frac{m_2}{2} + \frac{7}{6}\right) \quad (2-31)$$

and

$$t_3 = -\left(\frac{t_1}{2} + \frac{t_2}{2} + 1\right) . \quad (2-32)$$

## 2.6 Bed Load Function

The bed load function used herein is modeled after Einstein's bed load function. This function is developed for a single representative bed material size  $D$ . For this condition,

$$\phi_* = \phi = \frac{g_b}{S_s \gamma_w} \left[ \frac{\rho_f}{\rho_s - \rho_f} \right]^{1/2} \left( \frac{1}{gD^3} \right)^{1/2} \quad (2-33)$$

$$\psi_* = \psi = \left[ \frac{\rho_s - \rho_f}{\rho_f} \right] \frac{D}{h' S_f} \quad (2-34)$$

and

$$\phi_* = a_1 \psi_*^{b_1} \quad (2-35)$$

where  $\phi_*$  = the bed load transport intensity parameter,  $\psi_*$  = the shear intensity parameter and  $a_1, b_1$  = the coefficient and the exponent respectively obtained from Einstein's bed load function (Figure 9, reference [2]) to represent the  $\phi_*$ - $\psi_*$  relation over the range of interest. It is understood that 4 to 5 sets of  $(a_1, b_1)$  define the complete range of  $\phi_*$ - $\psi_*$  from the smallest to the largest practical transport rate. It is also possible to adjust the bed load function in a particular model by obtaining  $a_1, b_1$  from calibration or from equilibrium data applicable to the channel.

From Equations (2-33) through (2-35) and using the expressions for  $h'$  and  $S_f$  in Equations (2-17) and (2-18), the bed load per unit width is:

$$g_b = \ell_4 h^{m_4} B^{t_4} \quad (2-36)$$

where

$$\ell_4 = a_1 \sqrt{g} \left[ \frac{\rho_s - \rho_f}{\rho_f} \right]^{b_1 + 1/2} \frac{D^{b_1 + 3/2} S_s \gamma_w}{(\ell_1 \ell_2)^{b_1}}, \quad (2-37)$$

$$m_4 = -b_1 (m_1 + m_2), \quad (2-38)$$

and

$$t_4 = -b_1 (t_1 + t_2). \quad (2-39)$$

## 2.7 Suspended Load Function

The vertical distribution of bed material concentration is not very sensitive to the underlying assumption of the distribution of sediment diffusion coefficient  $\epsilon_s$  (or the shear distribution) in the depth of flow. The major uncertainty in the computation of suspended load comes through the selection of an appropriate value of the Rouse number,  $Z$  [3]. For simplicity, it is assumed herein that the turbulent diffusivity  $\epsilon_s$ , varies linearly in the depth of flow as follows:

$$\epsilon_s = \kappa U_* y \quad (2-40)$$

where  $\kappa$  = Von Karman's constant and  $y$  = distance from the local bed level. The resulting bed material concentration profile is:

$$\frac{C_y}{C_a} = \left( \frac{a}{y} \right)^Z \quad (2-41)$$

with

$$Z = \frac{w}{\kappa U_*} \quad (2-42)$$

where  $C_y$  and  $C_a$  are the bed material concentration at distance  $y$  and distance  $a$  from the bed level, respectively, and  $w$  is the fall velocity of the representative size,  $D$ . Note that the total shear velocity,  $U_*$  is used in Equation (2-42) to define  $Z$  in keeping with the writers' personal experience.

Following the bed material transport functions used herein [2,3], the reference concentration  $C_a$  is defined in a bed layer of thickness  $2D$ . It is assumed that the bed load is moving with a velocity of  $11.6 U_*'$  in the bed layer, so that

$$C_a = \frac{g_b}{(11.6 U_*') (2D)} \quad (2-43)$$

The suspended bed material load,  $g_s$  can then be evaluated as:

$$g_s = \int_{2D}^h C_y u_y dy = \int_{2D}^h C_a \left(\frac{2D}{y}\right)^Z U_*' a_2 \left(\frac{y}{D}\right)^{b_2} dy \quad (2-44)$$

Simplifying Equation (2-44)

$$g_s = \ell_5 h^{m_5} t_5 + \ell_6 h^{m_6} t_6 \quad (2-45)$$

where

$$\ell_5 = \frac{\frac{b_2}{2} \ell_3 \ell_4}{11.6 (b_2 - Z + 1) (2D)^{b_2 - Z + 1}} \quad (2-46)$$

$$m_5 = m_3 + m_4 + (b_2 - Z + 1), \quad (2-47)$$

$$t_5 = t_3 + t_4 \quad (2-48)$$

$$\ell_6 = - \frac{\frac{b_2}{2} \ell_3 \ell_4}{11.6 (b_2 - Z + 1)} \quad (2-49)$$

$$m_6 = m_3 + m_4 \quad (2-50)$$

and

$$t_6 = t_3 + t_4 \quad (2-50a)$$

The average spatial concentration  $C_s$  in the vertical can be calculated as:

$$C_s = \frac{1}{h} \int_{2D}^h C_y dy = \frac{1}{h} \int_{2D}^h C_a \left(\frac{2D}{y}\right)^Z dy \quad (2-51)$$

Simplifying Equation (2-51)

$$C_s h = \ell_7 h^{m_7} t_7 + \ell_8 h^{m_8} t_8 \quad (2-52)$$

where

$$\ell_7 = \frac{\ell_4}{11.6(1-Z) \sqrt{g \ell_1 \ell_2} (2D)^{1-Z}} \quad (2-53)$$

$$m_7 = -\frac{m_1}{2} - \frac{m_2}{2} + m_4 + 1-Z \quad (2-54)$$

$$t_7 = -\frac{t_1}{2} - \frac{t_2}{2} + t_4 \quad (2-55)$$

$$\ell_8 = -\frac{\ell_4}{11.6(1-Z) \sqrt{g \ell_1 \ell_2}} \quad (2-56)$$

$$m_8 = -\frac{m_1}{2} - \frac{m_2}{2} + m_4 \quad (2-57)$$

and

$$t_8 = -\frac{t_1}{2} - \frac{t_2}{2} + t_4 \quad (2-58)$$

## 2.8 Summary

In this chapter, the governing equations of one dimensional sedimentation transients, Equations (2-4) and (2-5), have been developed. These equations assume that: (1) the channel shape is constant, (2) the channel phenomena can be modeled as functions only of the linear dimension along the direction of flow and (3) the hydraulic transients travel much faster than sedimentation transients, so that for the time scale of the latter transients the flow can be considered as steady.

The governing equations form a set of hyperbolic, nonlinear partial differential equations. It is shown that their characteristic equation has two roots, one relating to the travel of small surface disturbances and the other relating to the travel of small bed waves. Consideration of the characteristics show that to be well posed, the problem of sedimentation transients, as defined by Equations (2-4) and (2-5), should have specified the initial conditions, the water-surface level in time at the downstream boundary and the sand-bed level in time at the upstream boundary. The governing equations separately consider the bed load and suspended bed material phases of sediment transport in the channel. These equations involve quantities relating to the resistance and transport phenomena such as  $S_f$ ,  $g_b$ ,  $g_s$ , and  $C_s$ . It is further assumed that the bed material size distribution in the channel is constant during a time interval and is specified a priori, so that the resistance and transport quantities are functions alone of the local depth of flow,  $h$ .

Supplementary equations have been developed expressing these quantities as explicit power functions of  $h$ . These are Equations (2-18), (2-36), (2-45) and (2-52). All the coefficients and power indices in these equations are determined from parameters  $k_1$ ,  $a$ ,  $b$ ,  $a_1$  and  $b_1$  that are specified for the alluvial channel flow. The supplementary equations are later used in this report to develop the numerical solution of the governing equations.

## CHAPTER III

## NUMERICAL SOLUTION

## 3.1 Finite Difference Scheme

Equations (2-4) and (2-5) governing the sedimentation transients in sand-bed channels are nonlinear hyperbolic partial differential equations. Herein these equations are numerically solved with a linearized implicit scheme, which is an extension of the implicit scheme described by Richtmyer and Morton [10] and Liggett and Cunge [11].

In this scheme, the functions and their derivatives are defined in the rectangular grid in the x-t plane as follows:

$$f(x,t) = \frac{\delta}{2} [f_{j+1}^{n+1} + f_j^{n+1}] + \frac{(1-\delta)}{2} [f_{j+1}^n + f_j^n] \quad (3-1)$$

$$\frac{\partial}{\partial t} f(x,t) = \frac{1}{2\Delta t} \left[ (f_{j+1}^{n+1} - f_{j+1}^n) + (f_j^{n+1} - f_j^n) \right] \quad (3-2)$$

$$\frac{\partial}{\partial x} f(x,t) = \frac{\delta}{\Delta x} [f_{j+1}^{n+1} - f_j^{n+1}] + \frac{(1-\delta)}{\Delta x} [f_{j+1}^n - f_j^n] \quad (3-3)$$

where  $f(x,t)$  is a function of  $x$  and  $t$  (e.g. the local bed level  $z$ );  $\Delta x$  and  $\Delta t$  are the discretization interval along the  $x$  and  $t$  axes, respectively;  $\delta$  is the weighting factor of the scheme, the superscript  $n$  refers to the time step and the subscript  $j$  to the space step (see Figure 3-1).

To linearize the difference equations, the functions at time step  $(n+1)$  are expressed as

$$f_j^{n+1} = f_j^n + \Delta f_j \quad (3-4)$$

where

$$\Delta f_j / f_j^n \ll 1$$

so that

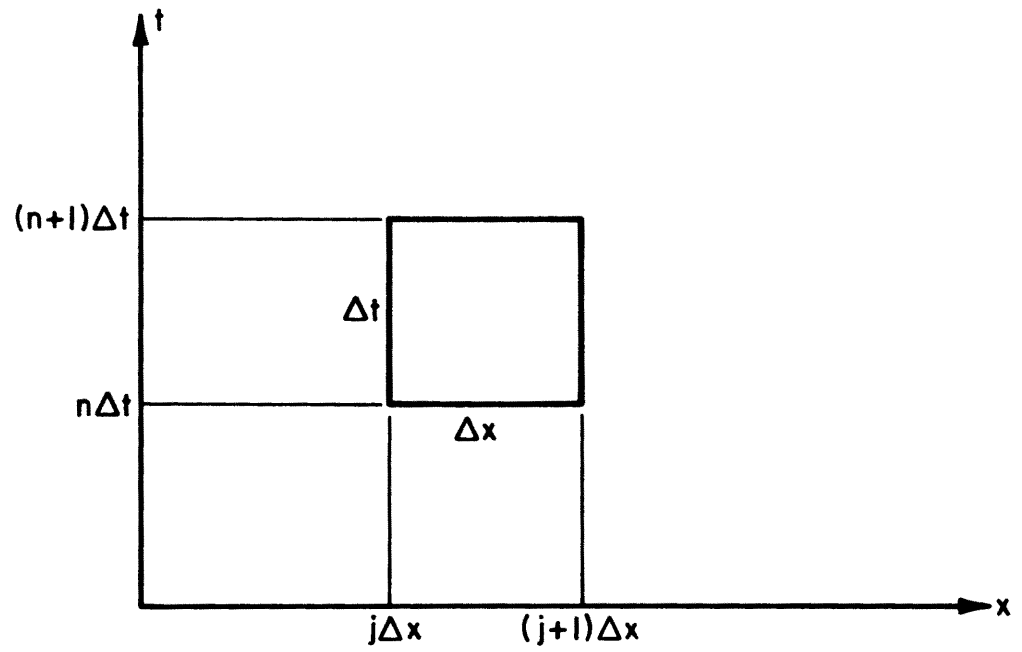


Fig. 3.1 Definition Sketch for the Finite Difference Scheme.

$$\left(f_j^{n+1}\right)^\alpha = \left(f_j^n\right)^\alpha + \alpha \left(f_j^n\right)^{\alpha-1} \Delta f_j \quad (3-5)$$

where  $\alpha$  is an exponent.

### 3.2 Discretization of the Equation for Bed Material Continuity

Equation (2-5) together with the supplementary equations developed in Chapter II, can be expressed as

$$\begin{aligned} \frac{\partial}{\partial x} \left( \sum_{i=4,5,6} \rho_i h_i^{m_i} B_i^{t_i} \right) + \frac{\partial}{\partial t} \left( \sum_{i=7,8} \rho_i h_i^{m_i} B_i^{t_i} \right) \\ + P_* \frac{\partial z}{\partial t} + \frac{1}{B} \frac{\partial B}{\partial x} \left( \sum_{i=4,5,6} \rho_i h_i^{m_i} B_i^{t_i} \right) = 0 \end{aligned} \quad (3-6)$$

The discretization of Equation (3-6) according to Equations (3-1) through (3-5) results in:

$$A_{*j} \Delta y_j + B_{*j} \Delta y_{j+1} + C_{*j} \Delta z_j + D_{*j} \Delta z_{j+1} - Q_{*j} = 0 \quad (3-7)$$

where

$$\begin{aligned} A_{*j} = & -\frac{\delta}{\Delta x} \left( \sum_{i=4,5,6} H_{ij} + \sum_{i=5,6} I_{ij} + J_{5j} \right) \\ & + \frac{1}{2\Delta t} \left( \sum_{i=7,8} H_{ij} + \sum_{i=7,8} I_{ij} + J_{7j} \right) \\ & + \frac{\delta}{2} \frac{B'_j}{B_j} \left( \sum_{i=4,5,6} H_{ij} + \sum_{i=5,6} I_{ij} + J_{5j} \right) \end{aligned} \quad (3-8)$$

$$\begin{aligned} B_{*j} = & \frac{\delta}{\Delta x} \left( \sum_{i=4,5,6} H_{i,j+1} + \sum_{i=5,6} I_{i,j+1} + J_{5,j+1} \right) \\ & + \frac{1}{2\Delta t} \left( \sum_{i=7,8} H_{i,j+1} + \sum_{i=7,8} I_{i,j+1} + J_{7,j+1} \right) \\ & + \frac{\delta}{2} \frac{B'_{j+1}}{B_{j+1}} \left( \sum_{i=4,5,6} H_{i,j+1} + \sum_{i=5,6} I_{i,j+1} + J_{5,j+1} \right) \end{aligned} \quad (3-9)$$

$$C_{*j} = \frac{P_*}{2\Delta t} - A_{*j} \quad (3-10)$$

$$D_{*j} = \frac{P_*}{2\Delta t} - B_{*j} \quad (3-11)$$

$$Q_{*j} = -\frac{1}{\Delta x} \left( \sum_{i=4,5,6} L_{i,j+1} - \sum_{i=4,5,6} L_{i,j} \right) - \frac{1}{2} \left[ \left( \frac{B'_{j+1}}{B_{j+1}} \right) \left( \sum_{i=4,5,6} L_{i,j+1} \right) + \left( \frac{B'_j}{B_j} \right) \left( \sum_{i=4,5,6} L_{i,j} \right) \right] \quad (3-12)$$

$$H_{i,j} = (\ell_{i,j}^n) (m_{i,j}^n) (h_j^n)^{m_{i,j}^n - 1} (B_j)^{t_i} \quad (3-13)$$

$$I_{i,j} = (\nabla \ell_{i,j}^n) (h_j^n)^{m_{i,j}^n} (B_j)^{t_i} \quad (3-14)$$

$$J_{i,j} = (\nabla m_{i,j}^n) (\ell_{i,j}^n) (h_j^n)^{m_{i,j}^n} \ln(h_j^n) (B_j)^{t_i} \quad (3-14a)$$

$$L_{i,j} = (\ell_{i,j}^n) (h_j^n)^{m_{i,j}^n} (B_j)^{t_i} \quad (3-15)$$

$$B'_j = \frac{\partial B_j}{\partial x} = \frac{B_{j+1} - B_j}{\Delta x} \quad (3-16)$$

$$\nabla \ell_{5j}^n = \frac{m_o \ell_{5j}^n Z_j^n}{h_j^n (b_2 + 1 - Z_j^n)} [(b_2 + 1 - Z_j^n) \ln(2D) + 1] \quad (3-17)$$

$$\nabla m_{5j}^n = -\frac{m_o Z_j^n}{h_j^n} \quad (3-17a)$$

$$\nabla \ell_{6j}^n = \frac{m_o \ell_{6j}^n Z_j^n}{h_j^n (b_2 + 1 - Z_j^n)} \quad (3-18)$$

$$\nabla \ell_{7j}^n = \frac{m_o \ell_{7j}^n Z_j^n}{h_j^n (1 - Z_j^n)} [(1 - Z_j^n) \ln(2D) + 1] \quad (3-19)$$

$$\nabla m_{7j}^n = \nabla m_{5j}^n \quad (3-19a)$$

$$\nabla \ell_8^n = \frac{m_o \ell_8^n Z_j^n}{h_j^n (1 - Z_j^n)} \quad (3-20)$$

$$Z_j^n = \ell_o (h_j^n)^{m_o} (B_j)^{t_o} \quad (3-21)$$

$$\ell_o = \frac{w}{\kappa (g \ell_2)^{1/2}} \quad (3-22)$$

$$m_o = -\frac{1}{2} (m_2 + 1) \quad (3-23)$$

$$t_o = -\frac{1}{2} t_2 \quad (3-24)$$

### 3.3 Discretization of the Equation of Motion

Equation 2-4 can be expressed as

$$\frac{Q^2}{2g} \frac{\partial}{\partial x} (Bh)^{-2} + \frac{\partial y}{\partial x} + \ell_2 h^{m_2} B^{t_2} = 0 \quad (3-25)$$

The discretization of Equation (3-25) according to Equations (3-1) through (3-5) results in:

$$E_{*j} \Delta y_j + F_{*j} \Delta y_{j+1} + G_{*j} \Delta z_j + H_{*j} \Delta z_{j+1} - R_{*j} = 0 \quad (3-26)$$

where

$$E_{*j} = -\frac{\delta}{\Delta x} [1 - (F_j^n)^2] + \frac{\delta}{2} H_{2j} \quad (3-27)$$

$$F_{*j} = \frac{\delta}{\Delta x} [1 - (F_{j+1}^n)^2] + \frac{\delta}{2} H_{2j+1} \quad (3-28)$$

$$G_{*j} = \frac{\delta}{\Delta x} [- (F_j^n)^2] - \frac{\delta}{2} H_{2j} \quad (3-29)$$

$$H_{*j} = \frac{\delta}{\Delta x} [+ (F_{j+1}^n)^2] - \frac{\delta}{2} H_{2j+1} \quad (3-30)$$

$$R_{*j} = - \left[ \frac{1}{2\Delta x} \{ (F_{j+1}^n)^2 (h_{j+1}^n) - (F_j^n)^2 (h_j^n) \} \right. \\ \left. + \frac{1}{\Delta x} (y_{j+1}^n - y_j^n) + \frac{1}{2} (L_{2j+1} + L_{2j}) \right] \quad (3-31)$$

$$F_j^n = \frac{Q}{[g(h_j^n)^3]^{1/2} B_j} \quad (3-32)$$

$$H_{2,j} = \ell_2 m_2 (h_j^n)^{m_2 - 1} (B_j)^{t_2} \quad (3-33)$$

$$L_{2,j} = \ell_2 (h_j^n)^{m_2} (B_j)^{t_2} \quad (3-34)$$

Equations (3-7) and (3-26) form a set of simultaneous linear equations in four unknowns  $\Delta y_j$ ,  $\Delta y_{j+1}$ ,  $\Delta z_j$  and  $\Delta z_{j+1}$  relating to spatial points  $j$  and  $j+1$ . All the coefficients in these equations are functions of quantities explicitly known for spatial point  $j$  and  $j+1$  at time step  $n$ . Evaluation of  $\Delta y_j$ ,  $\Delta y_{j+1}$ ,  $\Delta z_j$  and  $\Delta z_{j+1}$  at time step  $n$ , allows the solution at points  $j$  and  $j+1$  to be advanced to time step  $n+1$  through Equation (3-4). If the channel reach being modeled is divided into  $(N-1)$  segments, there are  $N$  spatial points and there are  $2N$  unknown  $\Delta y$ 's and  $\Delta z$ 's as  $\Delta y_i$ ,  $\Delta z_i$ ,  $i=1,2,\dots,N$ . The number of equations (3-7 and 3-26) available for the discretized channel reach is  $2(N-1)$ . Two additional equations connecting  $\Delta y$ 's and  $\Delta z$ 's are therefore required to evaluate the  $2N$   $\Delta y$ 's and  $\Delta z$ 's. These additional equations are provided by the two boundary conditions.

### 3.4 Boundary Conditions

As discussed in Section 2.3, the mathematical problem of sedimentation transients in subcritical flow should have the following boundary conditions specified in addition to the initial values:

1. At the upstream boundary  
 $z(1,t), 0 \leq t \leq T$
2. At the downstream boundary  
 $y(N,t), 0 \leq t \leq T$

As shown subsequently, the change in the bed and water surface levels at a vertical  $j$ , over one time step  $n\Delta t$  to  $(n+1)\Delta t$  can be related as

$$\Delta y_j = S_{*j} \Delta z_j + T_{*j} \quad (3-35)$$

where  $\Delta y_j = y_j^{n+1} - y_j^n$ ,  $\Delta z_j = z_j^{n+1} - z_j^n$  and  $S_{*j}$  and  $T_{*j}$  are constants for a given time step. Equation (3-35) with appropriate values of  $S_{*j}$  and  $T_{*j}$  for  $j=1$  and  $N$  provides the two boundary conditions.

In practice the upstream boundary condition is generally available as the bed material load hydrograph or less frequently as the bed level hydrograph. The downstream boundary condition, however, depends on the physical constraint of the problem. For example, the downstream control may be the water surface level of the channel. The treatment of Equation (3-35) for these cases is illustrated below.

Upstream bed material load hydrograph: At any point in the channel,  $0 \leq x \leq L$ , supplementary equations (2-36) and (2-45) give

$$g_t = (g_b + g_s) = \sum_{i=4,5,6} \lambda_i h_i^{m_i} B_i^{t_i} \quad (3-36)$$

It is assumed that at the upstream boundary the flow depth instantaneously adjusts itself so that the transport past the boundary is equal to the bed material inflow. At two consecutive time steps,

$$g_t^n = \sum_{i=4,5,6} \lambda_i^n (h_1^n)^{m_i^n} (B_1)^{t_i} \quad (3-37)$$

and

$$g_t^{n+1} = \sum_{i=4,5,6} \lambda_i^{n+1} (h_1^{n+1})^{m_i^{n+1}} (B_1)^{t_i} \quad (3-38)$$

where  $g_t$  is the bed material inflow at the upstream boundary and superscripts  $n$  and  $n+1$  relate to the time step  $n\Delta t$  and  $(n+1)\Delta t$ , respectively. In Equation (3-38),  $h_1^{n+1}$  can be solved by iterative procedures, so that

$$\Delta h_1 = h_1^{n+1} - h_1^n = \Delta y_1 - \Delta z_1$$

The boundary condition, Equation (3-35) is then specified with

$$S_{*1} = 1$$

and

$$T_{*1} = \Delta h_1$$

Upstream bed level hydrograph: If the upstream bed level is specified as the boundary condition,

$$\Delta z_1 = z_1^{n+1} - z_1^n$$

is known at every time step. Then, Equation (3-35) is specified for this condition with  $S_{*1} =$  a very large number, say  $10^6$  and

$$T_{*1} = -S_{*1} \Delta z_1.$$

Downstream water surface-level hydrograph: The problem of specifying the downstream boundary condition is somewhat simpler. As shown subsequently (refer Equations (3-40), (3-41)), the values of  $S_{*N}$  and  $T_{*N}$  are available in the solution algorithm. The value of  $\Delta y_N$  is known at each time step from the water surface-level hydrograph available at the downstream boundary. Equation (3-35) is then specified for the calculated  $S_{*N}$  and  $T_{*N}$  and the available  $\Delta y_N$ .

### 3.5 Solution Algorithm

The following system of  $2N$  linear equations is available to solve for  $2N$  unknowns:

Equation 3-35	Upstream Boundary Condition	1 grid point
Equation 3-7	Equation of Bed Material Continuity	$N-1$ grid spaces
Equation 3-26	Equation of Motion	$N-1$ grid spaces
Equation 3-35	Downstream Boundary Condition	1 grid point
Unknowns:	$\Delta y_j, \Delta z_j, j = 1, 2, \dots, N.$	

The coefficient matrix for this set is a sparse diagonal matrix and is economically solved by the double sweep algorithm.

In the first sweep, the algorithm calculates three internal vectors  $T_{*j}$ ,  $S_{*j}$  and  $U_{*j}$ ,  $j = 2, 3, \dots, N$  with the following recursive equations:

$$U_{*j} = \frac{E_{*j-1} S_{*j-1} + G_{*j-1}}{A_{*j-1} S_{*j-1} + C_{*j-1}} \quad (3-39)$$

$$T_{*j} = \frac{(R_{*j-1} - E_{*j-1} T_{*j-1}) - U_{*j} (Q_{*j-1} - A_{*j-1} T_{*j-1})}{F_{*j-1} - U_{*j} B_{*j-1}} \quad (3-40)$$

$$S_{*j} = - \frac{H_{*j-1} - U_{*j} D_{*j-1}}{F_{*j-1} - U_{*j} B_{*j-1}} \quad (3-41)$$

where the vectors  $A_*$ ,  $B_*$ ,  $C_*$ ,  $D_*$ ,  $E_*$ ,  $F_*$ ,  $G_*$ ,  $H_*$ ,  $Q_*$  and  $R_*$  are coefficients defined for Equations (3-7) and (3-26) and elements  $S_{*1}$  and  $T_{*1}$  are available from the upstream boundary condition, Equation (3-35).

In the second sweep,  $\Delta z$  and  $\Delta y$  are calculated from  $J = (N-1)$ , to  $J = 1$  by the following equation:

$$\Delta z_j = \frac{(Q_j^* - A_j^* T_j^*) - (B_j^* \Delta y_{j+1} + D_j^* \Delta z_{j+1})}{A_j^* S_j + C_j^*} \quad (3-42)$$

and

$$\Delta y_j = S_j^* \Delta z_j + T_j^* \quad (3-43)$$

where  $\Delta y_N$  and  $\Delta z_N$  are available from the downstream boundary condition, Equation (3-35).

Equations (3-42) to Equation (3-43) enable the calculation of the solution vectors of the system,  $\Delta y(N)$  and  $\Delta z(N)$  and the water surface and bed levels at time step  $(n+1)\Delta t$  are calculated by Equation (3-4) as

$$y_j^{n+1} = y_j^n + \Delta y_j, \quad j = 1, 2, \dots, N \quad (3-44)$$

$$z_j^{n+1} = z_j^n + \Delta z_j, \quad j = 1, 2, \dots, N \quad (3-45)$$

The solution can then be advanced to time  $(n+2)\Delta t$  by using values (3-44) and (3-45) as the initial conditions.

## CHAPTER IV

## STABILITY AND CONVERGENCE

## 4.1 Introduction

The numerical solution of the set of nonlinear partial differential equations, Equations (2-4) and (2-5), raises valid questions of stability and convergence. Stability is the property of the numerical scheme that assures that no part of the solution will grow in time without limit until it destroys the calculations. Convergence is tested by the ability of the scheme to reproduce the terms of the differential equations without introducing extraneous terms which are large enough to affect the solution.

There is no existing theory for analyzing the stability and convergence of numerical schemes for nonlinear partial differential equations. However, the experience of other workers and results of their numerical experiments [11] show that the small perturbation analysis may be applied to the system of linearized partial differential equations and its finite difference analog. This allows the estimation of the domain of stability and the convergence properties of the scheme.

In this chapter, the diffusion and dispersion characteristics of the governing equations (2-4) and (2-5) are studied for small amplitude perturbations. This is followed by a similar analysis of the finite difference equations based on the difference scheme adopted in Chapter III. The comparison of the two systems is used to study the convergence of the finite difference scheme.

## 4.2 Linearization of the Governing Equations

Equation (2-4) can be written as:

$$(1 - F^2) \frac{\partial y}{\partial x} + F^2 \frac{\partial z}{\partial x} - F^2 \frac{(y-z)}{B} \frac{\partial B}{\partial x} + S_f = 0 \quad (4-1)$$

Similarly Equation (2-5) taken together with the supplementary equations developed in Chapter II, can be written as:

$$\begin{aligned} & \left[ \sum_{i=4,5,6} (B^{t_i} \ell_i^{m_i} h^{m_i-1}) + \sum_{i=5,6} (B^{t_i} h^{m_i} \frac{\partial \ell_i}{\partial h}) + B^{t_5} \ell_5^{m_5} \ln(h) \frac{\partial m_5}{\partial h} \right] \frac{\partial h}{\partial x} \\ & + \left[ \sum_{i=7,8} (B^{t_i} \ell_i^{m_i} h^{m_i-1}) + \sum_{i=7,8} (B^{t_i} h^{m_i} \frac{\partial \ell_i}{\partial h}) \right. \\ & \left. + B^{t_7} \ell_7^{m_7} \ln(h) \frac{\partial m_7}{\partial h} \right] \frac{\partial h}{\partial t} + (1-p) S_s \gamma_w \frac{\partial z}{\partial t} \\ & + \left[ \sum_{i=4,5,6} \{ B^{t_i-1} \ell_i^{m_i} (1+t_i) h^{m_i} \} \right] \frac{\partial B}{\partial x} = 0 \end{aligned} \quad (4-2)$$

Defining

$$\tilde{H}_i = B^{t_i} \ell_i^{m_i} h^{m_i-1} \quad (4-3)$$

$$\tilde{I}_i = B^{t_i} h^{m_i} \frac{\partial \ell_i}{\partial h} \quad (4-4)$$

$$\tilde{J}_i = B^{t_i} \ell_i^{m_i} \ln(h) \frac{\partial m_i}{\partial h} \quad (4-5)$$

$$\tilde{K}_i = B^{t_i-1} \ell_i^{m_i} (1+t_i) h^{m_i} \quad (4-6)$$

Equation (4-2) can be stated as

$$\begin{aligned}
& \left[ \sum_{i=7,8} \tilde{H}_i + \sum_{i=7,8} \tilde{I}_i + \tilde{J}_7 \right] \frac{\partial y}{\partial t} + \left[ \sum_{i=4,5,6} \tilde{H}_i + \sum_{i=5,6} \tilde{I}_i + \tilde{J}_5 \right] \frac{\partial y}{\partial x} + \\
& \left[ (1-p)S_s \gamma_w - \left( \sum_{i=7,8} \tilde{H}_i + \sum_{i=7,8} \tilde{I}_i + \tilde{J}_7 \right) \right] \frac{\partial z}{\partial t} \\
& \left[ - \left( \sum_{i=4,5,6} \tilde{H}_i + \sum_{i=5,6} \tilde{I}_i + \tilde{J}_5 \right) \right] \frac{\partial z}{\partial x} + \left[ \sum_{i=4,5,6} \tilde{K}_i \right] \frac{\partial B}{\partial x} = 0 \quad (4-7)
\end{aligned}$$

Equations (4-1) and (4-7) are nonlinear in  $h$ . They are linearized around the uniform flow by writing:

$$y = y_o + \eta \quad (4-8)$$

$$z = z_o + \zeta \quad (4-9)$$

$$h = h_o + \eta - \zeta \quad (4-10)$$

where subscript  $o$  refers to the uniform flow condition and perturbations  $\eta \ll y_o$ ,  $\zeta \ll z_o$ , and  $(\eta - \zeta) \ll h_o$ .

In the general case of a variable coefficient  $P_i$  operating on a partial derivative, say  $\partial y / \partial t$ , the perturbations defined in Equations (4-8) through (4-10) will result in the following:

$$P_i \frac{\partial y}{\partial t} = [P_{i_o} + \pi_i] \left[ \frac{\partial y_o}{\partial t} + \frac{\partial \eta}{\partial t} \right] \quad (4-11)$$

$$= P_{i_o} \frac{\partial y_o}{\partial t} + \pi_i \frac{\partial \eta}{\partial t} + \pi_i \frac{\partial y_o}{\partial t} + P_{i_o} \frac{\partial \eta}{\partial t} \quad (4-12)$$

where  $P_{i_o}$  is the value of  $P_i$  associated with uniform flow and  $\pi_i$  is the perturbation in  $P_i$  due to  $\eta$  and  $\zeta$ . The first term in the expansion represents the uniform flow, and it drops out together with the uniform flow components of other terms in the perturbed equation. The second and third terms are dropped because they are of negligible magnitude compared to the remaining terms ( $\pi_i \ll P_{i_o}$ ). Thus the only remaining term on the right hand side in Equation (4-12) is

$P_{i_0} \partial \eta / \partial t$ . Similar reasoning will apply to  $P_i \partial y / \partial x$ ,  $P_i \partial z / \partial t$ ,  $P_i \partial z / \partial x$  and the only terms remaining in the perturbed equations corresponding to these will be  $P_{i_0} \partial \eta / \partial x$ ,  $P_{i_0} \partial \zeta / \partial t$  and  $P_{i_0} \partial \zeta / \partial x$ .

Substituting Equations (4-8) through (4-10) into Equations (4-1) and (4-7), and considering the foregoing simplification based on an order of magnitude analysis, the following system is obtained:

$$\begin{bmatrix} P_1 & P_2 & P_3 - P_1 & -P_2 \\ 0 & P_5 & 0 & 1 - P_5 \end{bmatrix} \begin{bmatrix} \frac{\partial \eta}{\partial t} \\ \frac{\partial \eta}{\partial x} \\ \frac{\partial \zeta}{\partial t} \\ \frac{\partial \zeta}{\partial x} \end{bmatrix} = \begin{bmatrix} -P_4 \\ -P_6 - P_7 \end{bmatrix} (\eta - \zeta) \quad (4-13)$$

where:

$$P_1 = \left[ \sum_{i=7,8} \tilde{H}_{i_0} + \sum_{i=7,8} \tilde{I}_{i_0} + \tilde{J}_{7_0} \right] \quad (4-14)$$

$$P_2 = \left[ \sum_{i=4,5,6} \tilde{H}_{i_0} + \sum_{i=5,6} \tilde{I}_{i_0} + \tilde{J}_{5_0} \right] \quad (4-15)$$

$$P_3 = p_* = (1-p) S_s \gamma_w \quad (4-16)$$

$$P_4 = \left[ \frac{1}{B} \frac{\partial B}{\partial x} \left( \sum_{i=4,5,6} (1+t_i) (\tilde{H}_{i_0}) + \sum_{i=5,6} (1+t_i) (\tilde{I}_{i_0}) \right) \right] \quad (4-17)$$

$$P_5 = 1 - F_o^2 \quad (4-18)$$

$$P_6 = H_{2_0} \quad (4-19)$$

$$P_7 = \frac{1}{B} \frac{\partial B}{\partial x} (2F_o^2) \quad (4-20)$$

and the subscript  $o$  refers to values of the subscripted quantities related to the equilibrium flow condition.

### 4.3 Diffusion and Dispersion Properties of the Differential System

For small perturbations, the linearized system (Equation (4-13)) approximates the behavior of the differential system (Equations (2-4) and (2-5)). The diffusion and dispersion properties of the differential system are therefore inferred in the following from a consideration of the linearized system.

The solution of  $\eta(x,t)$ ,  $\zeta(x,t)$  of Equation (4-13) is assumed to be differentiable at least once for all  $x$  and  $t$  including the boundaries. The solution can be written as a Fourier series:

$$\eta(x,t) = \sum_{m=1}^{\infty} \eta_{0m} \exp[i(\sigma_m x - \beta_m t)] \quad (4-21)$$

$$\zeta(x,t) = \sum_{m=1}^{\infty} \zeta_{0m} \exp[i(\sigma_m x - \beta_m t)] \quad (4-22)$$

where  $i = \sqrt{-1}$ ,  $\sigma_m = 2\pi/L_m$ ,  $L_m$  is the spatial wavelength,  $\beta_m = 2\pi/T_m$ ,  $T_m$  is the wave period, and subscript  $m$  refers to the  $m$ th component. Considering one such component and dropping the subscript, the substitution of Equations (4-21) and (4-22) into Equation (4-13) provides the following homogeneous system:

$$\begin{bmatrix} (P_1\beta - P_2\sigma + P_4i) & (P_3\beta - P_1\beta + P_2\sigma - P_4i) \\ (P_6i + P_7i - P_5\sigma) & (P_5\sigma - \sigma - P_6i - P_7i) \end{bmatrix} \begin{bmatrix} \eta_0 \\ \zeta_0 \end{bmatrix} = \begin{bmatrix} 0 \\ 0 \end{bmatrix} \quad (4-23)$$

For a nontrivial solution the determinant of the coefficient matrix of homogeneous Equation (4-23) must vanish. Accordingly:

$$\beta = - \frac{\sigma[P_2(P_3P_5 - P_1)\sigma^2 + P_3P_4(P_6 + P_7)] + i\sigma^2[P_2P_3(P_6 + P_7) - P_4(P_3P_5 - P_1)]}{(P_3P_5 - P_1)^2\sigma^2 + P_3^2(P_6 + P_7)^2} \quad (4-24)$$

Equation (4-23) shows  $\beta$  is a complex number with the real part

$$\beta_R = \frac{-\sigma[P_2(P_3P_5 - P_1)\sigma^2 + P_3P_4(P_6 + P_7)]}{(P_3P_5 - P_1)^2\sigma^2 + P_3^2(P_6 + P_7)^2} \quad (4-25)$$

and the imaginary part

$$\beta_I = \frac{-\sigma^2[P_2P_3(P_6 + P_7) - P_4(P_3P_5 - P_1)]}{(P_3P_5 - P_1)^2\sigma^2 + P_3^2(P_6 + P_7)^2} \quad (4-26)$$

Considering Equations (4-21) and (4-22), the amplification factor of Equation (4-13) is  $\exp[\beta_I]$  and the celerity of the  $m$ th Fourier component is  $[\beta_R/\sigma]_m$ . Equation (4-26) indicates that generally  $\beta_I \neq 0$  unless  $\frac{\partial B}{\partial x} = 0$  and  $S_f = 0$ . That is the frictional system, Equations (2-4) and (2-5), has a nonvanishing amplification factor. It is relevant to consider the celerity of a small perturbation in the system (Equations (2-4) and (2-5)) as affected by the frictional term and the nonprismatic channel shape. From Equation (4-25), one can define the small perturbation celerity for a frictionless prismatic channel,

$$c_o = \frac{-P_2}{(P_3P_5 - P_1)} \quad (4-27)$$

For a prismatic channel ( $\frac{\partial B}{\partial x} = 0$ ) with nonzero frictional term

$$c_f = \frac{-P_2(P_3P_5 - P_1)\sigma^2}{(P_3P_5 - P_1)^2\sigma^2 + P_3^2P_6^2} \quad (4-28)$$

or

$$c_f = \frac{c_o}{1 + \epsilon_f} \quad (4-29)$$

where

$$\epsilon_f = \frac{P_3P_6}{(P_3P_5 - P_1)\sigma} \quad (4-30)$$

In subcritical sand-bed channel flow generally,  $\epsilon_f < 0$ . For a nonprismatic channel ( $B' \neq 0$ ), with nonzero frictional term,

$$c_{fB} = \frac{c_o}{1 + \epsilon_{fB}} [1 + \epsilon_{fB} \epsilon_B] \quad (4-31)$$

where

$$\epsilon_{fB} = \epsilon_f \left[ 1 + \frac{P_7}{P_6} \right] \quad (4-32)$$

and

$$\epsilon_B = \frac{P_4}{P_2 \sigma} \quad (4-33)$$

From Equations (4-27) through (4-33), the following conclusions can be derived about the celerity of a small perturbation in the differential system (Equations (2-4) and (2-5)):

1. The celerity  $c_o$  in a prismatic, frictionless system increases as the rate of change of transport with the depth of flow ( $g_t'$ ), increases in absolute magnitude (smaller bed material size, etc.). Also  $c_o$  is independent of wave length.
2. The effect of frictional term ( $S_f$ ) is to decrease the celerity of a small perturbation. The correction  $\epsilon_f$  (Equation (4-29)) depends on the wave length of the perturbation and is larger in absolute magnitude for longer waves than for the shorter waves.
3. For a nonprismatic channel, the effect of  $B' \neq 0$  is to change  $\epsilon_f$  as well as to introduce another correction (Equation (4-31)). For a contracting subcritical flow sand-bed channel ( $B' < 0$ ), the celerity will generally be greater than for a corresponding prismatic channel.

4. In a frictionless system, small perturbations will travel without dispersion (Equation (4-27)). However in a frictional and nonprismatic system, dispersion of the waves is experienced. The absolute magnitude of both  $\epsilon_f$  and  $\epsilon_B$  increase with increasing wavelength of the component wave.

The effect of frictional and nonprismatic terms on the damping factor  $\exp[\beta_I]$  can be similarly studied by considering Equation (4-26). Rewriting this equation

$$(\beta_I)_{fB} = \frac{c_o \sigma}{1 + \epsilon_{fB}} [\epsilon_{fB} - \epsilon_B] \quad (4-34)$$

where all these terms have been previously defined. For a prismatic channel,  $P_4 = 0$ ,  $P_7 = 0$ ,  $\epsilon_B = 0$ , and  $\epsilon_{fB} = \epsilon_f$ , so that

$$(\beta_I)_f = \frac{c_o \sigma \epsilon_f}{1 + \epsilon_f} \quad (4-35)$$

and for a nonfrictional, prismatic channel,  $\epsilon_f = 0$ ,

$$(\beta_I)_o = 0 \quad (4-36)$$

Equations (4-34) through (4-36) show:

1. In a prismatic nonfrictional system the perturbations  $\eta$  and  $\zeta$  will not be amplified or damped.
2. For a subcritical flow in a prismatic sand-bed channel,  $\epsilon_f < 0$  and therefore  $\beta_I$  is negative, so that all wave components of the perturbations will be damped. The damping factor  $\exp[\beta_I]$  also depends on the wavelength, so that shorter wavelength components will be damped more than the longer wavelengths.

3. For a large enough positive value of  $B'$  (expanding channel),  $(\beta_I)_{fB}$  could become positive, so that the perturbation  $\eta$  and  $\zeta$  will be amplified.

#### 4.4 Diffusion and Dispersion Functions for the Difference System

Using the small perturbation linearized approximation (Equation (4-13)) to the differential system (Equations (2-4) and (2-5)) the diffusion and dispersion functions are developed for the difference scheme used herein. The discretization scheme of Equations (3-1) through (3-5) applied to Equation (4-13) yields:

$$\begin{aligned}
& \frac{P_1}{2\Delta t} [\eta_{j+1}^{n+1} - \eta_{j+1}^n + \eta_j^{n+1} - \eta_j^n] + \frac{P_2}{\Delta x} [\delta(\eta_{j+1}^{n+1} - \eta_j^{n+1}) + (1-\delta)(\eta_{j+1}^n - \eta_j^n)] \\
& + \frac{(P_3 - P_1)}{2\Delta t} [\zeta_{j+1}^{n+1} - \zeta_{j+1}^n + \zeta_j^{n+1} - \zeta_j^n] \\
& - \frac{P_1}{\Delta x} [\delta(\zeta_{j+1}^{n+1} - \zeta_j^{n+1}) + (1-\delta)(\zeta_{j+1}^n - \zeta_j^n)] \\
& + \frac{P_4}{2} \{ [\delta(\eta_{j+1}^{n+1} + \eta_j^{n+1}) + (1-\delta)(\eta_{j+1}^n + \eta_j^n)] \\
& - [\delta(\zeta_{j+1}^{n+1} + \zeta_j^{n+1}) + (1-\delta)(\zeta_{j+1}^n + \zeta_j^n)] \} = 0 \tag{4-37}
\end{aligned}$$

$$\begin{aligned}
& \frac{P_5}{\Delta x} [\delta(\eta_{j+1}^{n+1} - \eta_j^{n+1}) + (1-\delta)(\eta_{j+1}^n - \eta_j^n)] \\
& + \frac{(1-P_5)}{\Delta x} [\delta(\zeta_{j+1}^{n+1} - \zeta_j^{n+1}) + (1-\delta)(\zeta_{j+1}^n - \zeta_j^n)] \\
& + \frac{(P_6 + P_7)}{2} \{ [\delta(\eta_{j+1}^{n+1} + \eta_j^{n+1}) + (1-\delta)(\eta_{j+1}^n + \eta_j^n)] \\
& - [\delta(\zeta_{j+1}^{n+1} + \zeta_j^{n+1}) + (1-\delta)(\zeta_{j+1}^n + \zeta_j^n)] \} = 0 \tag{4-38}
\end{aligned}$$

Let the solution of Equations (4-37) and (4-38) be expressed as a Fourier series for a time and space grid point  $t = n\Delta t$  and  $x = j\Delta x$  as:

$$\eta_j^n = \sum_{m=1}^{\infty} \eta_{om} \exp[i(\sigma_m j\Delta x - \beta_m n\Delta t)] \quad (4-39)$$

$$\zeta_j^n = \sum_{m=1}^{\infty} \zeta_{om} \exp[i(\sigma_m j\Delta x - \beta_m n\Delta t)] \quad (4-40)$$

In Equations (4-39) and (4-40)  $\sigma_n (= 2\pi/L_m)$  and  $\beta_m (= 2\pi/T_m)$  are the wavelength and wave period for the  $m$ th Fourier component and in general  $\beta_m$  is complex. Considering one such component and dropping the subscript  $m$ , substitution of Equations (4-39) and (4-40) into (4-37) and (4-38) yields:

$$\begin{aligned} & \{P_1[\exp(-i\beta\Delta t)-1] + P_2 r i \tan\alpha[\delta\{\exp(-i\beta\Delta t)-1\}+1] \\ & + P_4\Delta t[\delta\{\exp(-i\beta\Delta t)-1\} + 1]\} \eta_o \\ & + \{(P_3-P_1)[\exp(-i\beta\Delta t)-1]-P_2 r i \tan\alpha[\delta\{\exp(-i\beta\Delta t)-1\} + 1] \\ & - P_4\Delta t[\delta\{\exp(-i\beta\Delta t)-1\} + 1]\} \zeta_o = 0 \end{aligned} \quad (4-41)$$

$$[iP_5 \tan\alpha + \frac{(P_6+P_7)\Delta x}{2}] \eta_o + [i(1-P_5) \tan\alpha - \frac{(P_6+P_7)\Delta x}{2}] \zeta_o = 0 \quad (4-42)$$

where

$$\alpha = \frac{\sigma\Delta x}{2} \quad (4-43)$$

and

$$r = \frac{2\Delta t}{\Delta x} \quad (4-44)$$

Equations (4-41) and (4-42) constitute a homogeneous system of algebraic equations in  $\eta_o$  and  $\zeta_o$ . For a nontrivial solution, the

determinant of the coefficient matrix should identically vanish. This condition yields:

$$\exp(-i\beta\Delta t) = 1 - \frac{(N-iQ)(M+N\delta) - i(N-iQ)(P-Q\delta)}{(M+N\delta)^2 + (P-Q\delta)^2} \quad (4-45)$$

where

$$M = \frac{P_3(P_6+P_7)\Delta x}{2} \quad (4-46)$$

$$N = P_2 r \tan^2 \alpha \quad (4-47)$$

$$P = (P_3 P_5 - P_1) \tan \alpha \quad (4-48)$$

$$Q = P_4 \Delta t \tan \alpha \quad (4-49)$$

Dividing Equation (4-45) by  $(P-Q\delta)^2$ :

$$\exp(-i\beta\Delta t) = 1 - \frac{(ST-U) - i(US+T)}{1+S^2} \quad (4-50)$$

where

$$S = \frac{M+N\delta}{P-Q\delta} \quad (4-51)$$

$$T = \frac{N}{P-Q\delta} \quad (4-52)$$

$$U = \frac{Q}{P-Q\delta} \quad (4-53)$$

Expressing the complex  $\beta$  as

$$\beta = \beta_R + i\beta_I \quad (4-54)$$

and separating Equation (4-50) into the real and imaginary components:

$$\exp(\beta_I \Delta t) \cos(\beta_R \Delta t) = \frac{1 + S^2 - ST + U}{(1+S^2)} \quad (4-55)$$

and

$$\exp(\beta_I \Delta t) \sin(\beta_R \Delta t) = - \frac{(US + T)}{1+S^2} \quad (4-56)$$

From Equations (4-55) and (4-56),

$$\tan(\beta_R \Delta t) = \frac{-(US + T)}{1+S^2-ST+U} \quad (4-57)$$

$$\sin(\beta_R \Delta t) = \frac{-(US+T)}{[(1+S^2-ST+U)^2 + (US+T)^2]^{1/2}} \quad (4-58)$$

and

$$\exp(\beta_I \Delta t) = \frac{[1+S^2-ST+U]^2 + (US+T)^2]^{1/2}}{1+S^2} \quad (4-59)$$

Equations (4-57) and (4-59), express the dispersion and diffusion functions for the finite difference analog of the linearized system (Equation (4-13)). The celerity of a Fourier component of solution Equations (4-39), (4-40) is given by  $\beta_R/\sigma$  and the amplification factor at time  $\Delta t$  is given by  $\exp[\beta_I \Delta t]$ . These functions are next used in studying the convergence ratios of the difference analog.

#### 4.5 Convergence Ratios

In the previous two sections, the diffusion and dispersion characteristics of the differential system (Equations (2-4) and (2-5)) have been developed for its linearized version (Equation (4-13)) and for the finite difference analog of Equation (4-13) based on the implicit difference scheme (Equations (3-1) through (3-5)). It is of considerable interest to study the closeness with which the finite difference analog represents the diffusion and dispersion characteristics of the differential system. Of necessity, this study can only be made approximately, in terms of the linearized system (Equation (4-13)) that is valid for small perturbations only. Two convergence ratios for one time step  $\Delta t$  are defined as:

$$R_1 = \frac{\text{wave damping in the finite difference system}}{\text{wave damping in the linearized differential system}}$$

and

$$R_2 = \frac{\text{wave celerity in the finite difference system}}{\text{wave celerity in the linearized differential system}}$$

From the results developed in Section 4.2 and 4.3, these ratios are:

$$R_1 = \frac{\exp(\beta_I \Delta t)}{\exp(\beta_I t)} \quad (4-60)$$

$$R_2 = \frac{B_R / \sigma}{c} \quad (4-61)$$

where  $t = \Delta t$ .

Substituting Equations (4-34) and (4-59) into Equation (4-60):

$$R_1 = \frac{[(1+S^2-ST+U)^2 + (US+T)^2]^{1/2}}{(1+S^2) \exp\left[\left(\frac{c_o \sigma \Delta t}{2}\right) (\epsilon_{fB} - \epsilon_B)\right]} \quad (4-62)$$

Similarly substituting Equation (4-31) and (4-57) into Equation (4-61):

$$R_2 = \frac{\tan^{-1}\left[\frac{-(US+T)}{1+S^2-ST+U}\right]}{\left(\frac{c_o \sigma \Delta t}{2}\right) (1+\epsilon_{fB} \epsilon_B)} \quad (4-63)$$

These ratios are next analyzed for frictional and nonfrictional systems.

#### 4.6 Convergence Ratios for Prismatic Frictionless Systems

The simplest case of the differential system is that of a prismatic, frictionless channel, that does not experience any dissipation or dispersion of the bed and water surface perturbations. For such a system:

$$\epsilon_{fB} = \epsilon_B = 0 \quad (4-64)$$

$$P_4 = P_6 = P_7 \equiv 0 \quad (4-65)$$

$$M = Q = U \equiv 0 \quad (4-66)$$

and Equations (4-62) and (4-63) simplify to:

$$R_1 = \frac{\left[ \left( 1 + \frac{N^2 \delta^2}{P^2} - \frac{N^2 \delta}{P^2} \right)^2 + \left( \frac{N}{P} \right)^2 \right]^{1/2}}{\left( 1 + \frac{N^2 \delta^2}{P^2} \right)} \quad (4-67)$$

$$R_2 = \frac{1}{\sigma \Delta t c_o} \tan^{-1} \left[ \frac{-\frac{N}{P}}{1 + \frac{N^2 \delta^2}{P^2} - \frac{N^2 \delta}{P^2}} \right] \quad (4-68)$$

From Equations (4-27), (4-47) and (4-48):

$$\frac{N}{P} = -c_o r \tan \alpha \quad (4-69)$$

so that

$$R_1 = \frac{\{ [1 + \delta(\delta-1)(c_o r \tan \alpha)^2]^2 + (c_o r \tan \alpha)^2 \}^{1/2}}{1 + (\delta c_o r \tan \alpha)^2} \quad (4-70)$$

$$R_2 = \frac{1}{\alpha c_o r} \tan^{-1} \left[ \frac{c_o r \tan \alpha}{1 + \delta(\delta-1)(c_o r \tan \alpha)^2} \right] \quad (4-71)$$

Equations (4-70) and (4-71) indicate that the convergence ratios are functions of dimensionless parameters  $c_o r$ ,  $\alpha$  and  $\delta$ . Also these ratios are expressed in terms of one time step  $\Delta t$ . As parameters  $c_o r$  and  $\alpha$  vary with a varying  $\Delta t$ , it is necessary to adopt a fixed typical time span over which the convergence ratios are studied. After Leendertse [12], the time  $T_L$  required for a wave to travel its original wavelength, is taken as such a time span. The number of time steps,  $N$ , contained in  $T_L$  is

$$N = \frac{L}{c_o \Delta T} = \frac{2\pi}{\alpha c_o r} \quad (4-72)$$

Based on the values of parameters  $c_o r$ ,  $\alpha$  and  $\delta$  used at the first time step, the cumulative product of the convergence ratios at time  $T_L$  are given as

$$R_{1*} = (R_1)^N \quad (4-73)$$

and

$$R_{2*} = (R_2)^N \quad (4-74)$$

Inspection of Equations (4-70) and (4-71) shows that for  $c_o r = 2$  and  $\delta = 0.5$ , the convergence ratios  $R_{1*}$  and  $R_{2*}$  are identically equal to 1. The variation of  $R_{1*}$  and  $R_{2*}$  with parameters  $c_o r$ ,  $\delta$  and  $\alpha$  is shown in Figure 4.1(a) through (c) for  $\alpha = \pi/40$ ,  $\pi/100$  and  $\pi/400$ . The results of these figures can be interpreted as:

1. The convergence ratio  $R_{1*}$  is greater than 1.0 for  $0 \leq \delta < 0.5$  for all values of  $c_o r$  and  $\alpha$ . Any perturbations resulting from truncations errors, etc., will therefore grow in time for this range of  $\delta$ . The finite difference analog is thus unstable for  $\delta < 0.5$  and this range should be avoided. In practice, the nonlinear systems always generate some high frequency perturbations [10] that can lead to instabilities unless some damping ( $R_{1*} < 1$ ) is provided in the finite difference analog. Therefore, a value of  $\delta > 0.5$  is necessary to assure the stability of the scheme.
2. A value of  $c_o r = 2$  provides a value of  $R_{1*} = R_{2*} = 1$  for  $\delta = 0.5$  and for all values of  $\alpha$  less than  $\pi/2$ . For other values of  $c_o r$ , ratios  $R_{1*}$  and  $R_{2*}$  are closest to 1 at different values of  $\delta$ . Physically,  $c_o r = 2$  amounts to following the perturbation along a characteristic direction.

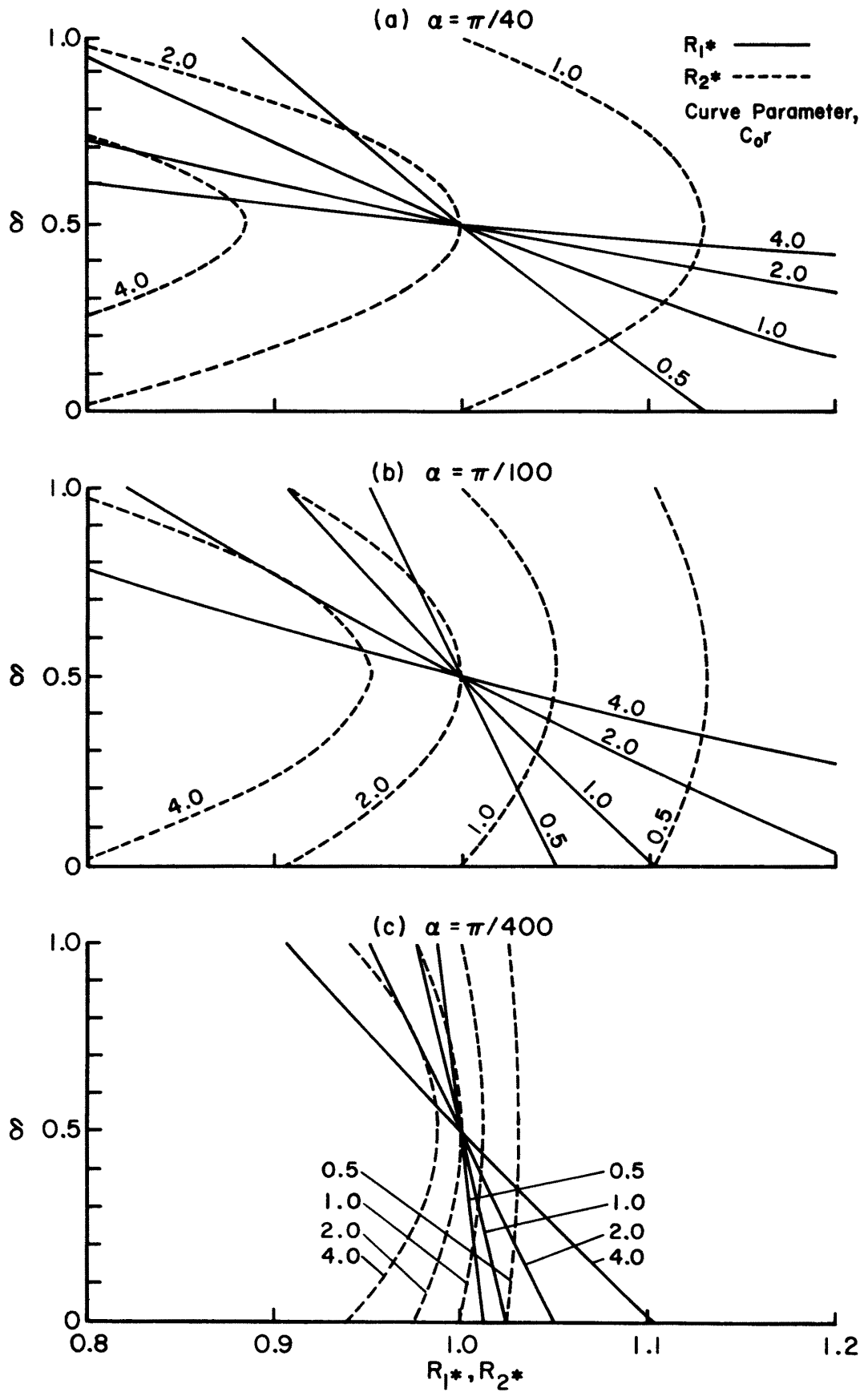


Fig. 4.1 Variation of Convergence Ratios  $R_1^*$  and  $R_2^*$  with Discretization Parameters in a Frictionless System.

#### 4.7 Convergence Ratios for Frictional Prismatic Channels

A more realistic case than the frictionless channel considered in the last section is that of a frictional channel. For a prismatic frictional channel,

$$\epsilon_B = 0 \quad (4-75)$$

$$\epsilon_{fB} = \epsilon_f \quad (4-76)$$

$$P_4 = P_7 \equiv 0 \quad (4-77)$$

and

$$Q = U \equiv 0 \quad (4-78)$$

Equations (4-62) and (4-63) can be accordingly simplified. The simplified equations indicate that the convergence ratios  $R_1$  and  $R_2$  are functions of terms pertaining to the resistance and transport functions such as  $P_1, P_2, P_3, P_5$  and  $P_6$ , as well as parameters  $c_f^r, \alpha$  and  $\delta$ . Therefore, parameters  $c_f^r, \alpha$  and  $\delta$  in frictional systems do not completely define the convergence ratios by themselves as they did in the nonfrictional systems. These ratios for frictional prismatic channels are not as simple as they were for the nonfrictional channels. However for a given problem, where values of  $P_1, P_2, P_3, P_5$  and  $P_6$  are fixed, it is possible to define the variation of  $R_1$  and  $R_2$  with the basic discretization variables  $\Delta x, \Delta t$  and  $\delta$ .

Another problem with the study of cumulative convergence ratios  $R_{1*}$  and  $R_{2*}$  in frictional systems arises from dispersion of waves. The celerity  $c_f$  (Equation (4-28)) depends on the wave number  $\sigma$  of a sinusoidal perturbation and  $\sigma$  changes continuously in time due to diffusion and dispersion. Ratios  $R_{1*}$  and  $R_{2*}$  in a frictional system are herein defined as

$$R_{1*} = (R_1)^{N_f} \quad (4-79)$$

$$R_{2*} = (R_2)^{N_f} \quad (4-80)$$

where

$$N_f = \frac{L}{c_f \Delta t} = \frac{2\pi(1 + \epsilon_f^2)}{\alpha c_o r} \quad (4-81)$$

In Equations (4-79) through (4-81),  $R_1$ ,  $R_2$ ,  $L$  and  $c_f$  pertain to the initial values of channel and wave parameters. It can be shown that in subcritical flow in prismatic sand-bed channels, these equations represent the upper bounds of  $|1-R_{1*}|$  and  $|1-R_{2*}|$  calculated from updating the values of  $L$  and  $c_f$  at each time step  $\Delta t$  with new values of  $\alpha$ ,  $\delta$  and  $c_f r$ .

The variation in  $R_{1*}$  and  $R_{2*}$  with  $\alpha$ ,  $\delta$  and  $c_f r$  is shown in Figures 4.2(a) through (c). These graphs pertain to the numerical problem studied in Chapter V. For this problem the equilibrium data are:

$$Q = 15000 \text{ cfs (424.752 m}^3/\text{sec)}$$

$$B = 300 \text{ ft (91.44 m)}$$

$$F = 0.20$$

$$S_f = 0.0001$$

$$g_b = 0.1030 \text{ lbs/ft/sec (1.50 N/m/sec)}$$

$$g_s = 0.2528 \text{ lbs/ft/sec (3.68 N/m/sec)}$$

and

$$g_t = 0.3558 \text{ lbs/ft/sec (5.18 N/m/sec)}$$

The value of resistance and transport parameters are:

$$P_1 = -0.002565 \text{ lbs/cu. ft.}$$

$$P_2 = -0.015862 \text{ lbs/sec/ft}^2$$

$$P_3 = 107.484 \text{ lbs/cu. ft.}$$

$$P_5 = 0.96021$$

$$P_6 = -0.0000019344 \text{ ft}^{-1}$$

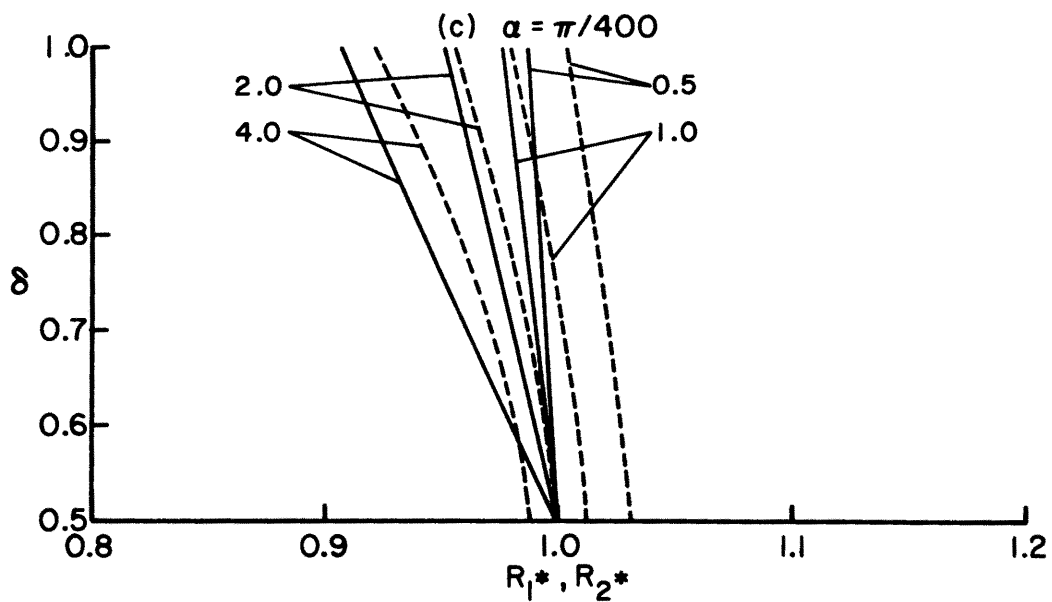
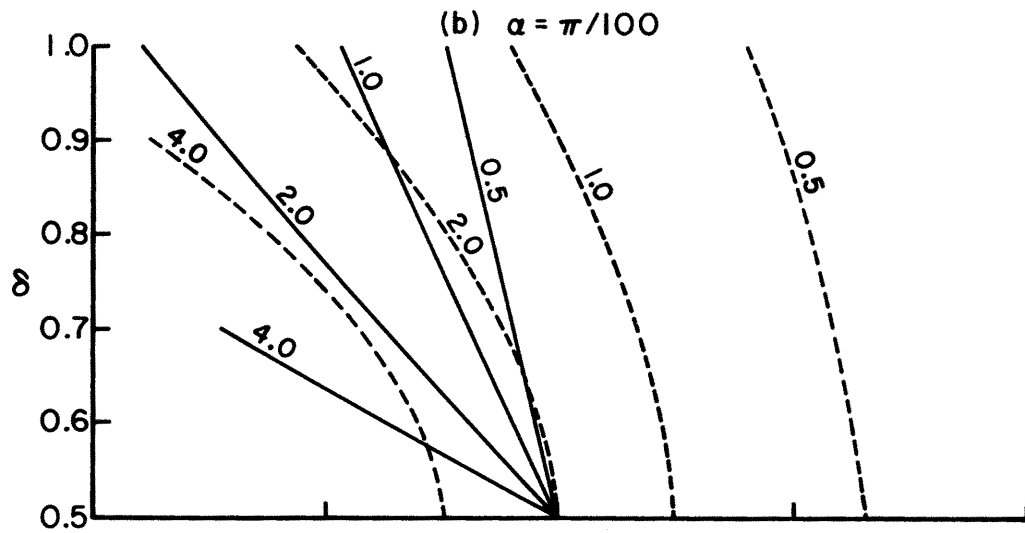
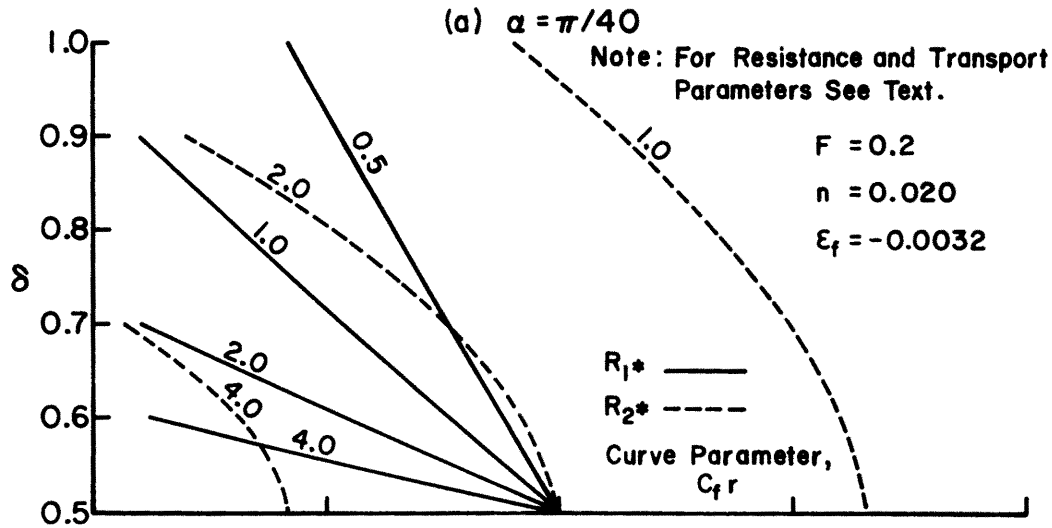


Fig. 4.2 Variation of Convergence Ratios  $R_1^*$  and  $R_2^*$  with Discretization Parameters in a Frictional System.

Figures 4.2 show:

1. For all values of  $\alpha$  and  $c_f r$ ,  $\delta = 0.5$  gives  $R_{1*} = 1.0$ . However, for reasons discussed in nonfrictional system, it may be necessary in practice to use  $\delta > 0.5$ .
2. Only for  $c_f r = 2$ , and  $\delta = 0.5$  both  $R_{1*}$  and  $R_{2*}$  are equal to 1 for all values of  $\alpha < \pi/2$ . For  $c_f r \geq 2$ , the values of  $R_{1*}$  and  $R_{2*}$  depart from 1. Note that a value of  $c_f r = 2$  corresponds to following a perturbation along the characteristic.
3. For all values of  $\delta$  and  $c_f r$  the values of  $R_{1*}$  and  $R_{2*}$  closest to 1 are found for the smallest values of  $\alpha$ . Apparently, the number of discretization points per wavelength are more important in determining the convergence ratios than the choice of  $\delta$  and  $c_f r$ .

The variation in  $R_{1*}$  and  $R_{2*}$  was also studied by increasing the resistance and sediment transport values used in Figure 4.2.

Figure 4.3 shows the variation in convergence ratios for the channel in Figure 4.2, if the Manning's  $n$  is increased by 50 percent for all values of the Froude number. Similarly, the variation in the convergence ratios for the same channel is shown in Figure 4.4 if the bed material load is increased threefold at all values of  $F$ . These figures show that the individual values of  $R_{1*}$  and  $R_{2*}$  are somewhat affected by these variations but the general conclusions stated above remain valid.

#### 4.8 Convergence Ratios for Frictional Nonprismatic Channels

In natural and man-made channels, the channel width may be contracting or expanding along the direction of flow. The general

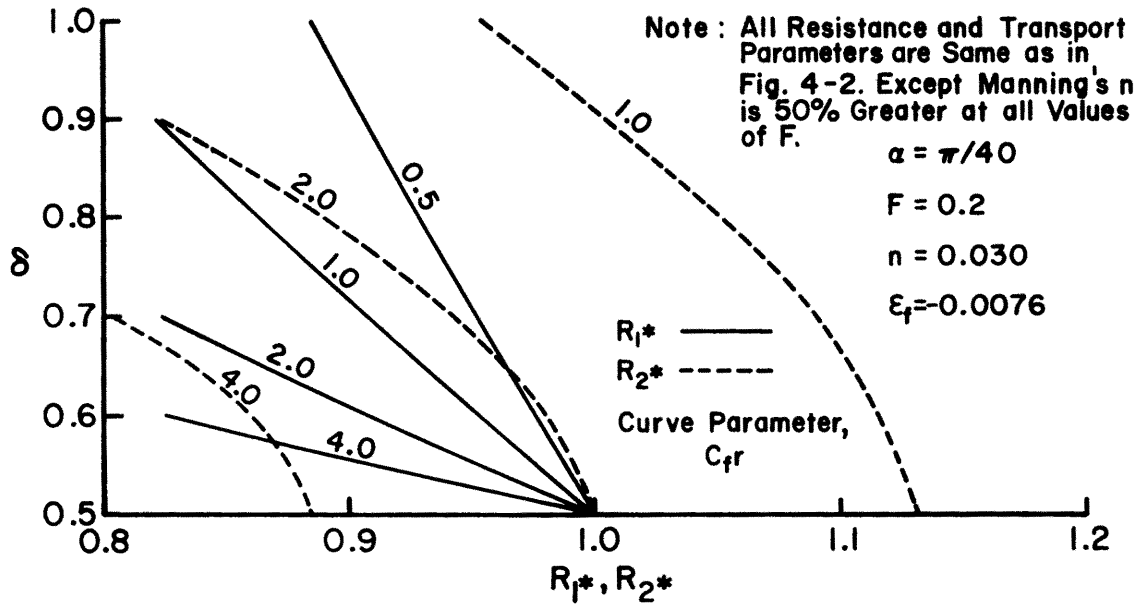


Fig. 4.3 Variation of Convergence Ratios  $R_1^*$  and  $R_2^*$  with Discretization Parameters (effect of increased frictional resistance).

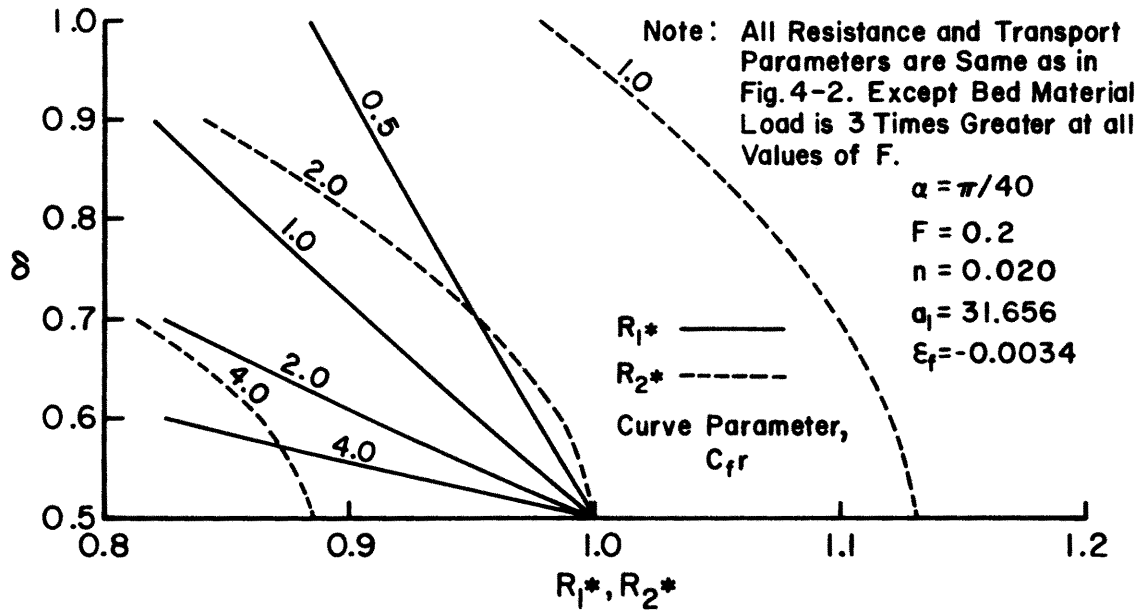


Fig. 4.4 Variation of Convergence Ratios  $R_1^*$  and  $R_2^*$  with Discretization Parameters (effect of increased bed material load).

problem treated in Chapters II and III therefore provided for a linearly varying channel width. For such a case, Equations (4-62) and (4-63) apply in full.

The celerity of a small disturbance in a frictional, nonprismatic channel,  $c_{fB}$  is given by Equation (4-31). One can therefore define the convergence ratios  $R_1$  and  $R_2$  in terms of parameters  $c_{fB}r$ ,  $\alpha$  and  $\delta$  as well as the resistance and transport parameters  $P_1, P_2, P_3, P_4, P_5, P_6$  and  $P_7$ . The cumulative values of convergence ratios  $R_{1*}$  and  $R_{2*}$  are defined as

$$R_{1*} = (R_1)^{N_{fB}} \quad (4-82)$$

$$R_{2*} = (R_2)^{N_{fB}} \quad (4-83)$$

where

$$N_{fB} = \frac{L}{c_{fB}\Delta t} = \frac{2\pi}{\alpha c_{fB}r} \quad (4-84)$$

and celerity  $c_{fB}$  is defined by Equation (4-31).

The variation in  $R_{1*}$  and  $R_{2*}$  with  $\alpha, \delta$  and  $c_{fB}r$  is shown in Figures 4.5(a) and (b). These graphs pertain to the channel used in Section 4.6 and with  $B' = 0.01$ . Similar graphs for  $B' = -0.01$  are shown in Figures 4.6(a) and (b). The scales in these two figures are different from the scales used in Figures 4.1 through 4.4. The following conclusions can be drawn from Figures 4.5 and 4.6 regarding the convergence ratios in nonprismatic frictional channels.

1. The behavior of  $R_{1*}$  is qualitatively similar for prismatic and nonprismatic channels.
2. The behavior of  $R_{2*}$  for nonprismatic channels departs considerably from that for prismatic channels, as shown by Figures 4.5 and 4.6. In general, it is more difficult to

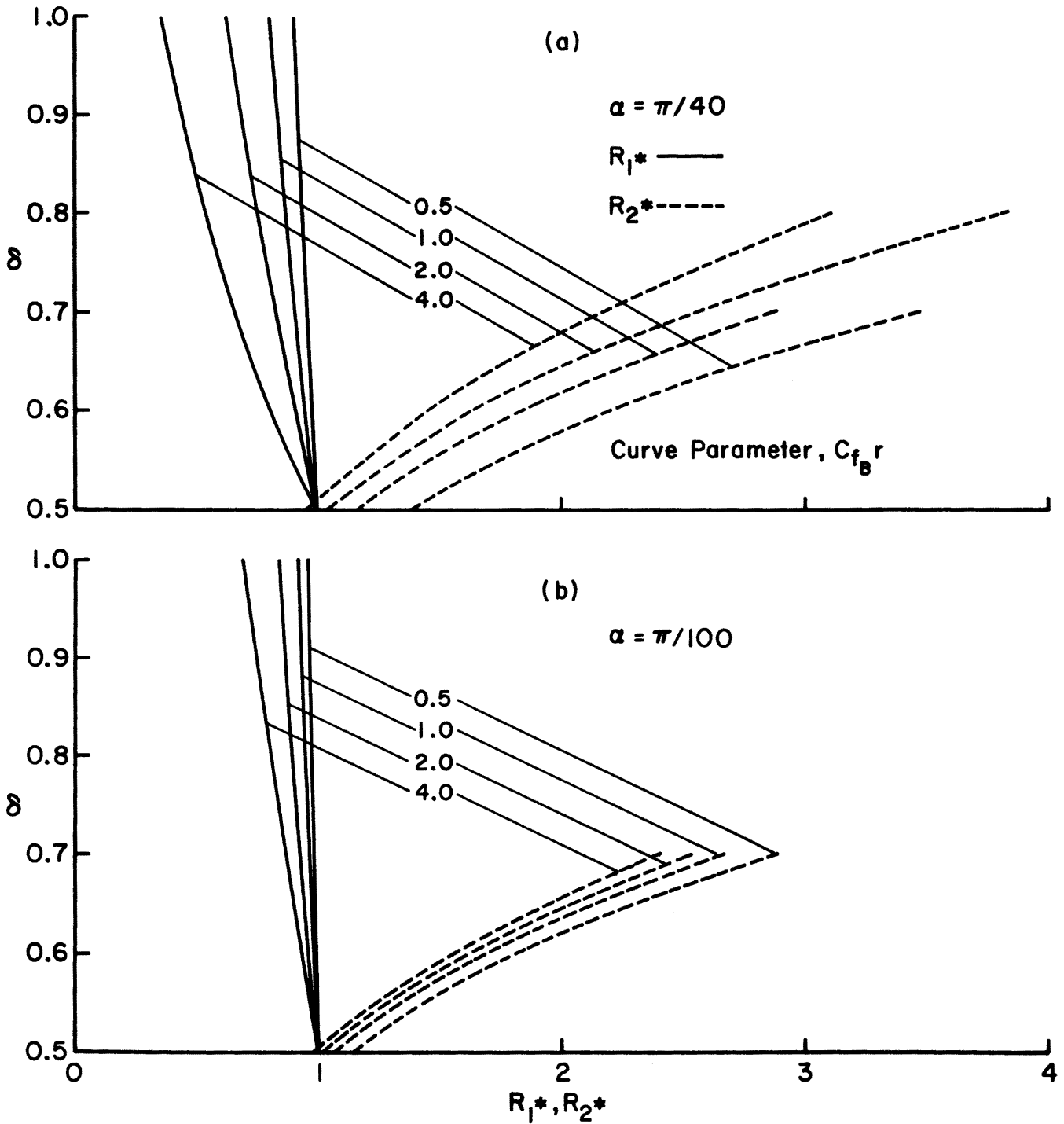


Fig. 4.5 Variation of Convergence Ratios  $R_1^*$  and  $R_2^*$  with Discretization Parameters for a Nonprismatic Channel,  $dB/dx = +0.01$ .

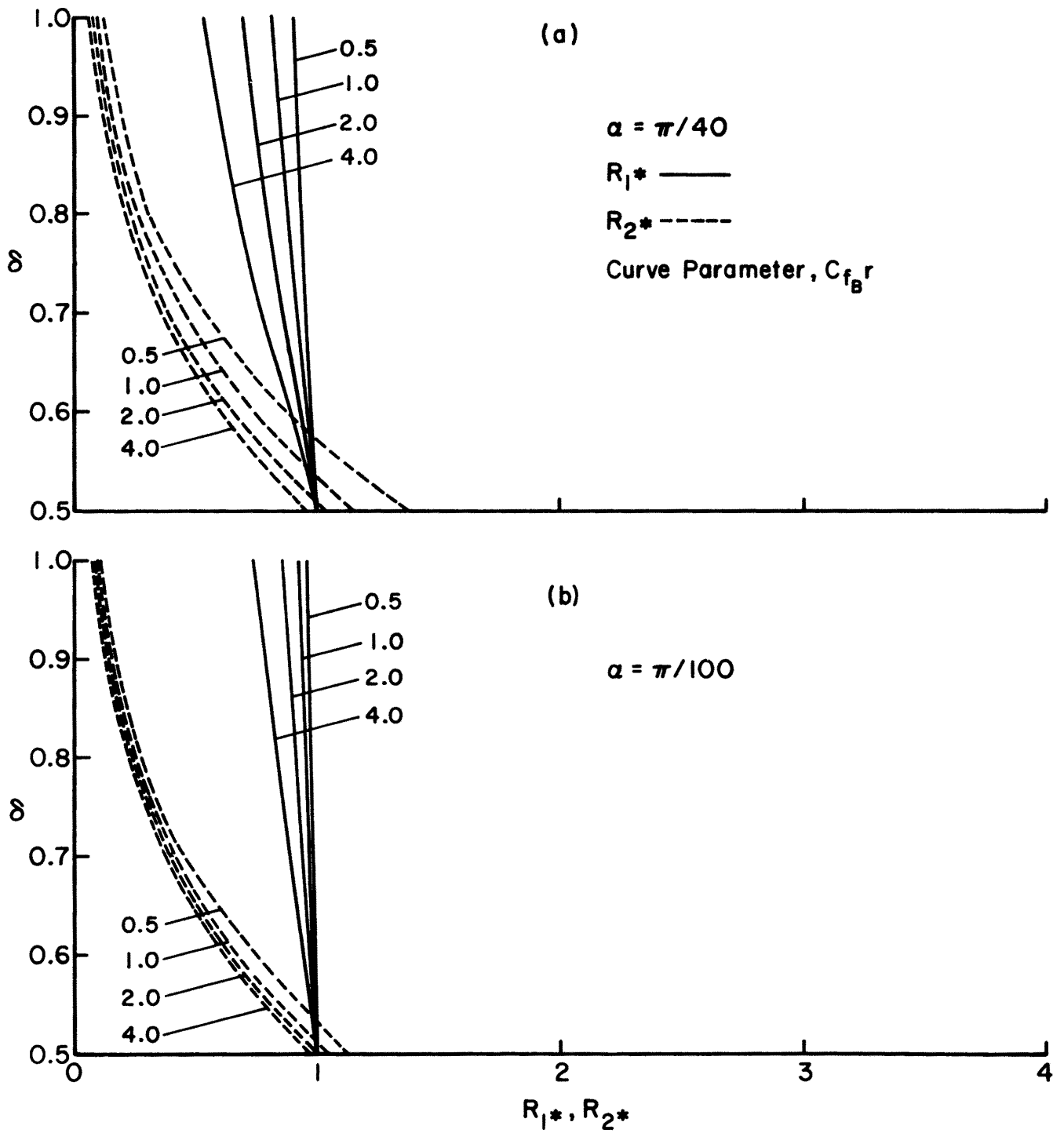


Fig. 4.6 Variation of Convergence Ratios  $R_1^*$  and  $R_2^*$  with Discretization Parameters for a Nonprismatic Channel,  $dB/dx = -0.01$ .

maintain  $R_{2*}$  close to unity than with the prismatic channel. Gross inaccuracies may result for values of  $\delta$  not in the vicinity of 0.5, for all values of  $c_{fB}r$ .

#### 4.9 Summary

The stability and convergence properties of the numerical scheme developed in Chapter III have been analyzed by using linearized versions of both the system of partial differential equations, Equation (4-13), and its finite difference analog, Equation (4-37) and (4-38). These properties have been expressed as the aggregate values of the dispersion and damping ratios over the time required for a wave to travel its own length. The following conclusions are drawn from this analysis:

1. Frictionless Prismatic Systems: the convergence ratios are functions of the dimensionless parameters  $c_0r$ ,  $\alpha$  and  $\delta$ . Ideally, for  $c_0r = 2$  and  $\delta = 0.5$ , the convergence ratios  $R_{1*}$  and  $R_{2*}$  are identically equal to 1, regardless of the value of  $\alpha$ . For  $0 \leq \delta < 0.5$ ,  $R_{1*}$  is greater than 1, and the numerical scheme is unstable. For  $0.5 \leq \delta \leq 1.0$ ,  $R_{1*}$  is less than 1, and artificial damping results in a stable scheme. In practice, however, high frequency perturbations are generated by the nonlinear system. Therefore, a value of  $\delta$  near 0.70 may be necessary to provide numerical damping required for stability.
2. Frictional Prismatic Systems: the convergence ratios are functions of the dimensionless parameter  $c_0r$ ,  $\alpha$  and  $\delta$ , and of the resistance and transport functions. The variation of  $R_{1*}$  and  $R_{2*}$ , however, show qualitatively similar behavior as that observed for ideal frictionless systems.

3. Frictional Nonprismatic Systems: the convergence ratios are functions of the dimensionless parameters  $c_o r$ ,  $\alpha$  and  $\delta$ , the resistance and transport functions, and the specified width variation.  $R_{1*}$  shows qualitatively similar behavior as that observed for prismatic systems. However, the behavior of  $R_{2*}$  represents a considerable departure from that observed for prismatic channels, and large amounts of dispersion and damping can occur for values of  $\delta$  not in the neighborhood of 0.5.

The preceding conclusions on the convergence ratios are of a qualitative nature and the actual magnitude of damping and dispersion can only be obtained through model verification based on experimental data.

## CHAPTER V

## NUMERICAL EXPERIMENTS

## 5.1 Introduction

The numerical model developed in Chapter III was simulated on the Colorado State University CDC 6400 digital computer. This chapter presents the results of numerical experiments carried out to assess the capabilities and limitations of the model.

In this phase of testing, various physical phenomena were hypothetically simulated with the numerical model, and the results are judged primarily on the realism of results obtained. The following test runs were carried out:

Test Run	Objective and Description
1	<ul style="list-style-type: none"> <li>(a) The formation and migration of a bed wave in the upstream reach of a channel due to a nonequilibrium sediment inflow hydrograph imposed on the upstream boundary.</li> <li>(b) The migration of a bed wave specified as initial condition on the channel bed.</li> </ul>
2	<ul style="list-style-type: none"> <li>(a) The phenomena posed by two bed waves of different celerity coalescing to form a larger wave.</li> <li>(b) The effect of the variation of the tail water elevation on the evolution of the channel bed configuration.</li> </ul>
3	The formation of a negative bed wave in the upstream reach of a channel due to a nonequilibrium sediment inflow hydrograph.

- 4                    The effect of local sediment removal mechanisms (dredging, sediment ejectors, etc.) on the configuration of the channel bed.

In these test runs particular attention was given to the practical value of the dimensionless discretization parameters  $\delta$ ,  $cr$  and  $\alpha$ .

The following were given due consideration:

1. Selection of  $\delta$  to provide sufficient numerical damping to preclude instability caused by high frequency perturbations generated by the nonlinear system.
2. Selection of  $\Delta t$  and  $\Delta x$  to ensure a value of  $cr$  consistent with the convergence criteria developed in Chapter IV.
3. Selection of  $\alpha$  to avoid the errors due to insufficient amount of discretization.

In addition, the accuracy of the linearized version was assessed by testing the satisfaction of the governing equations for all space intervals at every time step.

## 5.2 Test Reach

A simulated test reach was used for all test runs. The equilibrium properties of the test reach are the following:

Discharge	15,000 cfs
Average width	300 ft
Average depth	12.5 ft
Froude number	0.20
Energy gradient	0.0001
Bed material transport	114 ppm, 0.3558 lbs/sec/ft
Median bed material size	0.25 mm

The resistance function was expressed as follows:

$$\eta = 0.00380/F^{1.03} \quad (5-1)$$

following Equation (2-14), where

$$K_1 = 0.00380$$

$$a = 0$$

$$b = 1.03$$

For the transport function, the bed load function  $\phi-\psi$  is used as given by Einstein (Figure 9, reference [2]) except the coefficient  $a_1$  was multiplied by a factor of 2.0, so that the bed material load is increased by the same factor. For the equilibrium data,

$$a_1 = 21.104$$

$$b_1 = -1.67$$

in Equation (2-35).

The length of the channel is 12 miles. The celerity of small perturbations is 0.00049 fps or 0.008 miles/day. From Chapter IV, a value  $cr = 2$  is indicated to minimize the convergence error.

Expressed in terms of  $\Delta t$  and  $\Delta x$  the condition is:

$$c \frac{\Delta t}{\Delta x} = 1 \quad (5-2)$$

Taking  $\Delta t = 10$  days, it follows that  $\Delta x = 0.08$  miles if Equation (5-2) is to be satisfied. Note that a smaller value of  $\Delta t$  will require a smaller value of  $\Delta x$  to maintain the same values of convergence ratios.

For  $\Delta x = 0.08$  miles, the number of computational reaches in the 12 mile-long channel is 150.

The simulation can be carried out for any number of time steps. However, for this particular example, a small wave will travel the whole length of the channel in 1500 days or a total number of 150 time steps.

In test runs 1 and 2 the simulation was carried over 100 time steps. Note here that by fixing  $\Delta x$  the value of  $\alpha$  has already been fixed. In effect,

$$\alpha = \frac{\pi}{L/\Delta x} \quad (5-3)$$

and since  $L$ , the wavelength of the disturbance is a characteristic of a given problem and independent of the discretization parameters, fixing  $\Delta x$  is tantamount to fixing  $\alpha$ . Caution should be used, however, to avoid values of  $\alpha$  greater than  $\frac{\pi}{10}$ , since this could introduce wave distortion and damping due to insufficient amounts of discretization (refer to Figure 4.1).

A summary of the discretization characteristics for the test reach follows:

$$\Delta x = 0.08 \text{ mi}$$

$$\Delta t = 10 \text{ days}$$

$$c = 0.008 \text{ mile/day}$$

$$cr = 2$$

$$\text{number of computational reaches} = 150$$

$$\text{number of time steps} = 100$$

### 5.3 Test Run 1: Formation and Migration of a Bed Wave

Two problems were simultaneously studied as part of Test Run 1:

1. The migration and dissipation of a bed wave specified as initial condition on the channel bed. This wave was made trapezoidal in shape, with an amplitude of 2 ft and wavelength of 2.4 miles. The initial value of  $\alpha$  for this test run is  $\pi/30$ .
2. The formation of a bed wave in the upstream reach of the channel due to a nonequilibrium sediment inflow hydrograph

imposed on the upstream boundary. For test run 1, the nonequilibrium sediment hydrograph was made triangular in shape, with an amplitude of 2.25 times the equilibrium transport rate and a duration of 100 days.

Figure 5.1 shows the bed elevation of the channel at 20, 40, 60, 80, 100, 120, 250, 750 and 1000 days.

The following observations are made regarding test run 1:

1. The theoretical analysis of stability and convergence made on a linearized version of the system has focused on the necessity of keeping  $\delta$  equal to or greater than 0.5 to avoid instability. In practice, however, a value of  $\delta$  in the neighborhood of 0.70 appears to be the smallest value that will numerically dampen the instabilities of the nonlinear system. Trial runs with a value of  $\delta$  of 0.60 showed a marked tendency to instability, as shown in Figures 5.2 and 5.3.
2. The accuracy of the linearized numerical scheme has been studied by testing the satisfaction of the governing equations at every time step. This was done by using the values of  $y$  and  $z$  for time steps  $n\Delta t$  and  $(n+1)\Delta t$  to calculate the various terms of the governing equations for every time and space interval. These discrete values were used in Equations (2-4) and (2-5) as follows:

$$\frac{\partial}{\partial x} (g_b) = \frac{0.5}{\Delta x} [g_{b,j+1}^{n+1} - g_{b,j}^{n+1} + g_{b,j+1}^n - g_{b,j}^n] = \Delta_1 \quad (5-4)$$

$$\frac{\partial}{\partial x} (g_s) = \frac{0.5}{\Delta x} [g_{s,j+1}^{n+1} - g_{s,j}^{n+1} - g_{s,j+1}^n - g_{s,j}^n] = \Delta_2 \quad (5-5)$$

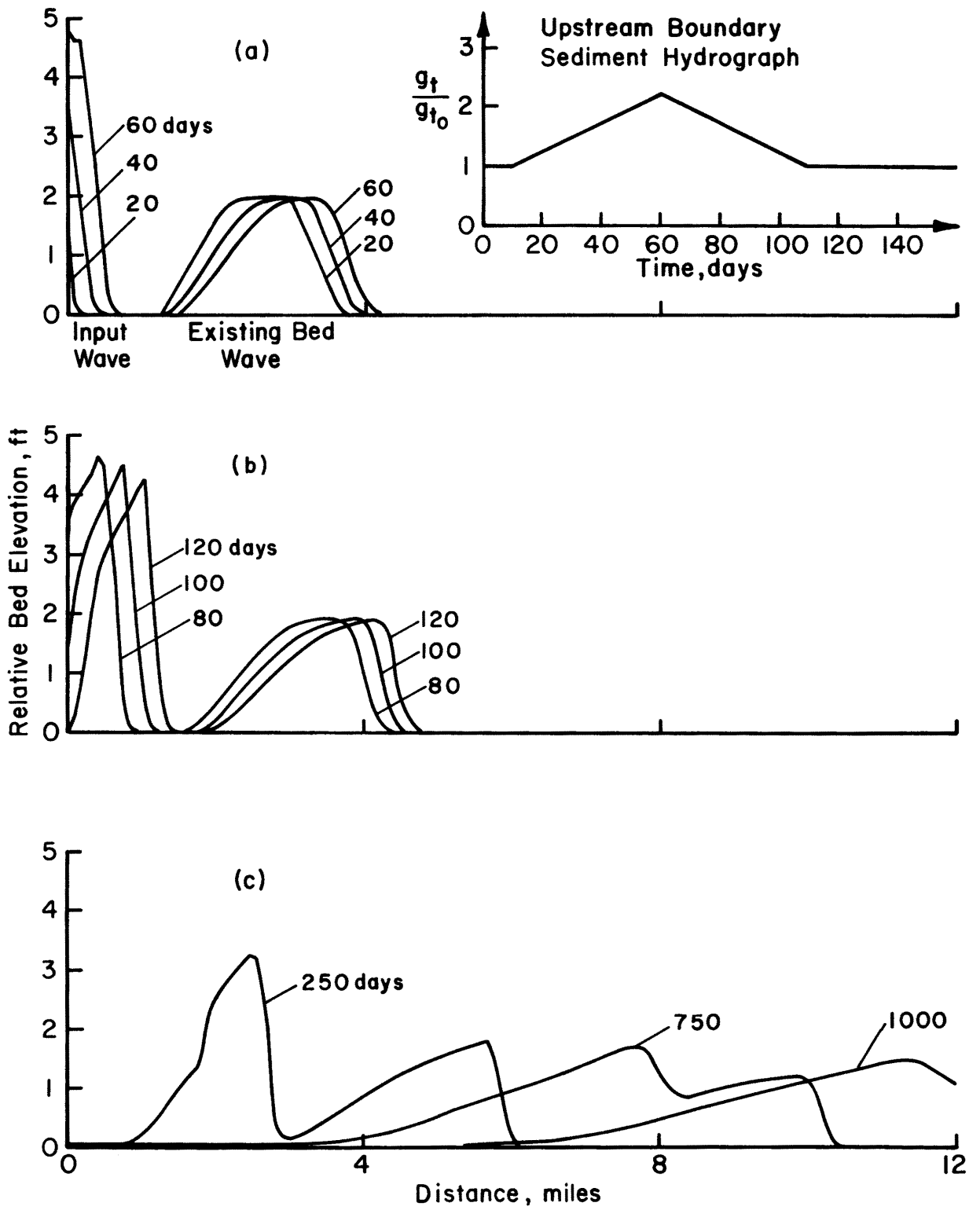


Fig. 5.1 Bed Elevation of the Channel, Test Run 1.  $\delta = 0.70$ .

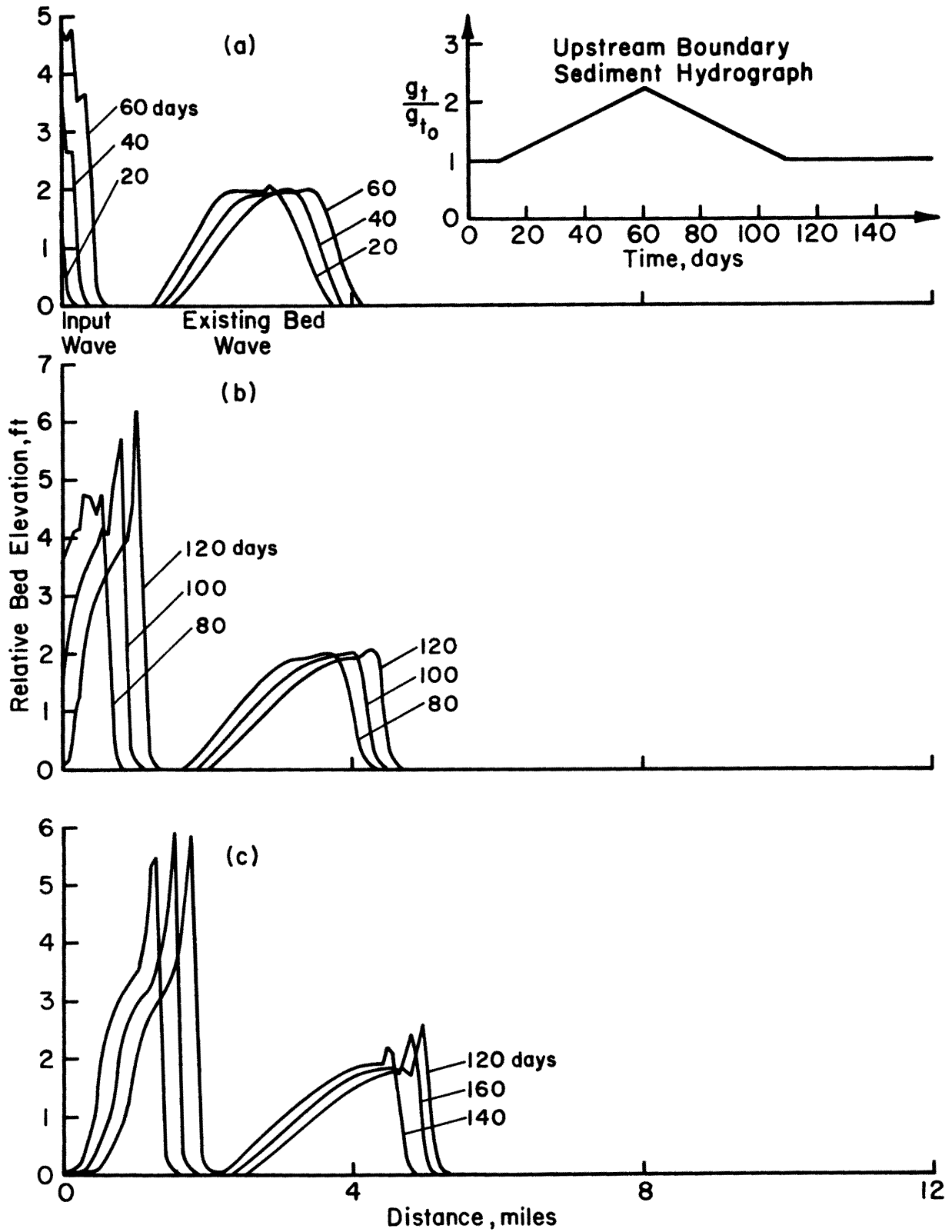


Fig. 5.2 Bed Elevation of the Channel, Test Run 1.  $\delta = 0.60$ .

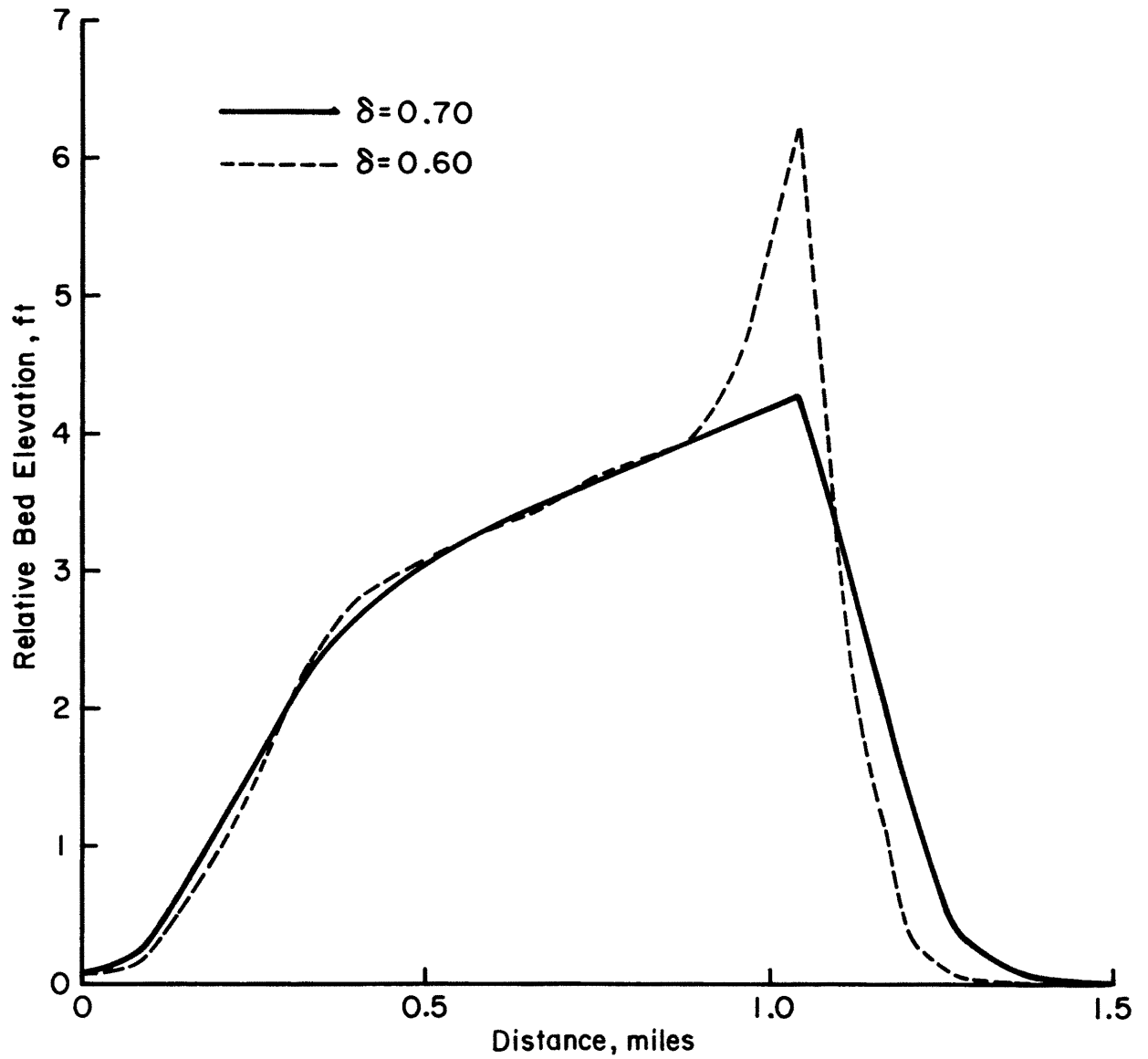


Fig. 5.3 Test Run 1: Comparison of Results of the Formation of the Bed Wave, for  $t = 120$  days.

$$\frac{\partial}{\partial t} (C_s h) = \frac{0.5}{\Delta t} [(C_s h)_{j+1}^{n+1} + (C_s h)_j^{n+1} - (C_s h)_{j+1}^n - (C_s h)_j^n] = \Delta_3 \quad (5-6)$$

$$P_* \frac{\partial}{\partial t} (z) = \frac{0.5}{\Delta t} P_* [z_{j+1}^{n+1} + z_j^{n+1} - z_{j+1}^n - z_j^n] = \Delta_4 \quad (5-7)$$

$$(g_b + g_s) \frac{B'}{B} = \frac{1}{4} \left\{ \left[ \frac{B'}{B} (g_b + g_s) \right]_{j+1}^{n+1} + \left[ \frac{B'}{B} (g_b + g_s) \right]_j^{n+1} \right. \\ \left. + \left[ \frac{B'}{B} (g_b + g_s) \right]_{j+1}^n + \left[ \frac{B'}{B} (g_b + g_s) \right]_j^n \right\} = \Delta_5 \quad (5-8)$$

$$\frac{\partial}{\partial x} \left( \frac{Q^2}{2gB^2 h^2} + y \right) = \frac{0.5}{\Delta x} [H_{T,j+1}^{n+1} - H_{T,j}^{n+1} + H_{T,j+1}^n - H_{T,j}^n] = \Delta_6 \quad (5-9)$$

$$\frac{\partial}{\partial x} (S_f) = \frac{0.5}{\Delta x} [S_{f,j+1}^{n+1} - S_{f,j}^{n+1} + S_{f,j+1}^n - S_{f,j}^n] = \Delta_7 \quad (5-10)$$

The errors in satisfying the sediment continuity and momentum equations were then expressed as:

$$\epsilon_s = \Delta_1 + \Delta_2 + \Delta_3 + \Delta_4 + \Delta_5$$

$$\epsilon_m = \Delta_6 + \Delta_7$$

Ideally, in a discretization scheme that introduces no errors,  $\epsilon_s = \epsilon_m = 0$ . However, the linearized numerical scheme always introduces truncation errors. These errors are taken as a measure of the inaccuracy of the numerical scheme.

This test run showed that the linearized version is an accurate representation of the governing equations. However, at points of discontinuity in the first derivative of the dependent variable, the governing equations may not be rigorously satisfied. This effect is likely to be of a secondary nature because it occurs only at local points and it is counteracted by the numerical damping provided in the scheme.

3. The existing bed wave travels downstream, and it is subject to damping and dispersion as will also occur in a natural system. However, the damping and dispersion of the simulated bed wave have two components: (1) a physical (natural) component, governed by the value of  $\epsilon_f$  (see Chapter IV, Equation (4-30)), and (2) a numerical (artificial) component, governed by the discretization parameters  $\delta$ ,  $cr$  and  $\alpha$ .

The amount of physical damping in the linearized equations can be assessed by calculating the value of the amplitude logarithmic decrement after one period of propagation. From Equation (4-35), for a prismatic channel:

$$\exp[(B_I)_f t] = \exp \frac{c_o \sigma \epsilon_f t}{1 + \epsilon_f} \quad (5-11)$$

For  $t = T$ , and using Equation (4-29)

$$\exp[(B_I)_f T] = \exp[c_f \sigma \epsilon_f T] \quad (5-12)$$

Since  $c_f T = L$ , and  $L\sigma = 2\pi$ ,

$$\exp[(B_I)_f T] = \exp[2\pi \epsilon_f] \quad (5-13)$$

And the amplitude decrement after one period of propagation can be related by the following equation:

$$\ln\left(\frac{z_1}{z_0}\right) = 2\pi \epsilon_f \quad (5-14)$$

where  $z_1$  is the bed elevation after one period of propagation,  $z_0$  is the bed elevation at the beginning of the period, and  $\epsilon_f$ , the frictional parameter given by Equation (4-30), is a function of the channel flow and wave characteristics.

The numerical damping in the linearized system can be estimated from Figure 4.1. This figure gives the value of  $R_{1*}$  for one period, for given  $\delta$ ,  $cr$  and  $\alpha$ . Since the convergence ratios are based on linearized equations and  $cr$  and  $\alpha$  vary in time, the value obtained from Figure 4.1 represents only a qualitative indication of the actual amount of numerical damping.

In the absence of closed form solutions of the governing equations it is difficult to separate the physical and numerical components of damping except by a qualitative estimation of the latter. For this reason, it is necessary to verify the model with data obtained from physical systems.

4. A bed wave is generated in time in the upstream reach of the channel, due to a sediment inflow hydrograph that exceeds the equilibrium transport rate for a given time period (see Figure 5.1). A significant feature of the nonlinear formulation of the upstream boundary condition is that the channel bed at the upstream boundary recedes to its equilibrium value as the inflow hydrograph recedes to equilibrium. This feature, that otherwise would be considered normal, has shown not to be possible with a strictly linear formulation of the boundary condition, see for instance Cunge and Perdreau [7].
5. In modeling the formation of a bed wave caused by a non-equilibrium sediment inflow values of  $cr$  less than 2 are not practical. With  $cr < 2$ , local oscillations are generated that may not preclude stability but are of

sufficient magnitude to render the solution meaningless.

In practice, both for convergence purposes and for eliminating oscillations when modeling nonequilibrium sediment inflow into a channel, a value of  $cr$  equal to or slightly greater than 2 is indicated.

6. The bed wave generated at the upstream boundary travels downstream subject to damping and dispersion. The foregoing comments regarding natural and artificial damping are also applicable to the bed waves.
7. The linearized numerical scheme is based on the assumption that over a time step  $\Delta t$  the change  $\Delta h$  in a quantity  $h$  is small enough so that second and higher order terms in  $\Delta h/h$  can be neglected without considerably impairing the accuracy of the solution. In general, a limit of  $\Delta h/h < 0.10$  is indicated. Larger values of  $\Delta h/h$  for any given time step will generate local instability that may or may not be dissipated by the numerical damping provided in the system. Maximum local values of  $\Delta h/h$  for test run 1 are of the order of 0.10.

In this respect, the shape of the sediment inflow hydrograph may impose a significant limitation on the discretization parameters. In theory, any shape of sediment inflow hydrograph can be modeled provided  $\Delta t$  can be adjusted to keep  $\Delta h/h$  within a specified tolerance, say 0.10. In practice, however, it is also necessary to keep  $cr \geq 2$  to avoid oscillations and to improve convergence. Thus, reducing  $\Delta t$  should be accompanied by a decrease in

$\Delta x$ , and this may extend computer time and core requirements. When core requirement is a limitation and large values of  $\Delta h/h$  are anticipated, the modeling may be carried out in two sequential stages: (1) modeling the formation of the bed wave, and (2) modeling the migration of the bed wave. In modeling the formation of the bed wave, the total length of the channel need not be taken. Instead, only a fraction of it, corresponding to an upstream reach of suitable length can be modeled as a first stage. This enables the decrease of  $\Delta x$  and  $\Delta t$ , thus distributing  $\Delta h$  over several time steps. Once the bed wave has formed on the upstream reach, its migration over the total length of the channel can be modeled as the second stage, with correspondingly larger values of  $\Delta x$  and  $\Delta t$ .

#### 5.4 Test Run 2: Coalescing of Bed Waves and Variation of Tail Water Elevation

Test run 2 was carried out using the discretizing parameters of Section 5.2, and a value of  $\delta$  of 0.70. Two problems were simultaneously studied:

1. The coalescing of two bed waves of different celerity: one specified as initial condition in the bed, and the other formed by a nonequilibrium sediment inflow hydrograph. For this problem, the nonequilibrium sediment inflow hydrograph was made trapezoidal in shape with an amplitude of 2.5 times the equilibrium transport rate and a duration of 120 days (see Figure 5.4). The maximum value of  $\Delta h/h$  was 0.14.
2. The effect of the variation of the tail water elevation on the channel bed configuration. For this problem, the tail

water elevation was increased 1 foot in the 250-500 day simulation interval, and decreased 1 foot in the 750-1000 day interval.

Figure 5.4 shows the bed elevation of the channel at 20, 40, 60, 80, 100, 120, 140, 160, 180, 200, 400, 600, 800 and 1000 days.

The following observations are made on test run 2:

1. Two waves of different celerity can coalesce and form larger waves (Figure 5.4).
2. The effect of the cyclical variation of the tail water level on the channel bed level is manifested by a cyclical change in the bed level. This change is qualitatively the same as caused by a cyclical variation in the sediment inflow. In this run a decrease of 1 foot in the tail water level caused a readjustment of the bed level to reflect that decrease. In the long run, the channel would have achieved a new equilibrium with the bed level lowered by 1 foot throughout.
3. The local instabilities shown are attributed to the high value of  $\Delta h/h$ , 0.14. At such a value, some high frequency perturbations are still being amplified, even though damping is provided.

### 5.5 Test Run 3: Formation of a Negative Bed Wave

Test run 3 was carried out using the discretizing parameters of Section 5.2, and a value of  $\delta$  of 0.70. In this test run, the degradation of the channel and formation of a negative bed wave following a decrease in the equilibrium sediment inflow hydrograph was modeled.

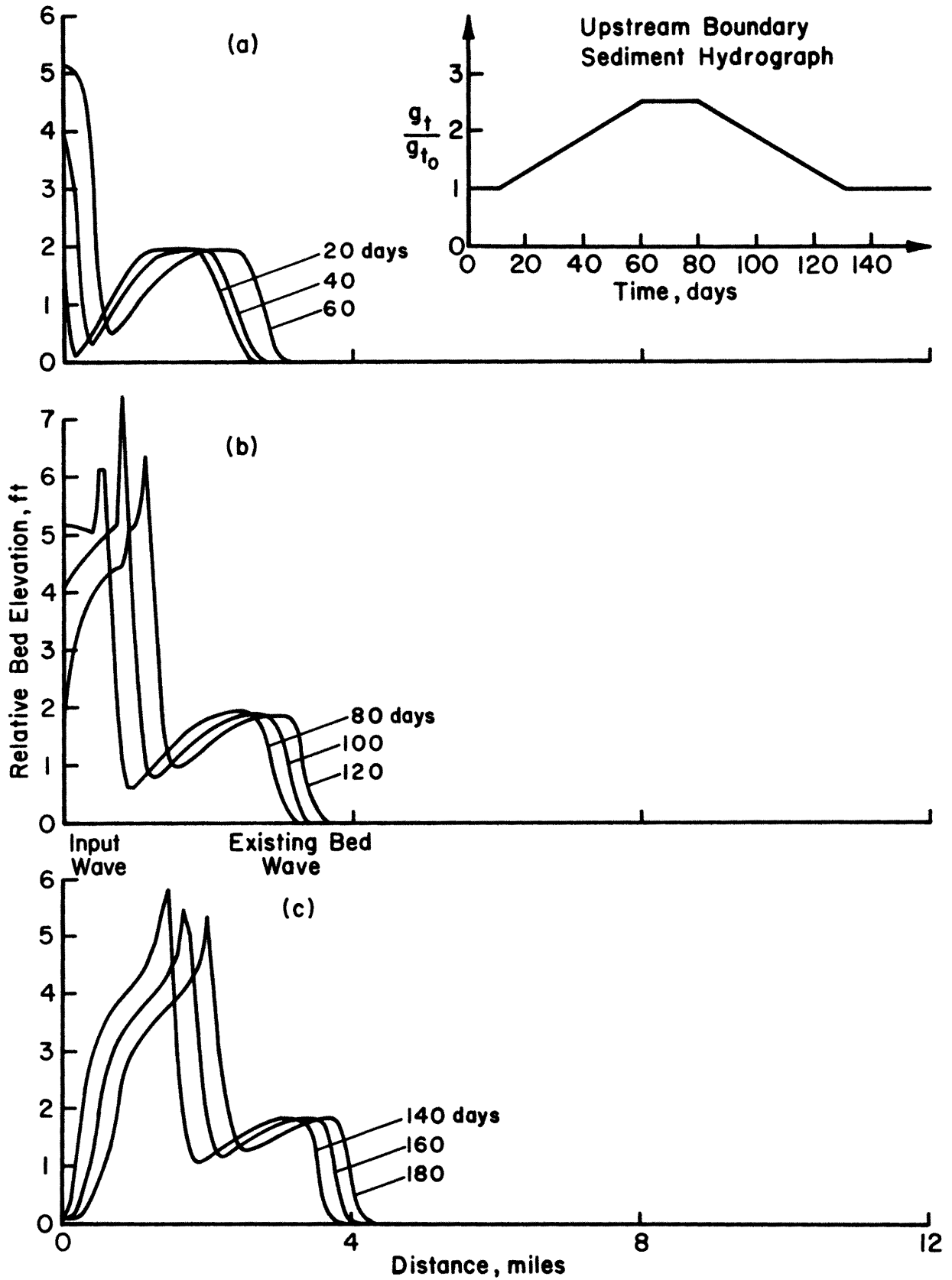


Fig. 5.4 Bed Elevation of the Channel, Test Run 2.  $\delta = 0.70$ .

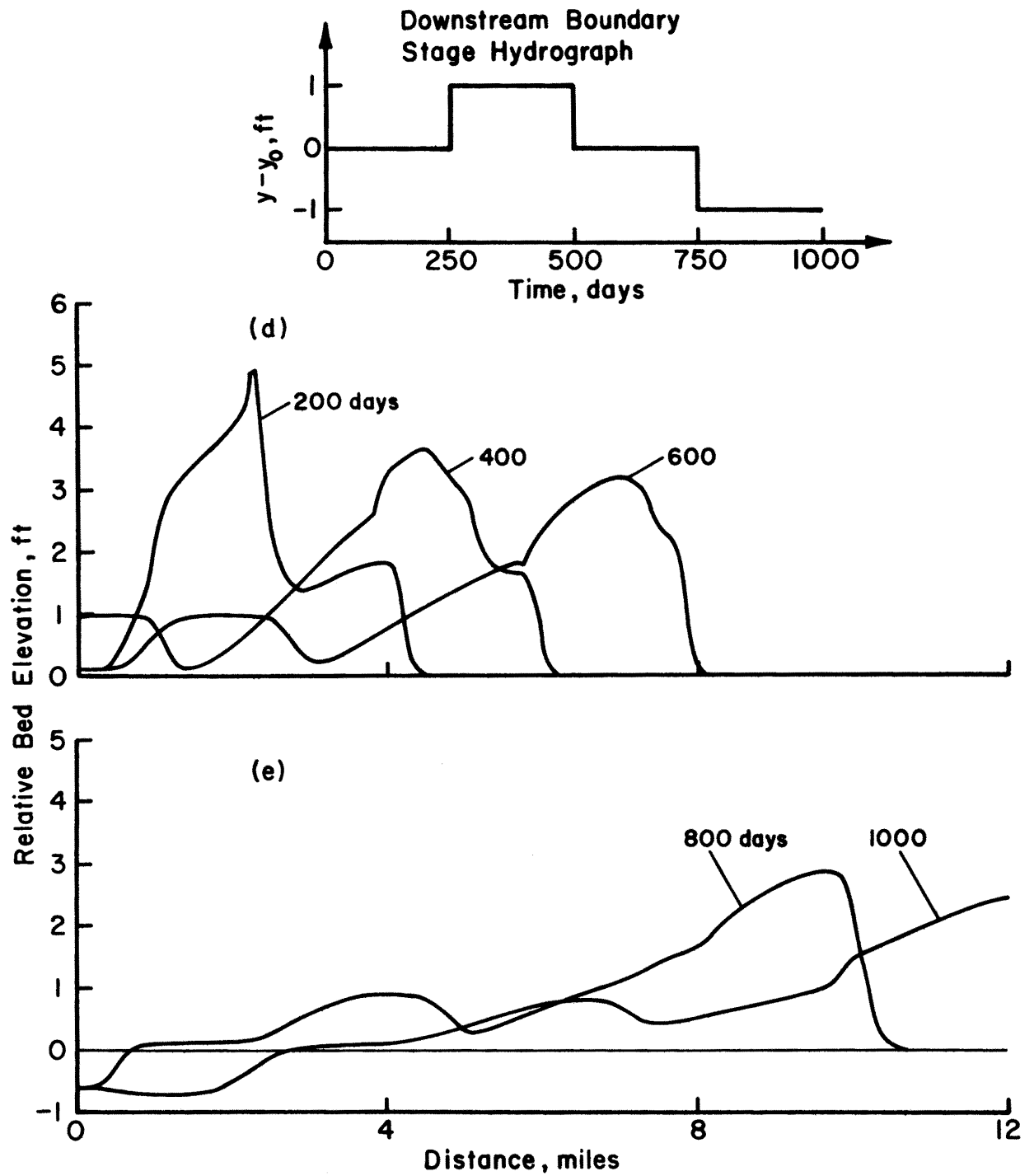


Fig. 5.4 Continued.

Figure 5.5 shows the results of bed elevation for 20, 40, 60, 80, 100, 120 and 140 days. The results are physically realistic and show the versatility of the scheme for modeling bed waves of sinusoidal shape.

#### 5.6 Test Run 4: The Effect of Local Sediment Removal

Test run 4 was carried out using the discretizing parameters of Section 5.2, and a value of  $\delta$  of 0.70. In this test run, the degradation of the channel bed following localized sediment removal was modeled. An amount of sediment equal to one-half of the equilibrium transport rate was removed at a distance of 3.2 miles from the upstream boundary. This was accomplished by balancing the sediment continuity equation at  $x = 3.2$  miles to reflect a distributed sediment sink over the length  $\Delta x$ . Figure 5.6 shows the results of bed elevation for 20, 40, 60, 80, 100, 120 and 140 days. The following observations are made on the results of this run:

1. The localized sediment removal causes local degradation that propagates downstream in time. If the rate of sediment removal is kept constant, new equilibrium conditions are reached at the point of removal.
2. The disturbance originated in the bed does not travel upstream. A theoretical explanation for this behavior lies in the fact that there is only one characteristic direction for the propagation of a bed discontinuity in subcritical flow, and this is in the downstream direction.

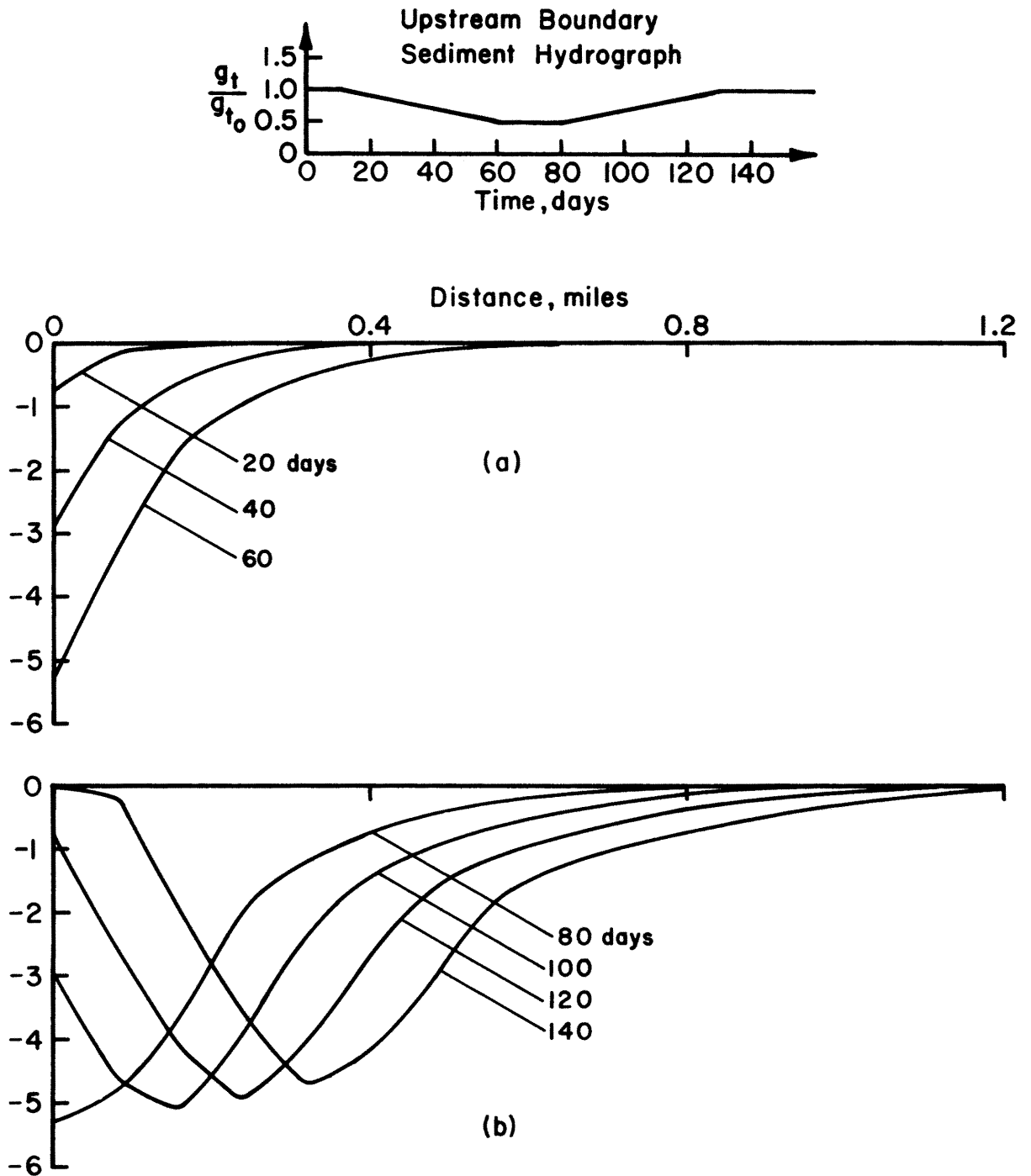


Fig. 5.5 Bed Elevation of the Channel, Test Run 3.  $\delta = 0.70$ .

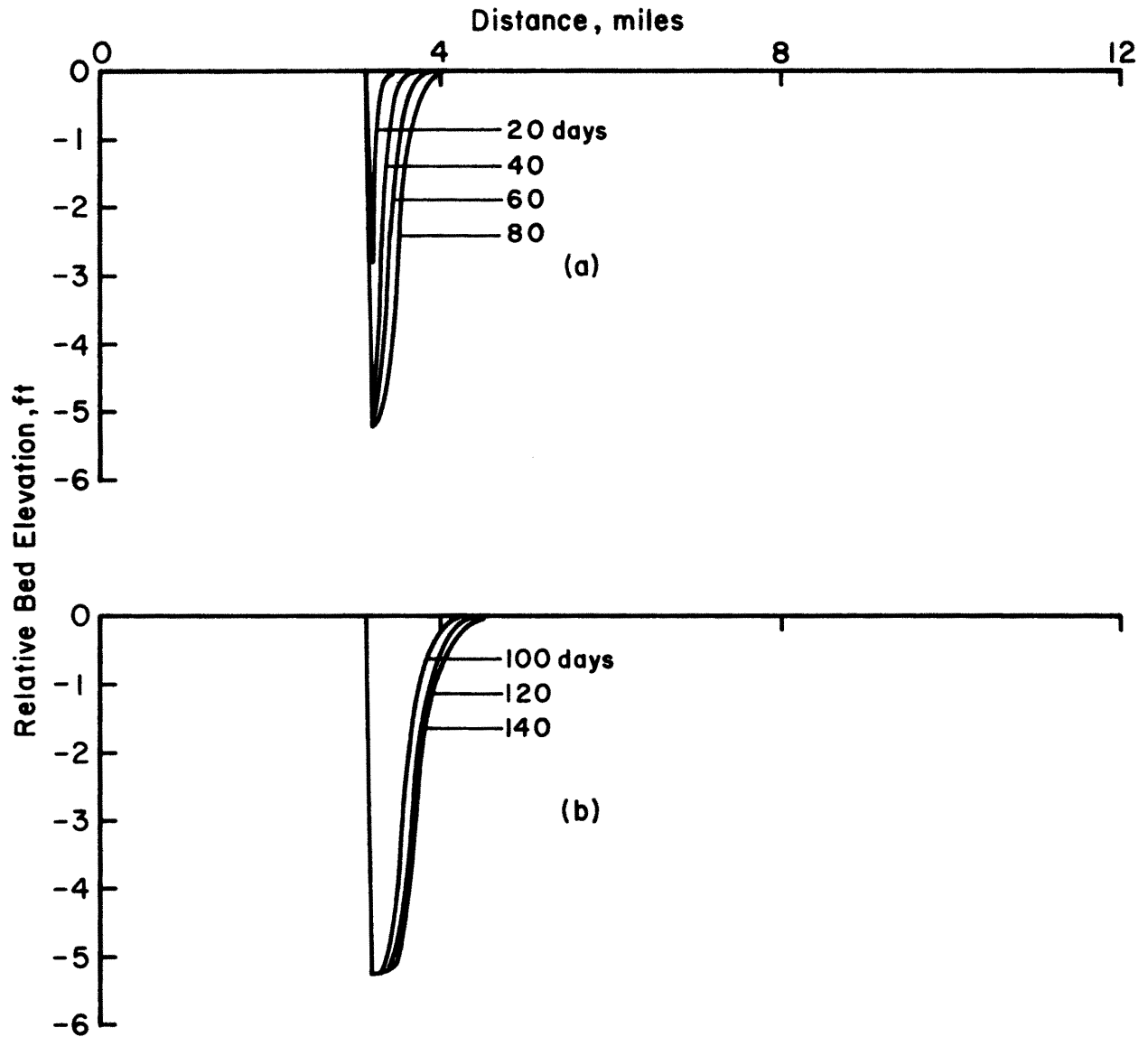


Fig. 5.6 Bed Elevation of the Channel, Test Run 4.  $\delta = 0.70$ .

## CHAPTER VI

## CONCLUSIONS AND RECOMMENDATIONS

A mathematical model of sedimentation transients in straight alluvial channels has been developed for subcritical flow. The model has a sound phenomenological structure inasmuch as it is based on widely accepted bed material transport functions and separately considers the bed load and suspended load components of the transport. It has considerable versatility and can successfully simulate various transients yielding realistic solutions. The model uses the momentum and sediment continuity equations in a coupled mode with the result that it can use rather long time steps. This represents a significant advantage because sedimentation transients are exceedingly slow phenomena.

Underlying assumptions: The mathematical model is based on the following simplifying assumptions. It is assumed that the sedimentation transients are a very slow process when compared to the water transients. Therefore, for the time scale used for these transients, the water discharge is considered invariant. This is a realistic assumption. On the upstream boundary, it is assumed that the bed level instantaneously adjusts to the flow depth and the prevailing transport rate. In actual channels, there is a developing flow region extending over some tens of hydraulic depth. However, in the length span of the channel, it represents a small segment and the physical dissipation evens out the conditions in time and space. This assumption is very convenient and enables the modeling of a sediment inflow hydrograph.

Boundary conditions: The implicit numerical scheme can be solved by resorting to a double sweep algorithm, provided the boundary

conditions are well posed. It is shown here that for the upstream boundary, either  $h$  or  $z$  need to be specified at every time step. Alternatively, since the bed material transport  $g_t$  is directly related to the depth of flow  $h$ , a hydrograph of  $g_t$  can be specified at the upstream boundary in lieu of  $h$ . For the downstream boundary, the model requires that stage  $y$  be specified at every time step.

Numerical analog: The governing equations for sedimentation transient are nonlinear. In the model presented herein, the resistance and sediment transport functions are expressed as power functions of the flow depth and the nonlinear character of the governing equation is maintained. A linear numerical analog of these equations is used in the model. This analog is based on the assumption that the proportional increment in the depth of flow, over one time step is small enough (say under 10 percent) so that second and higher order terms in  $\Delta h/h$  can be ignored. In the course of this study, a nonlinear numerical solution was also developed, using the Newton-Raphson technique. This solution has not been presented herein. Experience with the nonlinear solution shows that for similar space and time spans of simulation it is considerably more expensive in computational time than the linearized solution.

Convergence ratios: The convergence ratios, as criteria of the stability and convergence of the numerical analog, have been derived herein. These are also based on linearized equations. General expressions are developed for the convergence ratios  $R_{1*}$  and  $R_{2*}$  for frictional nonprismatic channels. A study of these ratios shows that for the simplified case of nonfrictional prismatic channels convergence is a function of three dimensionless discretization

parameters:  $\delta$ ,  $c_o r$  and  $\alpha$ . Both  $R_{1*}$  and  $R_{2*}$  are identically equal to 1 for  $\delta = 0.50$  and  $c_o r = 2$  for all  $\alpha < \frac{\pi}{2}$ . As  $\delta$  and  $c_o r$  depart from 0.5 and 2.0, respectively, the value of  $\alpha$  becomes increasingly relevant for convergence. Very low values of  $\alpha$  ( $\alpha \leq \pi/100$ ) assure a high degree of convergence even though  $\delta$  might not be in the neighborhood of 0.5 and  $c_o r$  may differ from 2.0.

Convergence for frictional prismatic channels is a function of  $\delta$ ,  $c_f r$  and  $\alpha$ , as well as of the resistance and transport parameters. A sensitivity study of  $R_{1*}$  and  $R_{2*}$  shows that variations in the resistance and transport parameters do not affect them to a significant degree.

Convergence for frictional nonprismatic channels is a function of  $\delta$ ,  $c_{fB} r$  and  $\alpha$ , as well as of the resistance and transport parameters and the specified channel width variation. Although  $R_{1*}$  does not seem to be appreciably affected by the width variation effect,  $R_{2*}$  for nonprismatic channels differ considerably from that of its prismatic counterpart, and it is difficult to generalize its behavior. In nonprismatic channels, it will be necessary to study the values of  $R_{1*}$  and  $R_{2*}$  for the selection of discretization parameters.

The results of actual test runs carried out to test the performance of the model indicate that a value of  $\delta$  of 0.70 is necessary to provide sufficient numerical damping to counteract the high frequency perturbations introduced by the nonlinearity of the system.

Test runs: The numerical model presented herein effectively simulates the formation of a bed wave due to a nonequilibrium sediment inflow hydrograph. There is no limitation to the shape of the sediment hydrograph that can be modeled, provided the linearization is valid ( $\Delta h/h \leq 0.10$ ) and  $cr$  is equal to or slightly greater than 2.

The numerical model presented herein can be used to model the transient phases of various types of aggradation and degradation problems. The examples presented herein relate to: (1) the formation and migration of positive and negative bed waves, (2) the effect of the variation of the tail water elevation on the channel bed configuration, and (3) the transient effect of local sediment removal.

Model limitations: The suspended bed material model cannot effectively account for values of the Rouse number  $Z$  equal to 1.1667 and 1.0. Coefficients  $k_5$ ,  $k_6$ ,  $k_7$  and  $k_8$  (Equations (2-46), (2-49), (2-53) and (2-56), respectively) contain terms such that they increase unbounded as  $Z \rightarrow 1.1667$  for  $k_5$  and  $k_6$ , and as  $Z \rightarrow 1.0$  for  $k_7$  and  $k_8$ . In practice, this condition will need to be monitored in the numerical solution, and if present, it will be necessary to modify the transport function to circumvent the numerical instability.

The linearized model is based on  $\Delta h/h \leq 0.10$ . In general, the discretization can be arranged so that this condition is satisfied. In certain cases of rapid change, it may be necessary to isolate different reaches and progress the solution sequentially in time with a small enough  $\Delta t$  in the region of rapid change.

Although the mathematical model presented herein has a sound phenomenological structure and the hypothetical test runs have yielded realistic results, it is necessary to verify it over some transient phenomena. This is needed more so because the governing equation of the phenomena are nonlinear and the convergence ratios are particularly sensitive to the discretization parameters. Data are now being especially collected on the Alluvial Channels Observation Project in Pakistan on sedimentation transients for the verification of the mathematical model developed herein.

**APPENDIX I**  
**REFERENCES**

## APPENDIX I

## REFERENCES

1. Mahmood, K. and Akhtar, A. B., Artificial Cutoff at Islam Headworks, Paper No. 352, Annual Proceedings, West Pakistan Engineering Congress, Lahore, 1962.
2. Einstein, H. A., The Bed Load Function for Sediment Transportation in Open Channel Flow, Tech. Bul. No. 1026, U.S. Dept. of Agriculture, Soil Conservation Service, 1950.
3. Mahmood, K., Flow in Sand Bed Channels, CUSUSWASH Water Management Technical Report No. 11, Colorado State University, Fort Collins, Colorado, 1971.
4. Mahmood, K., Variation of Regime Coefficients in Pakistan Canals, Journal of the Waterways, Harbors and Coastal Engineering Division, Proceedings ASCE, Vol. 100, No. WW2, May 1974.
5. Iwagaki, Yuichi, On the River-Bed Variation and its Stability, Proceedings 6th Japan National Congress for Applied Mechanics, 1956.
6. Vries, M. de, Solving River Problems by Hydraulic and Mathematical Models, Publication No. 76 II, Delft Hydraulics Laboratory, 1971.
7. Cunge, J. A., and Perdreau, M., Mobile Bed Fluvial Mathematical Model, La Hoille Blanche, No. 7, 1973.
8. Liggett, J. A., Basic Equations of Unsteady Flow, Chapter 2, Vol. I, Unsteady Flow in Open Channels, Editors K. Mahmood and V. Yevjevich, Water Resources Publications, Fort Collins, Colorado, 1975.
9. Mahmood, K., Mathematical Modeling of Morphological Transients in Sandbed Channels, Proceedings 16th Congress of the IAHR, Vol. 2, Sao Paulo, Brazil, 1975.
10. Richtmyer, R. D., and Morton, K. W., Difference Methods for Initial-Value Problems, Wiley & Sons, New York, 1967.
11. Liggett, J. A., and Cunge, J. A., Numerical Methods of Solution of Unsteady Flow Equations, Chapter 4, Vol. I, Unsteady Flow in Open Channels, Editors K. Mahmood and V. Yevjevich, Water Resources Publications, Fort Collins, Colorado, 1975.
12. Leendertse, J. S., Aspects of a Computational Model for Long-Period Water Wave Propagation, U.S. Air Force Project Rand, The Rand Corp., Santa Monica, California, 1967.

APPENDIX II  
DESCRIPTION OF PROGRAM SETRAN

## APPENDIX II

## DESCRIPTION OF PROGRAM SETRAN

Program SETRAN calculates the sedimentation transients in alluvial channels, according to the mathematical model presented in this report. A description of the structure of the program follows. Input-output examples are also given.

## 1. Program SETRAN

SETRAN is the name of the main program. It reads the input data and executes the main steps in the calculation. Program SETRAN calls ten subroutines for the execution of various aspects of the calculation.

## 2. Input Description

The input to SETRAN consists of the following:

Card No. 1, Format (2I10)

This card reads in the integer indicators INDU and INDT that provide for alternative choices in the upstream boundary condition and transport function, respectively. The following values of the indicators are used:

- a) INDU = 1: the inflow sediment hydrograph  $g_t(t)$  is specified as the upstream boundary condition, at every time step.
- b) INDU = 2: the bed level hydrograph  $z_1(t)$  is specified as the upstream boundary condition, at every time step.
- c) INDT = 1: the  $\phi - \psi$  relationship from Einstein's transport function, Figure 9, reference [2], will be used.
- d) INDT = 2: the user has the option of specifying one set of transport parameters  $a_1$  and  $b_1$  (Equation 2-35), obtained from experimental data. This set should cover the total range of transport experienced in a particular problem.

Card No. 2, Format (6F10.0)

This card reads in the following real variables: viscosity of water, bed material properties, and the resistance parameters  $k_1$ ,  $a$  and  $b$  (Equation 2-14).

Variable	Units	FORTTRAN NAME
Kinematic viscosity $\nu$	sq ft/sec	VNU
Channel bed porosity $p$	--	POR
Median bed material size $D$	ft	DIA
Coefficient $k_1$ in Equation 2-14	(Empirical)	CK
Exponent $a$ in Equation 2-14	--	CA
Exponent $b$ in Equation 2-14	--	CB

Card No. 3, Format (2F10.0)

This card reads in the minimum and maximum values of the Froude number to be expected at the upstream boundary. These values are needed in the calculation of the upstream depth of flow from the specified inflow sediment hydrograph.

Variable	Units	FORTTRAN NAME
Minimum Froude Number	--	FRMIN
Maximum Froude Number	--	FRMAX

Card No. 4, Format (3F10.0, 2I10)

This card reads in the information related to the discretization.

Variable	Units	FORTTRAN NAME
Weighting factor $\delta$	--	DEL
Reach length	miles	RLENGTH
Total time	days	TTIME
Number of space intervals	--	NL
Number of time intervals	--	NT

Card (Sequence) No. 5, Format (4F10.0)

The next input is a sequence of (NT + 1) cards with the information related to the boundary conditions at every time step. The following variables are read in:

Variable	Units	FORTTRAN NAME
Water discharge (upstream boundary)	cfs	QU(J)
Bed material concentration (upstream boundary)	ppm	CU(J)
Bed elevation (upstream boundary)	ft	ZU(J)
Water surface elevation (downstream boundary)	ft	YD(J)

Note 1: Depending on the available boundary conditions (refer to Card No. 1) either CU or ZU will be known in a problem. The field for variable unavailable in a problem should be left blank on every card.

Card (Sequence) No. 6, Format (5F10.0)

The next input is a sequence of (NL + 1) cards with the information related to the initial conditions at every space grid point. The following variables are read in:

Variable	Units	FORTTRAN NAME
Horizontal relative distance	mile	X(J)
Channel width	ft	BZ(J)
Water surface elevation	ft	YO(J)
Bed elevation	ft	ZO(J)
Reference bed elevation	ft	ZREF(J)

The reference bed elevation is the elevation to which the bed level will be referenced at every time step. Either the initial bed elevation or any other suitable reference elevation should be read in as reference bed elevation.

Card No. 7, Format (2F10.0)

If INDT = 2, an additional card which constitutes the last card in the input logical record should be read in. This card contains the values of  $a_1$  and  $b_1$  in Equation 2-35; Format (2F10.0)

Variable	Units	FORTTRAN NAME
$a_1$	--	EA
$b_1$	--	EB

## 3. Description of the Main Program

A flow chart shown in Figure A-1 depicts the structure of the main program. A brief description of the subroutines is given in the following section.

## 4. Description of Subroutines

Subroutine ULMT

This subroutine calculates variables  $\lambda_i$ ,  $m_i$ , and  $t_i$ , for  $i = 0, 1, 2, 3$ .

Variable	Units	FORTTRAN NAME
$\lambda_0, m_0, t_0$	--	UL(4), UM(4), UT(4)
$\lambda_1, m_1, t_1$	--	UL(1), UM(1), UT(1)
$\lambda_2, m_2, t_2$	--	UL(2), UM(2), UT(2)
$\lambda_3, m_3, t_3$	--	UL(3), UM(3), UT(3)

Subroutine VLMT

This subroutine calculates variables  $\lambda_i$ ,  $m_i$  and  $t_i$ , for  $i = 5, 6, 7, 8$ . It also calculates the local value of the shear intensity parameter  $\psi$  and the Rouse number  $Z$ .

Variable	Units	FORTTRAN NAME
$l_5, m_5, t_5$	--	VL(5), VM(5), VT(5)
$l_6, m_6, t_6$	--	VL(6), VM(6), VT(6)
$l_7, m_7, t_7$	--	VL(7), VM(7), VT(7)
$l_8, m_8, t_8$	--	VL(8), VM(8), VT(8)
$\psi$	--	PSI
Z	--	ROU

### Subroutine VARI

This subroutine calculates the following variables at each space grid point, and prints them out at every time step.

Variable	Units	FORTTRAN NAME
Referenced bed elevation	ft	ZPLOT(J)
Average velocity	fps	V
Froude number	--	FR
Bed load transport	lbs/sec/ft	GBE(J)
Suspended load transport	lbs/sec/ft	GSU(J)
Bed material concentration x h	lbs-ft/ft <sup>3</sup>	CSH(J)
$p \cdot \Delta Z_j$	lbs-ft/ft <sup>3</sup>	PZ(J)
Total energy	ft	HT(J)
Energy gradient	ft/ft	SF(J)

Subroutine MOMENT

This subroutine computes the statistical parameters of the first bed wave from the upstream boundary.

Variable	Units	FORTRAN NAME
Mode	mile	XMD
Z plot - mode	ft	ZMD
Mean $\bar{X}$	mile	XMN
Standard deviation $\sigma$	--	SD
Coefficient of variation $c_v$	--	CV
Skewness coefficient $\gamma_1$	--	SKC
Kurtosis coefficient $\gamma_2$	--	CKU

Subroutine HZUP

This subroutine calculates the value of the depth of flow at the upstream boundary corresponding to the specified inflow sediment hydrograph, (INDU = 1). It uses successive interpolations starting with two extreme values provided by FRMIN and FRMAX. The maximum number of iterations provided is 20, which is sufficient for most cases. If the Rouse number is near 1.00 or 1.1667 (see Chapter 6, Limitations), subroutine HZUP may not converge in 20 iterations.

Variable	Units	FORTRAN NAME
Trial $h_1$	ft	H3TRY
Trial $g_{t1}$	lbs/sec/ft <sup>2</sup>	G3TRY
Interpolated $h_1$	ft	HZB

Subroutine COEF

This subroutine calculates the values of the entries to the coefficient matrix. It also calculates the value of the bed wave celerity at the upstream boundary, to be used as a guide for the discretization.

Variable	Units	FORTTRAN NAME
Parameter $P_1$	lbs/cu ft	P1
Parameter $P_2$	lbs/sec/ft <sup>2</sup>	P2
Parameter $P_3$	lbs/cu ft	P3
Parameter $P_5$	--	P5
Parameter $P_6$	ft <sup>-1</sup>	P6
Bed celerity $c_f$	ft/sec	CNF
$A_{*j}$	lbs/sec/ft <sup>3</sup>	AS(J)
$B_{*j}$	lbs/sec/ft <sup>3</sup>	BS(J)
$C_{*j}$	lbs/sec/ft <sup>3</sup>	CS(J)
$D_{*j}$	lbs/sec/ft <sup>3</sup>	DS(J)
$E_{*j}$	ft <sup>-1</sup>	ES(J)
$F_{*j}$	ft <sup>-1</sup>	FS(J)
$G_{*j}$	ft <sup>-1</sup>	GS(J)
$H_{*j}$	ft <sup>-1</sup>	HS(J)
$Q_{*j}$	lbs/sec/ft <sup>2</sup>	QS(J)
$R_{*j}$	ft/ft	RS(J)

Subroutine DSWP

This subroutine calculates the values of  $\Delta y_j$  and  $\Delta z_j$  for  $j = 1, 2, \dots, (NL + 1)$ , by a double sweep algorithm. In a first sweep, the upstream boundary conditions are picked up, and intermediate vectors  $S_{*j}$ ,  $T_{*j}$ , and  $U_{*j}$  are calculated. In a second sweep, the downstream boundary conditions are picked up, and  $\Delta y_j$  and  $\Delta z_j$  are calculated based on the intermediate vectors.

Variable	Units	FORTRAN NAME
$S_{*j}$	--	SS(J)
$T_{*j}$	--	TS(J)
$U_{*j}$	--	US(J)
$\Delta y_j$	ft	DY(J)
$\Delta z_j$	ft	DZ(J)

Subroutine TEST2

This subroutine checks the solution vector at each time step by testing the balance achieved on the governing equations, using the values of the variables at time steps  $n\Delta t$  and  $(n + 1)\Delta t$ , for all space intervals. It is based on Equations 5-4 to 5-10.

Subroutine GT

This subroutine calculates the local value of the bed material transport for the specified values of  $K_1$ ,  $a$ ,  $b$ ,  $a_1$  and  $b_1$ .

Subroutine BACKW

This subroutine calculates a backwater curve for the new value of water discharge, thus readjusting the water surface level to the change in water discharge at every time step.

## 5. List of Variables (Arrays) in SETRANS

FORTTRAN	Variable	Symbol	Units
BZ	channel width	B	ft
BZP	dB/dx	B'	ft/ft
CSH	concentration xh	$(C_s h)$	lbs/ft <sup>2</sup>
* CSHO	concentration xh	$(C_s h)_o$	lbs/ft <sup>2</sup>
CU	concentration upstream	$c_1$	ppm
DY	change in y	$\Delta y$	ft
DZ	change in z	$\Delta z$	ft
GBE	bed load transport	$g_b$	lbs/sec/ft
* GBEO	bed load transport	$(g_b)_o$	lbs/sec/ft
GSB	upstream bed material transport	$g_{t1}$	lbs/sec/ft
GSU	suspended load	$g_s$	lbs/sec/ft
* GSUO	suspended load	$(g_s)_o$	lbs/sec/ft
HT	total energy	$H_T$	ft
* HTO	total energy	$(H_T)_o$	ft
HZ	flow depth	h	ft
* HZO	flow depth	$h_o$	ft
PZ	$p_* z_j$	$p_* z_j$	lbs/ft <sup>2</sup>
* PZO	$p_* z_j$	$p_* z_{jo}$	lbs/ft <sup>2</sup>
QU	water discharge	Q	cfs
SF	energy gradient	$S_f$	ft/ft
* SFO	energy gradient	$S_{fo}$	ft/ft
X	horizontal relative distance	x	ft
YD	downstream stage	$y_N$	ft
* YO	stage	$y_o$	ft

	Z	bed level	z	ft
*	Z0	bed level	$z_0$	ft
	ZU	upstream bed level	$z_1$	ft
	ZPLOT	plot bed level	--	ft
	ZREF	reference bed level	--	ft

\* Subscript 0 refers to conditions at the previous time step  $n\Delta t$ .

## 6. Input and Output Examples

Follows a sequence of cards as an example of an input logical record, with the corresponding output.











Card Sequence VI

Card VI-A

X(1)	BZ(1)	YO(1)	ZO(1)	ZREF(1)	
0.00	300.0	132.500	120.000	120.000	
<b>FORTRAN STATEMENT</b>					IDENTIFICATION
FOR COMMENT					
STATEMENT NUMBER					
1	1	1	1	1	1
2	2	2	2	2	2
3	3	3	3	3	3
4	4	4	4	4	4
5	5	5	5	5	5
6	6	6	6	6	6
7	7	7	7	7	7
8	8	8	8	8	8
9	9	9	9	9	9
10	10	10	10	10	10
11	11	11	11	11	11
12	12	12	12	12	12
13	13	13	13	13	13
14	14	14	14	14	14
15	15	15	15	15	15
16	16	16	16	16	16
17	17	17	17	17	17
18	18	18	18	18	18
19	19	19	19	19	19
20	20	20	20	20	20
21	21	21	21	21	21
22	22	22	22	22	22
23	23	23	23	23	23
24	24	24	24	24	24
25	25	25	25	25	25
26	26	26	26	26	26
27	27	27	27	27	27
28	28	28	28	28	28
29	29	29	29	29	29
30	30	30	30	30	30
31	31	31	31	31	31
32	32	32	32	32	32
33	33	33	33	33	33
34	34	34	34	34	34
35	35	35	35	35	35
36	36	36	36	36	36
37	37	37	37	37	37
38	38	38	38	38	38
39	39	39	39	39	39
40	40	40	40	40	40
41	41	41	41	41	41
42	42	42	42	42	42
43	43	43	43	43	43
44	44	44	44	44	44
45	45	45	45	45	45
46	46	46	46	46	46
47	47	47	47	47	47
48	48	48	48	48	48
49	49	49	49	49	49
50	50	50	50	50	50
51	51	51	51	51	51
52	52	52	52	52	52
53	53	53	53	53	53
54	54	54	54	54	54
55	55	55	55	55	55
56	56	56	56	56	56
57	57	57	57	57	57
58	58	58	58	58	58
59	59	59	59	59	59
60	60	60	60	60	60
61	61	61	61	61	61
62	62	62	62	62	62
63	63	63	63	63	63
64	64	64	64	64	64
65	65	65	65	65	65
66	66	66	66	66	66
67	67	67	67	67	67
68	68	68	68	68	68
69	69	69	69	69	69
70	70	70	70	70	70
71	71	71	71	71	71
72	72	72	72	72	72
73	73	73	73	73	73
74	74	74	74	74	74
75	75	75	75	75	75
76	76	76	76	76	76
77	77	77	77	77	77
78	78	78	78	78	78
79	79	79	79	79	79
80	80	80	80	80	80
UNIVERSITY COMPUTER CENTER					
GLOBE 507847					

Card VI-B

X(2)	BZ(2)	YO(2)	ZO(2)	ZREF(2)	
0.08	300.0	132.458	119.958	119.958	
<b>FORTRAN STATEMENT</b>					IDENTIFICATION
FOR COMMENT					
STATEMENT NUMBER					
1	1	1	1	1	1
2	2	2	2	2	2
3	3	3	3	3	3
4	4	4	4	4	4
5	5	5	5	5	5
6	6	6	6	6	6
7	7	7	7	7	7
8	8	8	8	8	8
9	9	9	9	9	9
10	10	10	10	10	10
11	11	11	11	11	11
12	12	12	12	12	12
13	13	13	13	13	13
14	14	14	14	14	14
15	15	15	15	15	15
16	16	16	16	16	16
17	17	17	17	17	17
18	18	18	18	18	18
19	19	19	19	19	19
20	20	20	20	20	20
21	21	21	21	21	21
22	22	22	22	22	22
23	23	23	23	23	23
24	24	24	24	24	24
25	25	25	25	25	25
26	26	26	26	26	26
27	27	27	27	27	27
28	28	28	28	28	28
29	29	29	29	29	29
30	30	30	30	30	30
31	31	31	31	31	31
32	32	32	32	32	32
33	33	33	33	33	33
34	34	34	34	34	34
35	35	35	35	35	35
36	36	36	36	36	36
37	37	37	37	37	37
38	38	38	38	38	38
39	39	39	39	39	39
40	40	40	40	40	40
41	41	41	41	41	41
42	42	42	42	42	42
43	43	43	43	43	43
44	44	44	44	44	44
45	45	45	45	45	45
46	46	46	46	46	46
47	47	47	47	47	47
48	48	48	48	48	48
49	49	49	49	49	49
50	50	50	50	50	50
51	51	51	51	51	51
52	52	52	52	52	52
53	53	53	53	53	53
54	54	54	54	54	54
55	55	55	55	55	55
56	56	56	56	56	56
57	57	57	57	57	57
58	58	58	58	58	58
59	59	59	59	59	59
60	60	60	60	60	60
61	61	61	61	61	61
62	62	62	62	62	62
63	63	63	63	63	63
64	64	64	64	64	64
65	65	65	65	65	65
66	66	66	66	66	66
67	67	67	67	67	67
68	68	68	68	68	68
69	69	69	69	69	69
70	70	70	70	70	70
71	71	71	71	71	71
72	72	72	72	72	72
73	73	73	73	73	73
74	74	74	74	74	74
75	75	75	75	75	75
76	76	76	76	76	76
77	77	77	77	77	77
78	78	78	78	78	78
79	79	79	79	79	79
80	80	80	80	80	80
UNIVERSITY COMPUTER CENTER					
GLOBE 507847					







Card VI-I

X(9)	BZ(9)	YO(9)	ZO(9)	ZREF(9)
0.64	300.0	132.162	119.662	119.662
<b>FORTRAN STATEMENT</b>				IDENTIFICATION
1	1	1	1	1
2	2	2	2	2
3	3	3	3	3
4	4	4	4	4
5	5	5	5	5
6	6	6	6	6
7	7	7	7	7
8	8	8	8	8
9	9	9	9	9
10	10	10	10	10



UNIVERSITY COMPUTER CENTER

GLOBE 507547

Card VI-J

X(10)	BZ(10)	YO(10)	ZO(10)	ZREF(10)
0.72	300.0	132.120	119.620	119.620
<b>FORTRAN STATEMENT</b>				IDENTIFICATION
1	1	1	1	1
2	2	2	2	2
3	3	3	3	3
4	4	4	4	4
5	5	5	5	5
6	6	6	6	6
7	7	7	7	7
8	8	8	8	8
9	9	9	9	9
10	10	10	10	10



UNIVERSITY COMPUTER CENTER

GLOBE 507547



Description of the Output: The following is a list and explanation of the output from Setran. Some of the output is self-explanatory.

First Page: Initial Data and Calculations.

Variable	Description
K1, A, B	Empirical coefficients of resistance equation, see Equation (2-14)
NL, NT	Number of intervals of space and time
J	Grid point in the space discretization
X	Distance in miles from upstream end of reach
ZPLOT	Referenced bed elevation, ft
BZ	Channel width, ft
Y	Water surface elevation, ft
Z	Bed elevation, ft
HZ	Channel depth, ft
V	Velocity, ft/sec
FR	Froude number
GBE	Bed load transport, lbs/sec/ft
GSU	Suspended load transport, lbs/sec/ft
CSH	Spatial concentration of bed material times depth, lbs/ft <sup>2</sup>
PZ	$P_*$ times bed elevation, lbs/ft <sup>2</sup> , see Equation (2-4)
HT	Total head above selected datum, ft
SF	Energy gradient

If  $INDU = 1$ , subroutine HZUP is used to calculate the upstream depth from the given sediment hydrograph. The number of iterations to achieve this is printed.

Following Pages: Data and calculations at each time step

Variable	Description
Parameter P1, P2 P3, P5, P6	Calculation of parameters given in Equations (4-14) through (4-19) at the upstream grid point.
Bed Wave Celerity	Celerity at upstream grid point, given by Equation (4-27)
D1, D2, D3, D4, D5	Accuracy of terms of continuity equation, see Equations (5-4) through (5-8)
ES	$\epsilon_s$ , given on page 66
D6, D7	Accuracy of terms of equation of motion, see Equations (5-9) and (5-10)
EM	$\epsilon_m$ , given on page 66

The root mean square of  $\epsilon_s$  and  $\epsilon_m$  summed over all grid points is also given.

The shape of the bed wave is defined by the following moments of ZPLOT. For this purpose values of  $ZPLOT \geq 0.01$  ft only are considered. If there are not at least five such grid points, the moments are not calculated.

<u>Variable</u>	<u>Description</u>
XMODE	Distance in miles from upstream boundary to ZMODE
ZMODE	Greatest value of ZPLOT along the reach
XMEAN	Distance in miles from upstream boundary to center of gravity of the wave
STAND. DEV.	Standard deviation of the wave description
COEFF. VAR.	Coefficient of variation of the wave distribution
SKEW COEFF.	Skew coefficient of the wave distribution
KURTOSIS COEFF.	Kurtosis coefficient of the wave distribution

Note: This problem was set up as an example only. For more accurate modeling of the wave, a lower value of  $\alpha$  should be chosen (see page 61).

MATHEMATICAL MODELING OF SEDIMENTATION TRANSIENTS

KINEMATIC VISCOSITY= .00000927 SQ.FT./SEC.  
 POROSITY= .350  
 MEDIAN RED SIZE= .001 FT.  
 K1= .003803  
 A= 0.000  
 B= 1.030  
 FROUDE NO MINIMUM= .100  
 FROUDE NO MAXIMUM= .750  
 WEIGHT F. DELTA= .700  
 REACH LENGTH= .800 MILES  
 TOTAL TIME= 50. DAYS  
 NL= 10  
 NT= 5  
 INDU= 1  
 INDT= 1

J	X	ZPLOT	HZ	Y	Z	HZ	V	FR	GBE	GSU	CSH	PZ	HT	SF
1	0.000	0.000	300.000	132.500	120.000	12.500	4.00	.20	.10304E+00	.25278E+00	.16032E+00	.12898E+05	.13275E+03	.10000E-03
2	.080	0.000	300.000	132.458	119.958	12.500	4.00	.20	.10304E+00	.25278E+00	.16032E+00	.12894E+05	.13271E+03	.10000E-03
3	.160	0.000	300.000	132.416	119.916	12.500	4.00	.20	.10304E+00	.25278E+00	.16032E+00	.12889E+05	.13266E+03	.10000E-03
4	.240	0.000	300.000	132.373	119.873	12.500	4.00	.20	.10304E+00	.25278E+00	.16032E+00	.12884E+05	.13262E+03	.10000E-03
5	.320	0.000	300.000	132.331	119.831	12.500	4.00	.20	.10304E+00	.25278E+00	.16032E+00	.12880E+05	.13258E+03	.10000E-03
6	.400	0.000	300.000	132.289	119.789	12.500	4.00	.20	.10304E+00	.25278E+00	.16032E+00	.12875E+05	.13254E+03	.10000E-03
7	.480	0.000	300.000	132.247	119.747	12.500	4.00	.20	.10304E+00	.25278E+00	.16032E+00	.12871E+05	.13250E+03	.10000E-03
8	.560	0.000	300.000	132.204	119.704	12.500	4.00	.20	.10304E+00	.25278E+00	.16032E+00	.12866E+05	.13245E+03	.10000E-03
9	.640	0.000	300.000	132.162	119.662	12.500	4.00	.20	.10304E+00	.25278E+00	.16032E+00	.12862E+05	.13241E+03	.10000E-03
10	.720	0.000	300.000	132.120	119.620	12.500	4.00	.20	.10304E+00	.25278E+00	.16032E+00	.12857E+05	.13237E+03	.10000E-03
11	.800	0.000	300.000	132.078	119.578	12.500	4.00	.20	.10304E+00	.25278E+00	.16032E+00	.12853E+05	.13233E+03	.10000E-03

NUMBER OF ITERATIONS IN SUBROUTINE HZUP= 7

TIME STEP= 1

WATER DISCHARGE= 15000.00 CFS

PARAMETER P1= -.86858628E-02  
 PARAMETER P2= -.50567238E-01  
 PARAMETER P3= .10748400E+03  
 PARAMETER P5= .96021138E+00  
 PARAMETER P6= -.19466672E-05  
 RED WAVE CELERITY= .48991645E-03 FT./SEC.

NUMBER OF ITERATIONS IN SUBROUTINE HZUP= 7

J	X	ZPLOT	RZ	Y	Z	HZ	V	FR	GRF	GSU	CSH	PZ	HT	SF
1	0.000	.000	300.000	132.500	120.000	12.500	4.00	.20	.10304E+00	.25278E+00	.16032E+00	.12898E+05	.13275E+03	.10000E-03
2	.080	.000	300.000	132.458	119.958	12.500	4.00	.20	.10304E+00	.25278E+00	.16032E+00	.12894E+05	.13271E+03	.10000E-03
3	.160	-.000	300.000	132.416	119.916	12.500	4.00	.20	.10304E+00	.25278E+00	.16032E+00	.12889E+05	.13266E+03	.10000E-03
4	.240	-.000	300.000	132.373	119.873	12.500	4.00	.20	.10304E+00	.25278E+00	.16032E+00	.12884E+05	.13262E+03	.10000E-03
5	.320	-.000	300.000	132.331	119.831	12.500	4.00	.20	.10304E+00	.25278E+00	.16032E+00	.12880E+05	.13258E+03	.10000E-03
6	.400	-.000	300.000	132.289	119.789	12.500	4.00	.20	.10304E+00	.25278E+00	.16032E+00	.12875E+05	.13254E+03	.10000E-03
7	.480	-.000	300.000	132.247	119.747	12.500	4.00	.20	.10304E+00	.25278E+00	.16032E+00	.12871E+05	.13250E+03	.10000E-03
8	.560	-.000	300.000	132.204	119.704	12.500	4.00	.20	.10304E+00	.25278E+00	.16032E+00	.12866E+05	.13245E+03	.10000E-03
9	.640	-.000	300.000	132.162	119.662	12.500	4.00	.20	.10304E+00	.25278E+00	.16032E+00	.12862E+05	.13241E+03	.10000E-03
10	.720	-.000	300.000	132.120	119.620	12.500	4.00	.20	.10304E+00	.25278E+00	.16032E+00	.12857E+05	.13237E+03	.10000E-03
11	.800	-.000	300.000	132.078	119.578	12.500	4.00	.20	.10304E+00	.25278E+00	.16032E+00	.12853E+05	.13233E+03	.10000E-03

J	D1	D2	D3	D4	D5	ES	D6	D7	EM
1	-.446988E-11	-.604998E-11	-.631012E-15	.105204E-10	0.	-.652849E-16	-.100000E-03	.100000E-03	.406793E-15
2	-.278055E-12	-.376338E-12	-.130128E-14	.655712E-12	0.	.179323E-16	-.100000E-03	.100000E-03	.300194E-14
3	.424015E-12	.573892E-12	-.128067E-14	-.996739E-12	0.	-.112666E-15	-.100000E-03	.100000E-03	-.195677E-14
4	.541985E-12	.733582E-12	-.114430E-14	-.127447E-11	0.	-.487659E-16	-.100000E-03	.100000E-03	.809682E-15
5	.562112E-12	.760809E-12	-.988435E-15	-.132200E-11	0.	-.681512E-16	-.100000E-03	.100000E-03	.169743E-14
6	.565890E-12	.765926E-12	-.829203E-15	-.133096E-11	0.	.253790E-16	-.100000E-03	.100000E-03	.673506E-15
7	.566897E-12	.767324E-12	-.669286E-15	-.133359E-11	0.	-.368604E-16	-.100000E-03	.100000E-03	-.474013E-15
8	.567524E-12	.768145E-12	-.509131E-15	-.133527E-11	0.	-.112723E-15	-.100000E-03	.100000E-03	-.513478E-15
9	.567997E-12	.768763E-12	-.348830E-15	-.133652E-11	0.	-.107363E-15	-.100000E-03	.100000E-03	.248239E-14
10	.568487E-12	.769455E-12	-.188401E-15	-.133770E-11	0.	.559113E-16	-.100000E-03	.100000E-03	.113624E-15
		ROOT MEAN SQUARE				.732545E-16			.153818E-14

TIME STEP= 2

WATER DISCHARGE= 15000.00 CFS

PARAMETER P1= -.86858628E-02  
PARAMETER P2= -.50567238E-01  
PARAMETER P3= .10748400E+03  
PARAMETER P5= .96021138E+00  
PARAMETER P6= -.19466672E-05  
RED WAVE CELERITY= .48991645E-03 FT./SEC.

NUMBER OF ITERATIONS IN SUBROUTINE HZUP= 5

J	X	ZPLOT	BZ	Y	Z	HZ	V	FR	GBE	GSU	CSH	PZ	HT	SF
1	0.000	1.654	300.000	132.433	121.654	10.779	4.64	.25	.15160E+00	.31644E+00	.17851E+00	.13076E+05	.13277E+03	.10367E-03
2	.080	.277	300.000	132.446	120.235	12.212	4.09	.21	.10949E+00	.26148E+00	.16291F+00	.12923E+05	.13271E+03	.10057E-03
3	.160	.046	300.000	132.414	119.962	12.452	4.02	.20	.10408E+00	.25420E+00	.16074E+00	.12894E+05	.13266E+03	.10009E-03
4	.240	.008	300.000	132.373	119.881	12.492	4.00	.20	.10321E+00	.25302E+00	.16039E+00	.12885E+05	.13262E+03	.10002E-03
5	.320	.001	300.000	132.331	119.832	12.499	4.00	.20	.10307E+00	.25282E+00	.16034E+00	.12880E+05	.13258E+03	.10000E-03
6	.400	.000	300.000	132.289	119.789	12.500	4.00	.20	.10304E+00	.25279E+00	.16033E+00	.12875E+05	.13254E+03	.10000E-03
7	.480	.000	300.000	132.247	119.747	12.500	4.00	.20	.10304E+00	.25279E+00	.16032E+00	.12871E+05	.13250E+03	.10000E-03
8	.560	.000	300.000	132.204	119.704	12.500	4.00	.20	.10304E+00	.25279E+00	.16032E+00	.12866E+05	.13245E+03	.10000E-03
9	.640	.000	300.000	132.162	119.662	12.500	4.00	.20	.10304E+00	.25278E+00	.16032E+00	.12862E+05	.13241E+03	.10000E-03
10	.720	.000	300.000	132.120	119.620	12.500	4.00	.20	.10304E+00	.25278E+00	.16032E+00	.12857E+05	.13237E+03	.10000E-03
11	.800	.000	300.000	132.078	119.578	12.500	4.00	.20	.10304E+00	.25278E+00	.16032E+00	.12853E+05	.13233E+03	.10000E-03

J	D1	D2	D3	D4	D5	ES	D6	D7	EM
1	-.697732E-04	-.910778E-04	.120190E-07	.120076E-03	0.	-.407633E-04	-.129319E-03	.101484F-03	-.278355F-04
2	-.897120E-05	-.120745E-04	.173773E-08	.201001E-04	0.	-.943801E-06	-.100888E-03	.100232E-03	-.656124E-06
3	-.144145E-05	-.194919E-05	.284293E-09	.336467E-05	0.	-.256839E-07	-.100056E-03	.100038E-03	-.179016F-07
4	-.239662E-06	-.324332E-06	.474092E-10	.563230E-06	0.	-.716231E-09	-.100007E-03	.100006E-03	-.499425E-09
5	-.400725E-07	-.542367E-07	.793126E-11	.942811E-07	0.	-.200542E-10	-.100001E-03	.100001E-03	-.139820F-10
6	-.670621E-08	-.907682E-08	.132766E-11	.157811E-07	0.	-.562009E-12	-.100000E-03	.100000E-03	-.391431F-12
7	-.112208E-08	-.151874E-08	.222331E-12	.264058E-08	0.	-.157736E-13	-.100000E-03	.100000E-03	-.746885E-14
8	-.187359E-09	-.253590E-09	.372496E-13	.440912E-09	0.	-.593293E-15	-.100000E-03	.100000E-03	.277209E-14
9	-.308908E-10	-.418108E-10	.621045E-14	.726953E-10	0.	-.739202E-16	-.100000E-03	.100000E-03	.130408E-14
10	-.469842E-11	-.635930E-11	.957148E-15	.110566E-10	0.	-.136583E-15	-.100000E-03	.100000E-03	.177592F-14

ROOT MEAN SQUARE .128939F-04 .880482E-05

TIME STEP= 3

WATER DISCHARGE= 15000.00 CFS

PARAMETER P1= -.12774362E-01  
 PARAMETER P2= -.833A2962E-01  
 PARAMETER P3= .10748400E+03  
 PARAMETER P5= .93794635E+00  
 PARAMETER P6= -.23403616E-05  
 RED WAVE CELEIRITY= .82699041E-03 FT./SEC.

NUMFR OF ITERATIONS IN SUBROUTINE HZUP= 7

J	X	ZPLOT	HZ	Y	Z	HZ	V	FR	GBE	GSU	CSH	PZ	HT	SF
1	0.000	.015	300.000	132.515	120.015	12.500	4.00	.20	.10304E+00	.25278E+00	.16032F+00	.12900E+05	.13276E+03	.10000E-03
2	.080	.875	300.000	132.420	120.833	11.587	4.32	.22	.12557E+00	.28280E+00	.16910E+00	.12988E+05	.13271E+03	.10186E-03
3	.160	.375	300.000	132.400	120.291	12.110	4.13	.21	.11192E+00	.26473E+00	.16386E+00	.12929E+05	.13267E+03	.10078E-03
4	.240	.098	300.000	132.369	119.971	12.398	4.03	.20	.10525E+00	.25578E+00	.16122E+00	.12895E+05	.13262E+03	.10020E-03
5	.320	.022	300.000	132.330	119.853	12.477	4.01	.20	.10353E+00	.25345E+00	.16052F+00	.12882E+05	.13258E+03	.10004E-03
6	.400	.005	300.000	132.289	119.793	12.495	4.00	.20	.10314E+00	.25292E+00	.16036E+00	.12876E+05	.13254E+03	.10001E-03
7	.480	.001	300.000	132.247	119.747	12.499	4.00	.20	.10306E+00	.25281E+00	.16033E+00	.12871E+05	.13250E+03	.10000E-03
8	.560	.000	300.000	132.204	119.704	12.500	4.00	.20	.10304E+00	.25279E+00	.16033E+00	.12866E+05	.13245E+03	.10000E-03
9	.640	.000	300.000	132.162	119.662	12.500	4.00	.20	.10304E+00	.25279E+00	.16032E+00	.12862E+05	.13241E+03	.10000E-03
10	.720	.000	300.000	132.120	119.620	12.500	4.00	.20	.10304E+00	.25279E+00	.16032E+00	.12857E+05	.13237E+03	.10000E-03
11	.800	.000	300.000	132.078	119.578	12.500	4.00	.20	.10304E+00	.25278E+00	.16032E+00	.12853E+05	.13233E+03	.10000E-03

J	D1	D2	D3	D4	D5	ES	D6	D7	EM
1	.743615E-05	.107018E-04	-.694042E-08	-.647052E-04	0.	-.465742E-04	-.132383E-03	.101288E-03	-.310946E-04
2	-.264575E-04	-.351092E-04	.538864E-08	.576780E-04	0.	-.388331E-05	-.103670E-03	.101023E-03	-.264695E-05
3	-.116704E-04	-.156723E-04	.228014E-08	.260388E-04	0.	-.130170E-05	-.101260E-03	.100357E-03	-.902453E-06
4	-.296377E-05	-.400348E-05	.583818E-09	.687153E-05	0.	-.951269E-07	-.100154E-03	.100088E-03	-.662382E-07
5	-.660445E-06	-.893518E-06	.130559E-09	.154888E-05	0.	-.495338E-08	-.100023E-03	.100019E-03	-.345280E-08
6	-.138200E-06	-.187036E-06	.273452E-10	.324987E-06	0.	-.221807E-09	-.100004E-03	.100004E-03	-.154651E-09
7	-.277784E-07	-.375974E-07	.549720E-11	.653612E-07	0.	-.907951E-11	-.100001E-03	.100001E-03	-.632884E-11
8	-.542807E-08	-.734687E-08	.107381E-11	.127735E-07	0.	-.349708E-12	-.100000E-03	.100000E-03	-.240409E-12
9	-.103854E-08	-.140567E-08	.205040E-12	.244399E-08	0.	-.128892E-13	-.100000E-03	.100000E-03	-.738212E-14
10	-.195203E-09	-.264208E-09	.381491E-13	.459372E-09	0.	-.573209E-15	-.100000E-03	.100000E-03	-.944557E-15
		ROOT MEAN SQUARE				.147849E-04			.987270E-05

TIME STEP= 4

WATER DISCHARGE= 15000.00 CFS

PARAMETER P1= -.86858628E-02  
 PARAMETER P2= -.50567238E-01  
 PARAMETER P3= .10748400E+03  
 PARAMETER P5= .96021138E+00  
 PARAMETER P6= -.19466672E-05  
 RED WAVE CELERITY= .48991645E-03 FT./SEC.

NUMBER OF ITERATIONS IN SUBROUTINE HZUP= 7

J	X	ZPLOT	RZ	Y	Z	HZ	V	FR	GRF	GSU	CSH	PZ	HT	SF
1	0.000	-.005	300.000	132.495	119.995	12.500	4.00	.20	.10304E+00	.25278E+00	.16032E+00	.12898E+05	.13274E+03	.10000E-03
2	.080	.174	300.000	132.454	120.132	12.322	4.06	.20	.10696E+00	.25809E+00	.16190E+00	.12912E+05	.13271E+03	.10035E-03
3	.160	.620	300.000	132.389	120.535	11.853	4.22	.22	.11834E+00	.27326E+00	.16635E+00	.12956E+05	.13267E+03	.10130E-03
4	.240	.398	300.000	132.357	120.271	12.085	4.14	.21	.11251E+00	.26552E+00	.16409E+00	.12927E+05	.13262E+03	.10082E-03
5	.320	.141	300.000	132.325	119.972	12.353	4.05	.20	.10626E+00	.25714E+00	.16162E+00	.12895E+05	.13258E+03	.10029E-03
6	.400	.039	300.000	132.287	119.828	12.459	4.01	.20	.10392E+00	.25398E+00	.16068E+00	.12880E+05	.13254E+03	.10008E-03
7	.480	.010	300.000	132.246	119.756	12.490	4.00	.20	.10326E+00	.25308E+00	.16041E+00	.12872E+05	.13250E+03	.10002E-03
8	.560	.002	300.000	132.204	119.707	12.498	4.00	.20	.10309E+00	.25285E+00	.16034E+00	.12867E+05	.13245E+03	.10000E-03
9	.640	.001	300.000	132.162	119.663	12.499	4.00	.20	.10305E+00	.25280E+00	.16033E+00	.12862E+05	.13241E+03	.10000E-03
10	.720	.000	300.000	132.120	119.620	12.500	4.00	.20	.10304E+00	.25279E+00	.16032E+00	.12857E+05	.13237E+03	.10000E-03
11	.800	.000	300.000	132.078	119.578	12.500	4.00	.20	.10304E+00	.25279E+00	.16032E+00	.12853E+05	.13233E+03	.10000E-03

J	D1	D2	D3	D4	D5	ES	D6	D7	EM
1	.225115E-04	.300990E-04	-.416584E-08	-.448133E-04	0.	.779301E-05	-.950474E-04	.100402E-03	.535957E-05
2	.915468E-05	.123251E-04	-.272485E-08	-.283902E-04	0.	-.691317E-05	-.105683E-03	.100974E-03	-.470929E-05
3	-.143954E-04	-.192003E-04	.310497E-08	.339048E-04	0.	.312233E-06	-.100662E-03	.100890E-03	.228428E-06
4	-.115812E-04	-.155407E-04	.229926E-08	.261064E-04	0.	-.101323E-05	-.101126E-03	.100426E-03	-.700573E-06
5	-.414833E-05	-.559830E-05	.818422E-09	.958281E-05	0.	-.163003E-06	-.100250E-03	.100137E-03	-.113368E-06
6	-.116253E-05	-.157221E-05	.229751E-09	.272054E-05	0.	-.139654E-07	-.100046E-03	.100037E-03	-.973010E-08
7	-.291307E-06	-.394205E-06	.576214E-10	.684539E-06	0.	-.916103E-09	-.100010E-03	.100009E-03	-.638597E-09
8	-.681558E-07	-.922446E-07	.134791E-10	.160335E-06	0.	-.514601E-10	-.100002E-03	.100002E-03	-.358757E-10
9	-.151957E-07	-.205672E-07	.299872E-11	.357573E-07	0.	-.259841E-11	-.100000E-03	.100000E-03	-.180906E-11
10	-.326778E-08	-.442293E-08	.637987E-12	.768996E-08	0.	-.120471E-12	-.100000E-03	.100000E-03	-.805970E-13
		ROOT MEAN SQUARE				.331170E-05			.226844E-05

TIME STEP= 5

WATER DISCHARGE= 15000.00 CFS

PARAMETER P1= -.86858628E-02  
 PARAMETER P2= -.50567238E-01  
 PARAMETER P3= .10748400E+03  
 PARAMETER P5= .96021138E+00  
 PARAMETER P6= -.19466672E-05  
 BED WAVE CELERITY= .48991645E-03 FT./SEC.

NUMBER OF ITERATIONS IN SUBROUTINE HZUP= 7

J	X	ZPLOT	RZ	Y	Z	HZ	V	FR	GRF	GSU	CSH	PZ	HT	SF
1	0.000	.004	300.000	132.504	120.004	12.500	4.00	.20	.10304E+00	.25278E+00	.16032F+00	.12498E+05	.13275E+03	.10000E-03
2	.080	.027	300.000	132.457	119.985	12.472	4.01	.20	.10364E+00	.25360E+00	.16057E+00	.12496E+05	.13271E+03	.10005E-03
3	.160	.220	300.000	132.408	120.135	12.273	4.07	.21	.10808F+00	.25959E+00	.16235F+00	.12913E+05	.13267E+03	.10045E-03
4	.240	.491	300.000	132.352	120.365	11.988	4.17	.21	.11491E+00	.26872E+00	.16503E+00	.12937E+05	.13262E+03	.10102E-03
5	.320	.389	300.000	132.315	120.220	12.094	4.13	.21	.11229E+00	.26522E+00	.16401E+00	.12922E+05	.13258E+03	.10081E-03
6	.400	.173	300.000	132.282	119.962	12.320	4.06	.20	.10701F+00	.25815E+00	.16192E+00	.12494E+05	.13254E+03	.10035E-03
7	.480	.056	300.000	132.244	119.804	12.440	4.02	.20	.10434E+00	.25455E+00	.16085E+00	.12877E+05	.13250E+03	.10012E-03
8	.560	.017	300.000	132.204	119.721	12.483	4.01	.20	.10341E+00	.25329E+00	.16047E+00	.12868E+05	.13245E+03	.10003E-03
9	.640	.004	300.000	132.162	119.666	12.495	4.00	.20	.10314F+00	.25292E+00	.16036F+00	.12862E+05	.13241E+03	.10001E-03
10	.720	.001	300.000	132.120	119.621	12.499	4.00	.20	.10306F+00	.25282E+00	.16033F+00	.12857E+05	.13237E+03	.10000E-03
11	.800	.000	300.000	132.078	119.578	12.500	4.00	.20	.10304E+00	.25279E+00	.16033E+00	.12853E+05	.13233E+03	.10000E-03

J	D1	D2	D3	D4	D5	FS	D6	D7	EM
1	.378909E-05	.511672E-05	-.771778E-09	-.863847E-05	0.	.266559E-06	-.998848E-04	.100072E-03	.186736E-06
2	.154393E-04	.207031E-04	-.309025E-08	-.340202E-04	0.	.211909E-05	-.989582E-04	.100423E-03	.146503E-05
3	.718154E-05	.963041E-05	-.177554E-08	-.190691E-04	0.	-.225887E-05	-.102383E-03	.100834E-03	-.154940E-05
4	-.879037E-05	-.117518E-04	.192357E-08	.212354E-04	0.	.695158E-06	-.100321E-03	.100807E-03	.486621E-06
5	-.104020E-04	-.139569E-04	.209733E-08	.237611E-04	0.	-.595760E-06	-.100872E-03	.100461E-03	-.410477E-06
6	-.489911E-05	-.660657E-05	.969867E-09	.113074E-04	0.	-.197324E-06	-.100317E-03	.100180E-03	-.137058E-06
7	-.166263E-05	-.224766E-05	.328626E-09	.388402E-05	0.	-.259505E-07	-.100075E-03	.100057E-03	-.180699E-07
8	-.484807E-06	-.655962E-06	.958061E-10	.113832E-05	0.	-.235605E-08	-.100017E-03	.100016E-03	-.164191E-08
9	-.129115E-06	-.174742E-06	.254528E-10	.303658E-06	0.	-.173416E-09	-.100004E-03	.100004E-03	-.128886E-09
10	-.322776E-07	-.436868E-07	.629118E-11	.759471E-07	0.	-.110069E-10	-.100001E-03	.100001E-03	-.767475E-11
		ROOT MEAN SQUARE				.102674E-05			.707547E-06

XMODF= .2400E+00      ZMODE= .4913E+00      XMEAN= .280E+00      STAND.DEV.= .9253E-01  
 COEFF.VAR.= .3295E+00      SKFW.COEFF.= .4550E+00      KURTOSIS COEFF.= .3180E+01

APPENDIX III  
PROGRAM FLOWCHART AND LISTING

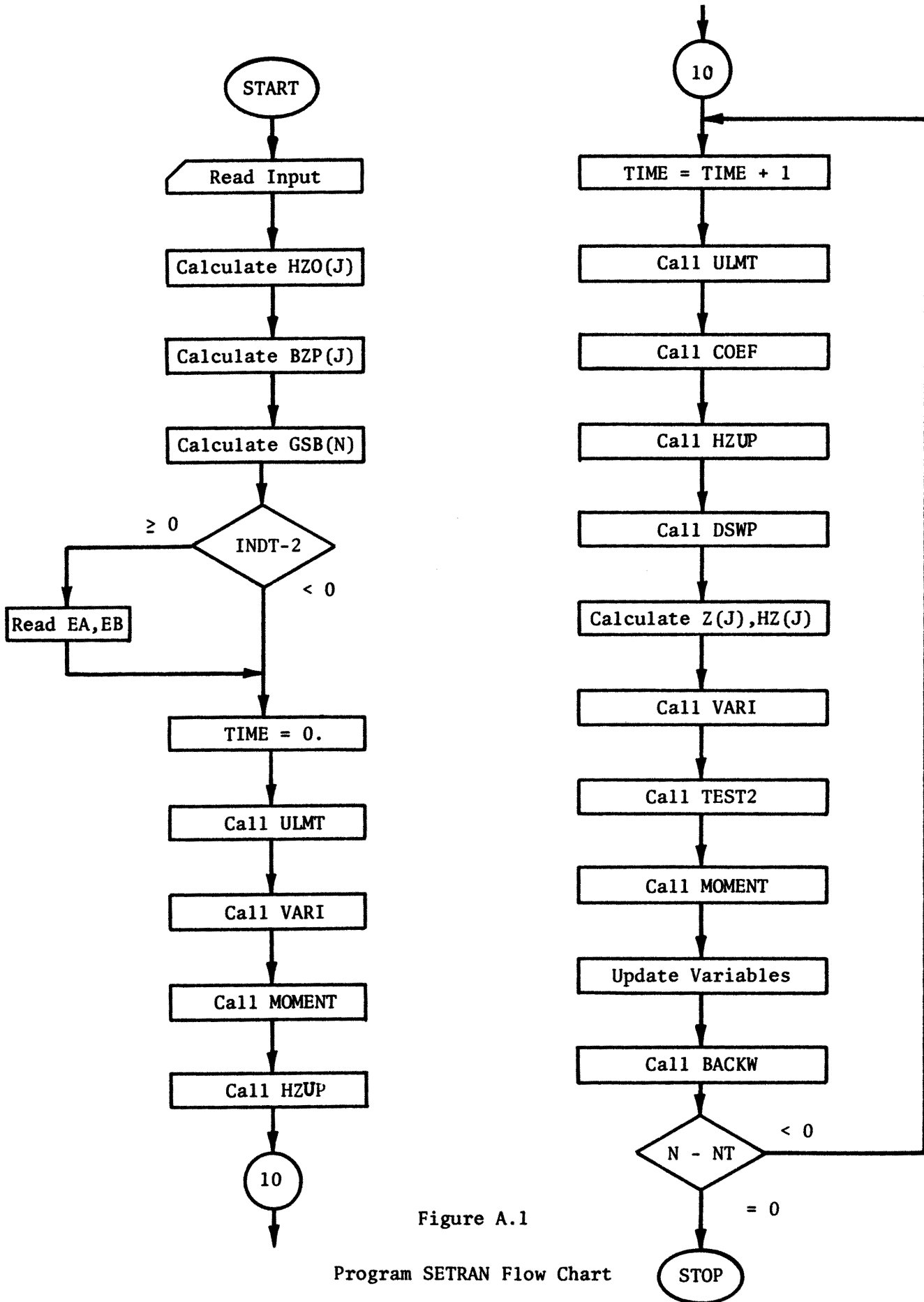


Figure A.1

Program SETRAN Flow Chart

```

PROGRAM SETRAN
1(INPUT,OUTPUT,PUNCH,TAPE5=INPUT,TAPE6=OUTPUT,TAPE7=PUNCH)
C**** PROGRAM SETRAN CALCULATES THE SEDIMENTATION TRANSIENTS IN ALLUVIAL
C**** CHANNELS, ACCORDING TO THE NUMERICAL MODEL DEVELOPED BY K. MAHMOOD
C**** AND V. M. PONCE.
COMMON/A/ GRAV,GAM,SS
COMMON/B/ POR,DIA,CK,CA,CB,VNU,WL,BR,MP
COMMON/C/ DEL
COMMON/D/ RLENGTH,NL,DX,NX,TTIME,NT,DT,NZ
COMMON/E/ TIME
COMMON/F/ FRMIN,FRMAX
COMMON/G/ INDT,EA,EB
COMMON/H/ INDU
COMMON/VC/ UL(4),UM(4),UT(4),VL(8),VM(8),VT(8)
COMMON/VA/ X(151),BZP(151),ZREF(151),ZPLOT(151)
DIMENSION QU(151),CU(151),ZU(151),YD(151)
DIMENSION HZO(151),HZ(151),ZO(151),Z(151),DY(151),DZ(151),BZ(151)
DIMENSION YO(151)
DIMENSION GSB(151)
DIMENSION GBE(151),GSU(151),CSH(151),PZ(151),HT(151),SF(151),
1GBEO(151),GSUO(151),CSHO(151),PZO(151),HTO(151),SFO(151)
WRITE(6,200)
GRAV= 32.17
GAM = 62.40
SS = 2.65
READ(5,105) INDU,INDT
READ(5,100) VNU,POR,DIA,CK,CA,CB
READ(5,100) FRMIN,FRMAX
READ(5,102) DEL,RLENGTH,TTIME,NL,NT
WRITE(6,110) VNU,POR,DIA,CK,CA,CB,FRMIN,FRMAX,DEL,RLENGTH,TTIME,
1NL,NT,INDU,INDT
DX= RLENGTH/FLOAT(NL)* 5280.
DT= TTIME /FLOAT(NT)*86400.
NX= NL+1
NZ= NT+1
DO 2 J=1,NZ
2 READ(5,100) QU(J),CU(J),ZU(J),YD(J)
DO 3 J=1,NX
3 READ(5,100) X(J),BZ(J),YO(J),ZO(J),ZREF(J)
DO 10 J=1,NX
10 HZO(J)= YO(J)-ZO(J)
BZP(1)= (BZ(2)-BZ(1))/DX
DO 15 J=2,NL
15 BZP(J)= (BZ(J+1)-BZ(J-1))/(2.*DX)
BZP(NX)= (BZ(NX)-BZ(NL))/DX
DO 20 J=1,NZ
20 GSB(J)= CU(J)*QU(J)/BZ(1)*GAM/10.**6.
IF(INDT.EQ.1) GO TO 9
READ(5,100) EA,EB
WRITE(6,112) EA,EB
9 CONTINUE
N=0
TIMF= 0.
EQ= QU(1)
CALL ULMT(EQ)
CALL VARI(HZO,ZO,BZ,GBEO,GSUO,CSHO,PZO,HTO,SFO,EQ)
CALL MOMENT
CALL HZUP(HZBO,BZ(1),GSB,N,EQ)
DO 60 N=1,NT

```

```

TIME= TIME+1.
WRITE(6,150) N,EQ
CALL ULMT(EQ)
CALL COEF(HZO,ZO,BZ,EQ)
CALL HZUP(HZB,BZ(1),GSB,N,EQ)
CALL DSWP(HZB,HZBO,ZU,YD,N,DY,DZ)
DO 40 J=1,NX
Z(J)= ZO(J)+DZ(J)
HZ(J)= HZO(J)+DY(J)-DZ(J)
40 CONTINUE
CALL VARI(HZ,Z,BZ,GBE,GSU,CSH,PZ,HT,SF,EQ)
CALL TEST2(GBE,GBEO,GSU,GSUO,CSH,CSHO,PZ,PZO,HT,HTO,SF,SFO,BZ,BZP)
41 CONTINUE
CALL MOMENT
HZBO= HZB
DO 50 J=1,NX
HZO(J)= HZ(J)
ZO(J)= Z(J)
GBEO(J)= GBE(J)
GSUO(J)= GSU(J)
CSHO(J)= CSH(J)
PZO(J)= PZ(J)
HTO(J)= HT(J)
SFO(J)= SF(J)
50 CONTINUE
EQ= QU(N+1)
CALL BACKW
60 CONTINUE
100 FORMAT (8F10.0)
101 FORMAT (I10)
102 FORMAT(3F10.0,2I10)
105 FORMAT(2I10)
110 FORMAT(* KINEMATIC VISCOSITY=*,F10.8,* SQ.FT./SEC.* /
1      * POROSITY=          *,F10.3,/
2      * MEDIAN BED SIZE=   *,F10.3,* FT.* /
3      * K1=                *,F10.6,/
4      * A=                  *,F10.3,/
5      * B=                  *,F10.3,/
6      * FROUDE NO MINIMUM= *,F10.3,/
7      * FROUDE NO MAXIMUM= *,F10.3,/
8      * WEIGHT F. DELTA=   *,F10.3,/
9      * REACH LENGTH=      *,F10.3,* MILES*/
9      * TOTAL TIME=        *,F10.0,* DAYS*/
1      * NL=                 *,I10,/
2      * NT=                 *,I10,/
3      * INDU=               *,I10,/
4      * INDT=               *,I10/)
111 FORMAT(7E15.8)
112 FORMAT(* TRANSPORT PARAMETER A1= *,F15.5,/
2      * TRANSPORT PARAMETER B1= *,F15.5/)
150 FORMAT(/// * TIME STEP= *I5, //
1      * WATER DISCHARGE=          *,F10.2,* CFS*/)
200 FORMAT(1H1,///,10X,* MATHEMATICAL MODELING OF SEDIMENTATION TRANSI
1ENTS *///)
STOP
END

```

```

SUBROUTINE GT(H,B,G)
COMMON/VC/ UL(4),UM(4),UT(4),VL(8),VM(8),VT(8)
G= VL(4)*H**VM(4)*B**VT(4)
1 +VL(5)*H**VM(5)*B**VT(5)
1 +VL(6)*H**VM(6)*B**VT(6)
RETURN
END

```

```

SUBROUTINE VARI(HZ,Z,HZ,GBE,GSU,CSH,PZ,HT,SF,EQ)
COMMON/A/ GRAV,GAM,SS
COMMON/B/ POR,DIA,CK,CA,CR,VNU,WL,BR,MP
COMMON/C/ DEL
COMMON/D/ RLENGTH,NL,DX,NX,TTIME,NT,DT,NZ
COMMON/E/ TIME
COMMON/VA/ X(151),BZP(151),ZREF(151),ZPLOT(151)
COMMON/VC/ UL(4),UM(4),UT(4),VL(8),VM(8),VT(8)
DIMENSION HZ(1),Z(1),RZ(1),GBE(1),GSU(1),CSH(1),PZ(1),HT(1),SF(1)
WRITE(6,300)
DO 10 J=1,NX
V= EQ/(HZ(J)*BZ(J))
FR= V/(GRAV*HZ(J)**0.5)
CALL VLMT(HZ(J),BZ(J))
GBE(J)= VL(4)*HZ(J)**VM(4)*BZ(J)**VT(4)
GSU(J)= VL(5)*HZ(J)**VM(5)*BZ(J)**VT(5)
1 +VL(6)*HZ(J)**VM(6)*BZ(J)**VT(6)
CSH(J)= VL(7)*HZ(J)**VM(7)*BZ(J)**VT(7)
1 +VL(8)*HZ(J)**VM(8)*BZ(J)**VT(8)
PZ(J)= (1.-POR)*SS*GAM*Z(J)
Y= Z(J)+HZ(J)
HT(J)= V*V/(2.*GRAV)+Y
SF(J)= UL(2)*HZ(J)**UM(2)*BZ(J)**UT(2)
ZPLOT(J)= Z(J)-ZREF(J)
WRITE(6,400) J,X(J),ZPLOT(J),BZ(J),Y,Z(J),HZ(J),V,FR,GBE(J),GSU(J)
1,CSH(J),PZ(J),HT(J),SF(J)
300 FORMAT(* J X ZPLOT BZ Y Z HZ V
1 FR GRE GSU CSH PZ HT
2 SF*/)
400 FORMAT(1X,I3,F7.3,5F8.3,2F5.2,6E12.5)
10 CONTINUE
RETURN
END

```

```

SUBROUTINE ULMT(EQ)
COMMON/A/ GRAV,GAM,SS
COMMON/B/ POR,DIA,CK,CA,CB,VNU,WL,BR,MP
COMMON/C/ DEL
COMMON/VC/ UL(4),UM(4),UT(4),VL(8),VM(8),VT(8)
VSS= ((2./3.*GRAV*(SS-1.)*DIA**3.+36.*VNU**2.))**0.5-6.*VNU)/DIA
XKAPPA= 0.4
UL(1)= ((0.0342*DIA**(0.1667-CA)*EQ**CB)/(CK*GRAV**(CB/2.)))**1.5
UM(1)= 1.-2.25*CB
UT(1)= -1.5*CB
UL(2)= ((CK*DIA**CA*EQ**(1.-CB)*GRAV**(CB/2.))/1.486)**2.
UM(2)= 3.*CB-10./3.
UT(2)= 2.*(CB-1.)
UL(3)= (7.*EQ*DIA**(1./6.))/(6.*(GRAV*UL(1)*UL(2))**0.5)
UM(3)= -(UM(1)/2.+UM(2)/2.+7./6.)
UT(3)= -(UT(1)/2.+UT(2)/2.+1.)
UL(4)= VSS/(XKAPPA*(GRAV*UL(2))**0.5)
UM(4)= -0.5*(UM(2)+1.)
UT(4)= -0.5*UT(2)
RETURN
END

```

```

SUBROUTINE VLMT(HZD,BZD)
COMMON/A/ GRAV,GAM,SS
COMMON/B/ POR,DIA,CK,CA,CB,VNU,WL,BR,MP
COMMON/G/ INDT,EA,EB
COMMON/VC/ UL(4),UM(4),UT(4),VL(8),VM(8),VT(8)
DIMENSION EINSA(8),EINSR(8)
DATA(EINSA(I),I=1,8)/7.714,7.357,10.552,25.668,138.263,1610.638,
136020496.,1395000000000000./
DATA(EINSB(I),I=1,8)/-1.01,-1.19,-1.67,-2.30,-3.23,-4.26,-7.81,
1-12.66/
IF(INDT.EQ.2) GO TO 10
PSI=(SS-1.)*DIA/(UL(1)*UL(2)*HZD**(UM(1)+UM(2))*BZD**(UT(1)+UT(2))
1)
IF(PSI.LE.0.77) IRANGE= 1
IF(PSI.GT.0.77.AND.PSI.LE.2.12) IRANGE=2
IF(PSI.GT.2.12.AND.PSI.LE.4.10) IRANGE=3
IF(PSI.GT.4.10.AND.PSI.LE.6.10) IRANGE=4
IF(PSI.GT.6.10.AND.PSI.LE.11.0) IRANGE=5
IF(PSI.GT.11.0.AND.PSI.LE.16.7) IRANGE=6
IF(PSI.GT.16.7.AND.PSI.LE.22.5) IRANGE=7
IF(PSI.GT.22.5) IRANGE=8
EA= EINSA(IRANGE)
EB= EINSB(IRANGE)
EA= 2.*EA
10 CONTINUE
VL(4)= EA*GRAV**0.5*(SS-1.)**(EB+0.5)*DIA**(EB+1.5)*SS*GAM/
1(UL(1)*UL(2))**EB
VM(4)= -EB*(UM(1)+UM(2))
VT(4)= -EB*(UT(1)+UT(2))
ROU= UL(4)*HZD**UM(4)*BZD**UT(4)
VL(5)= (2.**0.1667*UL(3)*VL(4))/(11.6*(1.1667-ROU)*(2.*DIA)**(1.16
167-ROU))
VM(5)= UM(3)+VM(4)+ 1.1667-ROU
VT(5)= UT(3) + VT(4)
VL(6)= -(2.**0.1667*UL(3)*VL(4))/(11.6*(1.1667-ROU))
VM(6)= UM(3)+VM(4)
VT(6)= VT(5)
VL(7)= VL(4)/(11.6*(1.-ROU)*(GRAV*UL(1)*UL(2))**0.5*(2.*DIA)**
1(1.-ROU))
VM(7)= -0.5*(UM(1)+UM(2))+VM(4)+1.-ROU
VT(7)= -0.5*(UT(1)+UT(2))+VT(4)
VL(8)= -VL(4)/(11.6*(1.-ROU)*(GRAV*UL(1)*UL(2))**0.5)
VM(8)= -0.5*(UM(1)+UM(2)) + VM(4)
VT(8)= VT(7)
RETURN
END

```

```

SUBROUTINE COEF(HZ,Z,BZ,EQ)
COMMON/A/ GRAV,GAM,SS
COMMON/B/ POR,DIA,CK,CA,CB,VNU,WL,BR,MP
COMMON/C/ DEL
COMMON/D/ RLENGTH,NL,DX,NX,TTIME,NT,DT,NZ
COMMON/VA/ X(151),BZP(151),ZREF(151),ZPLOT(151)
COMMON/VC/ UL(4),UM(4),UT(4),VL(8),VM(8),VT(8)
COMMON/VD/ AS(150),BS(150),CS(150),DS(150),ES(150),FS(150),GS(150)
1,HS(150),QS(150),RS(150)
DIMENSION HZ(1),Z(1),BZ(1)
CALL VLMT(HZ(1),BZ(1))
VL4L= VL(4) $ VM4L= VM(4) $ VT4L= VT(4)
VL5L= VL(5) $ VM5L= VM(5) $ VT5L= VT(5)
VL6L= VL(6) $ VM6L= VM(6) $ VT6L= VT(6)
VL7L= VL(7) $ VM7L= VM(7) $ VT7L= VT(7)
VL8L= VL(8) $ VM8L= VM(8) $ VT8L= VT(8)
H2L= UL(2)*UM(2)*HZ(1)**(UM(2)-1.)*BZ(1)**UT(2)
H4L= VL4L*VM4L*HZ(1)**(VM4L-1.)*BZ(1)**VT4L
H5L= VL5L*VM5L*HZ(1)**(VM5L-1.)*BZ(1)**VT5L
H6L= VL6L*VM6L*HZ(1)**(VM6L-1.)*BZ(1)**VT6L
H7L= VL7L*VM7L*HZ(1)**(VM7L-1.)*BZ(1)**VT7L
H8L= VL8L*VM8L*HZ(1)**(VM8L-1.)*BZ(1)**VT8L
FRL= EQ/(BZ(1)*(GRAV*HZ(1)**3.))**0.5)
ZRL= UL(4)*HZ(1)**UM(4)*BZ(1)**UT(4)
DL5L= UM(4)*VL5L*ZRL*((1.1667-ZRL)*ALOG(2.*DIA)+1.)/(HZ(1)*(1.166
17-ZRL))
DL6L= UM(4)*VL6L*ZRL/(HZ(1)*(1.1667-ZRL))
DL7L= UM(4)*VL7L*ZRL*((1.0000-ZRL)*ALOG(2.*DIA)+1.)/(HZ(1)*(1.000
10-ZRL))
DL8L= UM(4)*VL8L*ZRL/(HZ(1)*(1.0000-ZRL))
XI5L=DL5L*HZ(1)**VM5L*BZ(1)**VT5L
XI6L=DL6L*HZ(1)**VM6L*BZ(1)**VT6L
XI7L=DL7L*HZ(1)**VM7L*BZ(1)**VT7L
XI8L=DL8L*HZ(1)**VM8L*BZ(1)**VT8L
XL2L= UL(2)*HZ(1)**UM(2)*BZ(1)**UT(2)
XL4L= VL4L*HZ(1)**VM4L*BZ(1)**VT4L
XL5L= VL5L*HZ(1)**VM5L*BZ(1)**VT5L
XL6L= VL6L*HZ(1)**VM6L*BZ(1)**VT6L
DM5L= -UM(4)*ZRL/HZ(1)
DM7L= DM5L
XJ5L= DM5L*BZ(1)**VT5L*VL5L*HZ(1)**VM5L*ALOG(HZ(1))
XJ7L= DM7L*BZ(1)**VT7L*VL7L*HZ(1)**VM7L*ALOG(HZ(1))
XK4L= XL4L*(VT4L+1.)
XK5L= XL5L*(VT5L+1.)
XK6L= XL6L*(VT6L+1.)
10 CONTINUE
P1= H7L+H8L+XI7L+XI8L+XJ7L
P2= H4L+H5L+H6L+XI5L+XI6L+XJ5L
P3= (1.-POR)*SS*GAM
P5= 1.-FRL*FRL
P6= H2L
P8= P3*P5-P1
CNF= -P2/P8
WRITE(6,100) P1,P2,P3,P5,P6,CNF
DO 20 J=1,NL
CALL VLMT(HZ(J+1),BZ(J+1))
H2 = UL(2)*UM(2)*HZ(J+1)**(UM(2)-1.)*BZ(J+1)**UT(2)
H4 = VL(4)*VM(4)*HZ(J+1)**(VM(4)-1.)*BZ(J+1)**VT(4)
H5 = VL(5)*VM(5)*HZ(J+1)**(VM(5)-1.)*BZ(J+1)**VT(5)

```

```

H6 = VL(6)*VM(6)*HZ(J+1)**(VM(6)-1.)*BZ(J+1)**VT(6)
H7 = VL(7)*VM(7)*HZ(J+1)**(VM(7)-1.)*BZ(J+1)**VT(7)
H8 = VL(8)*VM(8)*HZ(J+1)**(VM(8)-1.)*BZ(J+1)**VT(8)
FR= EQ/(BZ(J+1)*(GRAV*HZ(J+1)**3.))**0.5)
ZR = UL(4)*HZ(J+1)**UM(4)*RZ(J+1)**UT(4)
DL5= UM(4)*VL(5)*ZR*((1.1667-ZR)*ALOG(2.*DIA)+1.)/(HZ(J+1)*(1.166
17-ZR))
DL6= UM(4)*VL(6)*ZR/(HZ(J+1)*(1.1667-ZR))
DL7= UM(4)*VL(7)*ZR*((1.0000-ZR)*ALOG(2.*DIA)+1.)/(HZ(J+1)*(1.000
10-ZR))
DL8= UM(4)*VL(8)*ZR/(HZ(J+1)*(1.0000-ZR))
XI5= DL5*HZ(J+1)**VM(5)*RZ(J+1)**VT(5)
XI6= DL6*HZ(J+1)**VM(6)*RZ(J+1)**VT(6)
XI7= DL7*HZ(J+1)**VM(7)*RZ(J+1)**VT(7)
XI8= DL8*HZ(J+1)**VM(8)*RZ(J+1)**VT(8)
XL2= UL(2)*HZ(J+1)**UM(2)*BZ(J+1)**UT(2)
XL4= VL(4)*HZ(J+1)**VM(4)*BZ(J+1)**VT(4)
XL5= VL(5)*HZ(J+1)**VM(5)*BZ(J+1)**VT(5)
XL6= VL(6)*HZ(J+1)**VM(6)*BZ(J+1)**VT(6)
DM5= -UM(4)*ZR/HZ(J+1)
DM7= DM5
XJ5= DM5*BZ(J+1)**VT(5)*VL(5)*HZ(J+1)**VM(5)*ALOG(HZ(J+1))
XJ7= DM5*BZ(J+1)**VT(7)*VL(7)*HZ(J+1)**VM(7)*ALOG(HZ(J+1))
XK4= XL4*(VT(4)+1.)
XK5= XL5*(VT(5)+1.)
XK6= XL6*(VT(6)+1.)
AS(J)= -(H4L+H5L+H6L+XI5L+XI6L+XJ5L)*DEL/DX
1      +( H7L+H8L+XI7L+XI8L+XJ7L)*0.5/DT
2      +(BZP(J)/BZ(J))*(H4L+H5L+H6L+XI5L+XI6L+XJ5L)*DEL/2.
BS(J)= +(H4+H5+H6+XI5+XI6+XJ5)*DEL/DX
1      +( H7+H8+XI7+XI8+XJ7)*0.5/DT
2      +(BZP(J+1)/BZ(J+1))*(H4+H5+H6+XI5+XI6+XJ5)*DEL/2.
TEM=0.5*(1.-POR)*SS*GAM/DT
CS(J)= TEM - AS(J)
DS(J)= TEM - BS(J)
QS(J)= -(XL4 +XL5 +XL6 )/DX
1      +(XL4L+XL5L+XL6L)/DX
ES(J)= -(1.-FRL**2.)*DEL/DX + H2L*DEL/2.
FS(J)= +(1.-FR**2.)*DEL/DX + H2 *DEL/2.
GS(J)= +(0.-FRL**2.)*DEL/DX - H2L*DEL/2.
HS(J)= +(0.+FR **2.)*DEL/DX - H2*DEL/2.
RS(J)= -(FR**2.*HZ(J+1)-FRL**2.*HZ(J))/(2.*DX)
1      -(HZ(J+1)+Z(J+1)-HZ(J)-Z(J))/DX
2      -(XL2+XL2L)/2.
H2L=H2 $ XL2L=XL2
H4L=H4 $ ZRL= ZR $ FRL= FR $ XL4L=XL4
H5L=H5 $ DL5L=DL5 $ XI5L=XI5 $ XL5L=XL5 $ DM5L=DM5 $ XJ5L=XJ5
H6L=H6 $ DL6L=DL6 $ XI6L=XI6 $ XL6L=XL6
H7L=H7 $ DL7L=DL7 $ XI7L=XI7 $ DM7L=DM7 $ XJ7L=XJ7
H8L=H8 $ DL8L=DL8 $ XI8L=XI8
XK4L= XK4
XK5L= XK5
XK6L= XK6
20 CONTINUE
100 FORMAT(/* PARAMETER P1= *E15.8/
1 * PARAMETER P2= *E15.8/
2 * PARAMETER P3= *E15.8/
3 * PARAMETER P5= *E15.8/
4 * PARAMETER P6= *E15.8/

```

```

5      * BED WAVE CELERITY=      *E15.8* FT./SEC.*//)
RETURN
END

```

```

SUBROUTINE DSWP(HZB,HZBO,ZU,YD,N,DY,DZ)
COMMON/D/ RLENGTH,NL,DX,NX,TTIME,NT,DT,NZ
COMMON/H/ INDU
COMMON/VD/ AS(150),BS(150),CS(150),DS(150),ES(150),FS(150),GS(150)
1,HS(150),QS(150),RS(150)
DIMENSION SS(151),TS(151),US(151)
DIMENSION ZU(1),YD(1),DY(1),DZ(1)
IF (INDU.EQ.2)GO TO 10
TS(1)= HZB-HZBO
SS(1)= 1.
GO TO 20
10 CONTINUE
DZ(1)= ZU(N+1)-ZU(N)
SS(1)= 1000000.
TS(1)= -SS(1)*DZ(1)
20 CONTINUE
DO 30 J=2,NX
US(J)= (ES(J-1)*SS(J-1)+GS(J-1))/(AS(J-1)*SS(J-1)+CS(J-1))
TS(J)= ((RS(J-1)-ES(J-1)*TS(J-1))-US(J)*(QS(J-1)-AS(J-1)*TS(J-1)))
1/(FS(J-1)-US(J)*RS(J-1))
SS(J)=-(HS(J-1)-US(J)*DS(J-1))/(FS(J-1)-US(J)*BS(J-1))
30 CONTINUE
DY(NX)= YD(N+1)-YD(N)
DZ(NX)= (DY(NX)-TS(NX))/SS(NX)
DO 70 J=2,NX
K= NX-J+1
DZ(K)= ((QS(K)-AS(K)*TS(K))- (BS(K)*DY(K+1)+DS(K)*DZ(K+1)))/(AS(K)*
1SS(K)+CS(K))
DY(K)= SS(K)*DZ(K)+ TS(K)
70 CONTINUE
RETURN
END

```

```

SUBROUTINE HZUP(HZB,BZ,GSR,N,EQ)
COMMON/A/ GRAV,GAM,SS
COMMON/C/ DEL
COMMON/F/ FRMIN,FRMAX
COMMON/VC/ UL(4),UM(4),UT(4),VL(8),VM(8),VT(8)
DIMENSION BZ(1),GSB(1)
HZMIN= (EQ/(BZ(1)*FRMAX*GRAV**0.5))**(2./3.)
HZMAX= (EQ/(BZ(1)*FRMIN*GRAV**0.5))**(2./3.)
CALL VLMT(HZMIN,BZ(1))
CALL GT(HZMIN,BZ(1),GSBMAX)
CALL VLMT(HZMAX,BZ(1))
CALL GT(HZMAX,BZ(1),GSBMIN)
KOUNT=0
H1= ALOG(HZMAX)
H2= ALOG(HZMIN)
G1= ALOG(GSBMIN)
G2= ALOG(GSBMAX)
G3= ALOG(GSB(N+1))
TOL= 0.000001*G3
TOL= ABS(TOL)
900 FORMAT(2(6E15.8/))
901 FORMAT(10X,E15.8)
10 KOUNT= KOUNT+1
IF(KOUNT.EQ.20) GO TO 40
H3TRY= H1-(H1-H2)*(G3-G1)/(G2-G1)
H3TRY= EXP(H3TRY)
CALL VLMT(H3TRY,BZ(1))
CALL GT(H3TRY,BZ(1),G3TRY)
G3TRY= ALOG(G3TRY)
TEMP= G3-G3TRY
IF(ABS(TEMP).LT.TOL) GO TO 40
IF(TEMP.LT.0) GO TO 20
H1= ALOG(H3TRY)
G1= G3TRY
GO TO 30
20 CONTINUE
H2= ALOG(H3TRY)
G2= G3TRY
30 CONTINUE
GO TO 10
40 CONTINUE
HZ9= H3TRY
45 WRITE(6,100) KOUNT
50 CONTINUE
100 FORMAT(/* NUMBER OF ITERATIONS IN SUBROUTINE HZUP= *I2/)
RETURN
END

```

```

SUBROUTINE MOMENT
COMMON/B/ POR,DIA,CK,CA,CB,VNU,WL,BR,MP
COMMON/D/ RLENGTH,NL,DX,NX,TTIME,NT,DT,NZ
COMMON/VA/ X(151),RZP(151),ZREF(151),ZPLOT(151)
DIMENSION XME(151),ZM(151)
BR= 0.01
MP=5
N= 0
DO 10 J= 1,NX
ZPLOT(J)= ZPLOT(J) - BR
IF(ZPLOT(J).LE.0.) GO TO 10
N= N+1
XME(N)= X(J)
ZM(N)= ZPLOT(J) + BR
10 CONTINUE
IF(N.LE.MP) RETURN
SUMA= 0.
SUMB= 0.
DO 20 J= 1,N
SUMA= SUMA + XME(J)*ZM(J)
SUMB= SUMB + ZM(J)
20 CONTINUE
XMN= SUMA/SUMB
NN= N-1
DO 30 J= 1,NN
CC= ZM(J+1)
DD= ZM(J)
IF(CC.LT.DD) GO TO 40
30 CONTINUE
40 ZMD= DD
XMD= XME(J)
SSD= 0.
SSK= 0.
SKU= 0.
DO 50 J= 1,N
UU= XME(J)-XMN
SSD= SSD + UU**2*ZM(J)/SUMB
SSK= SSK + UU**3*ZM(J)/SUMB
SKU= SKU + UU**4*ZM(J)/SUMB
50 CONTINUE
SD= SQRT(SSD)
CV= SD/XMN
SKC= SSK/SD**3
CKU= SKU/SD**4
PRINT 100, XMD,ZMD, XMN,SD,CV,SKC,CKU
100 FORMAT (1X,*XMODE=*,E11.4,10X,*ZMODE=*,E11.4,10X,*XMEAN=*,E11.4,10
1X,*STAND.DEV.=*,E11.4,/,1X,*COEFF.VAR.=*,E11.4,10X,*SKEW.COEFF.=*,
2E11.4,10X,*KURTOSIS COEFF.=*,E11.4)
RETURN
END

```

```

SUBROUTINE TEST2(A,B,A1,B1,A2,B2,C,D,E,F,G,H,BZ,BZP)
COMMON/C/ DEL
COMMON/D/ RLENGTH,NL,DX,NX,TTIME,NT,DT,NZ
DIMENSION A(1),B(1),A1(1),B1(1),A2(1),B2(1),C(1),D(1),E(1),F(1),
1G(1),H(1)
DIMENSION BZ(1),BZP(1)
SR= 0.
SU= 0.
XL= NL
PRINT 200
DO 10 J= 1,NL
P= DEL/DX*(A(J+1)-A(J))+ (1.-DEL)/DX*(B(J+1)-B(J))
P1= DEL/DX*(A1(J+1)-A1(J))+ (1.-DEL)/DX*(B1(J+1)-B1(J))
P2= 0.5/DT*(A2(J+1)+A2(J)-B2(J+1)-B2(J))
Q= 0.5/DT*(C(J+1)+C(J)-D(J+1)-D(J))
P3= P+P1+P2
P4= DEL/2.*(BZP(J+1)/BZ(J+1)*A(J+1)+BZP(J)/BZ(J)*A(J))+ (1.-DEL)/2.
1*(BZP(J+1)/BZ(J+1)*B(J+1)+BZP(J)/BZ(J)*B(J))
P5= DEL/2.*(BZP(J+1)/BZ(J+1)*A1(J+1)+BZP(J)/BZ(J)*A1(J))+ (1.-DEL)/
12.*(BZP(J+1)/BZ(J+1)*B1(J+1)+BZP(J)/BZ(J)*B1(J))
P6= P4+P5
R= P3+Q+P4+P5
SR= SR + R*R
S= DEL/DX*(E(J+1)-E(J))+ (1.-DEL)/DX*(F(J+1)-F(J))
T= DEL/2.*(G(J+1)+G(J))+ (1.-DEL)/2.*(H(J+1)+H(J))
U= S+T
SU= SU + U*U
PRINT 100,J,P,P1,P2,Q,P6,R,S,T,U
10 CONTINUE
V= SQRT(SR/XL)
W= SQRT(SU/XL)
PRINT 120, V,W
100 FORMAT(I10,9E13.6)
120 FORMAT(20X,*ROOT MEAN SQUARE*,37X,E15.6,24X,E15.6/)
200 FORMAT(/**
14          D5          D1          D2          D3          D
2*/)          ES          D6          D7          EM
RETURN
END

```